Control of Plant Wide Processes Using Fractional Order Controller

Soumya Ranjan Sahoo

Department of Chemical Engineering
National Institute of Technology Rourkela

Control of Plant Wide Processes Using Fractional Order Controller

Thesis submitted in partial fulfillment

of the requirements of the degree of

M. Tech Dual Degree

in

Chemical Enginnering
(*Specialization: Chemical Engineering*)

by

Soumya Ranjan Sahoo

(Roll Number: 711CH1025)

based on research carried out

under the supervision of

Prof. Madhusree Kundu

May, 2016

Department of Chemical Engineering
National Institute of Technology Rourkela

Department of Chemical Engineering
National Institute of Technology Rourkela

Prof. Madhusree Kundu
Associate Professor

May 26, 2016

Supervisor's Certificate

This is to certify that the work presented in the dissertation entitled *Control of Plant Wide Processes Using Fractional Order Controller* submitted by *Soumya Ranjan Sahoo*, Roll Number 711CH1025, is a record of original research carried out by him under my supervision and guidance in partial fulfillment of the requirements of the degree of *M. Tech Dual Degree* in *Chemical Enginnering.* Neither this thesis nor any part of it has been submitted earlier for any degree or diploma to any institute or university in India or abroad.

Madhusree Kundu

Declaration of Originality

I, *Soumya Ranjan Sahoo*, Roll Number *711CH1025* hereby declare that this dissertation entitled *Control of Plant Wide Processes Using Fractional Order Controller* presents my original work carried out as a postgraduate student of NIT Rourkela and, to the best of my knowledge, contains no material previously published or written by another person, nor any material presented by me for the award of any degree or diploma of NIT Rourkela or any other institution. Any contribution made to this research by others, with whom I have worked at NIT Rourkela or elsewhere, is explicitly acknowledged in the dissertation. Works of other authors cited in this dissertation have been duly acknowledged under the sections "Reference" or "Bibliography". I have also submitted my original research records to the scrutiny committee for evaluation of my dissertation.

I am fully aware that in case of any non-compliance detected in future, the Senate of NIT Rourkela may withdraw the degree awarded to me on the basis of the present dissertation.

May 26, 2016
NIT Rourkela

Soumya Ranjan Sahoo

Acknowledgment

This report would not have been possible without the positive input of great many individuals. It seems inevitable that I will fail to thank everyone, so accept my apology in advance. Most importantly I wish to express my heartily gratitude to my guide Prof. Dr. Madhusree Kundu for his invaluable guidance along with constant flow of existing & new ideas and contagious enthusiasm through my work. I want to thank madam for constantly motivating me through his valuable counsel as well as excellent tips to build my research and writing skills. I am obliged to all my friends for their friendships and encouragements. Finally, the thesis would not have been completed without the support of the most important people in my life -my family. I sincerely wish to thank my parents, for their unconditional love and constant encouragement.

May 26, 2016
NIT Rourkela

Soumya Ranjan Sahoo
Roll Number: 711CH1025

Abstract

Fractional order PID controller is gaining popularity because the presence of two extra degrees of freedom, which have the potential to meet up the extra degrees in terms of uncertainty, robustness, output controllability. In other words, the fractional order PID controller is the generalization of the conventional PID controller. In the current study the fractional order PID controller is designed and implemented for the complex and plant wide processes. Distillation is a the most effective separation process in the chemical and petroleum industries but with a drawback of energy intensivity To reduce the energy consumption two distillation columns can be combined into one column, which is known as dividing wall distillation column (DWC). Though the control of DWC has been addressed but it requires further R&D efforts considering the complexity in control of this process In this work the DWC is controlled by the advanced control strategy like fractional order PID controller. One of the challenging field in the process control is to design control system for entire chemical plant. We have presented the control system for the HDA plant by implementing the fractional order PID controller. Both the discussed processes are multi-input-multi-output (MIMO) system and these processes are difficult to tune because of the presence of the interaction between the control loops. For the DWC process the traditional simplified decoupler is used, while for the HDA plant process the equivalent transfer function model is used to handle the MIMO system. For tuning of the fractional order PID controllers the optimization techniques have been used. The DWC controllers have been tuned by the ev-MOGA multi objective algorithm and the HDA plant controllers are tuned by the cuckoo search method.

Keywords*: *Dividing wall column*; *HDA process plant*; *Equivalent transfer function*; *ev-MOGA*; *Cuckoo search method

Contents

List of Figures

List of Tables

Chapter 1

Introduction

1.1 Introduction

The most significant objective of any controller being designed is its ability to suppress the external disturbance creeping into the system. Due to the relatively simple structure and remarkable effectiveness of implementation, the proportional integral derivative (PID) controllers are so far prodigiously applied in industrial applications. It has been reported that more than 95% of the control loops in the process control industry are controlled by PID controllers. Fractional order PID controller is gaining popularity because of its extra flexibility in terms of its extra two degrees of freedom over the conventional PID controllers, which can meet up additional control objectives. Recently, due to the enhanced understanding of three centuries old fractional calculus, the implementation of fractional order controllers has become feasible. It is very difficult to design cost effective and high performance controllers. To design a controller by using some traditional trail and error method using design criterion in both the time and frequency domain is practically impossible. Robustness and performance can be represented as objective functions with respect to design parameters in controller design being formulated as optimization problem. The fractional order control design is formulated using the multi objective optimization technique (ev-MOGA). The fractional order controller can be used for different industrial process for high-performance and cost effective solutions.

Distillation has been a very effective separation process nonetheless with questionable sustainability due to its large energy intensive operation. To reduce the energy consumption, different types of technical solutions have been proposed at least over the last three decades, one of them is column sequencing. The number of columns required to isolate more than two components is the number of components minus one and the number of columns increases with the number of components. Therefore, an optimal sequencing strategy is necessary. One of the most important optimal fully thermally coupled columns is Petluyk column. This type of thermally coupled column consists of a prefractionator which is coupled with the main column with two recycle streams. One recycle is liquid which is fed into the top of the prefractionator and other one which is vapour is injected into the bottom of the prefractionator. The petluyk column got transformed into divided wall column by inserting a longitudinal partition in the middle section of the column. Feed is supplied into the side

wall of the prefractionator. The control of DWC has been a comparatively complex and challenging area needs further contributions.

One of the challenges for the process system engineer to design control system for the entire plant. Plant wide control is the effective control system for the plant to archive the demands of product rate and quality without violating safety and environmental regulation. For a plant wide control there are three main steps such as control structure design, controller design and implementation. The control structure can be subdivided into control objectives, manipulated variable, the control configuration, the selection of controller type. For the plant wide control, we have chosen the HDA process. The presence of reactor with exothermic reaction, distillation columns and high level interaction makes the plant really complex with plant-wide control as a challenging one.

1.1.1 Literature review

When more than two products need to be separated, the number of columns increases with the number of components One of the best way to handle this problem is optimal sequencing strategy. Systematic column sequencing is an area of research being addressed for quite a long time now [1-5]. Another effective technique proposed is thermally coupled distillation column [6]. Unlike Petlyuk column dividing wall column (DWC) is a full thermally coupled single shell distillation column, which has the capability to separate more than three components with high purity. From the previous studies it has been proved that DWC can save operating and capital expenditure up to $30 - 40\%$ and reduce the space requirement by 40 % [7-10]. Remarkably, DWC is not limited to three component separations, but has been extended in azeotropic separations [11], extractive distillation [12], and reactive distillation [13]. DWC is very appealing to the chemical industry since its first industrial application way back in 1985 with BASF, Montz GmbH, and UOP as the leading companies.Dejanovic et al. [9] evaluated the patents and research articles published till the end of 2009. One of the most important thermally coupled columns is the fully thermally coupled distillation column or Petlyuk column. This type of distillation column consists of a prefractionator, coupled main column and two recycle streams. One recycle is liquid which is fed into the top of the prefractionator and other one which is vapor is injected into the bottom of the prefractionator. The petluyk column got transformed into divided wall column by inserting a longitudinal partition in the middle section of the column. Feed is introduced into the prefractionator. The distillate product is the lightest component, while the heaviest component is the bottom product. The side stream product is the intermediate boiling component. There are several benefits of DWC (1) low capital expenditure and reduce space, (2) Higher product purity, (3) high efficiency in term of thermodynamics due to less remixing effect. (4) less cost of maintenance. The dynamic control of the DWC has been explored in a pretty conservative way perhaps steered by the notion that control in DWC would be more difficult than with a traditional two-column separation process because of the additional interface of the four coupled column [14]. Only few control structure were applied for DWC, while many types of controllers are used for

binary distillation column [15]. In most industrial processes PID loops are used to propel the system to desired steady state and to satisfy the goal of dynamic optimization [16]. It might not be inappropriate to summarize here briefly the previous contributions regarding the control in DWC, which may put our present work in the proper perspective. There are four degrees of freedom available in a DWC reflux flow rate (R), vapor boilup (V), side-stream flow rate (S), and the liquid split ratio, which can be used as manipulated variable to achieve four control objectives. The purities of all the product streams should be controlled output variables. Wolff and Skogestad (1995) proposed both three and four point decentralized control in DWC separating ethanol/propanol/butanol ternary system [17]. The three-point structure controlled distillate purity by manipulating reflux flow rate, sidestream purity by manipulating sidestream flow rate and bottoms purity manipulating vapor boilup. In the four-point structure, they proposed an additional loop to control side stream impurity by manipulating the liquid split ratio. Mutalib and Smith [1998] and Mutalib et al. [1998] proposed a new approach to assess the complexity of DWC control by using degrees of freedom approach. [18,19]. They proposed a control scheme with two temperatures in the system with side stream as constant and invited censure. For controlling three compositions one must require at least three temperatures so it is not possible for this work to satisfy the material balance limitation [14]. Lately, inferential temperature control has been adapted instead of composition control in DWC to avoid the costly and high-maintenance prone composition analyzers. Adrian et al. (2004) [20] reported the experimental studies in BASE laboratory for butanol/pentanol/hexanol. They proposed three output controls by manipulating reflux flow rate, liquid split and side stream flow rate. For MPC controller they have used the reboiler heat duty as an extra input. Without the proper reason behind this distinction, their claim of improved control using MPC over PID was not convincing [14]. Wang et al. (2008) also suggested control of product purities using inferential temperature control in DWC [21]. Ling and Luyben, (2009) proposed the output variables as three product streams and one component in the prefractionator by manipulating liquid split, side stream flow rate, vapour boilup and reflux flow rate. Later they proposed four point inferential temperature and differential temperature composition control loops [22]. The simulation result revealed the inferential control structure provides effective product purity for the feed flow rate and feed composition disturbances. At the same time, there remains a trade-off between energy efficiency and controllability while using classical multiloop decentralize control strategy [23]. Application of DMC/MPC in DWC control started by then as evidenced in the open literature. Serra et al. (2001) studied three different system with different relative volatility using 33 tray column and 99 % purity [24]. They showed that PID provides better load disturbance than the dynamic matrix control structure [24]. Woinaroschy and Isopescu (2010) showed the ability of iterative dynamic programming to solve time optimal control of DWC [25]. Kvernland, et al. (2010) applied MPC only to a particular case of DWC, namely the Kaibel column to minimize the total impurity flow [26]. MPC obtained typically less total impurity flow as compared to conventional decentralized control while subjected to disturbance. Rewagad and Kiss (2012) implemented MPC strategy to BTX system in a DWC and claimed the better performance

of it compared to the performances of PID controllers within a multi-loop framework. Application of advanced control strategies like MPC/DMC in DWC reveals the lack of consistency in the system chosen, disturbances chosen, criterion of optimization etc., which hindered the conclusiveness of their merits over conventional decentralized multiloop control in DWC. Apart from this, the inherent limitations of MPC strategy could not promote the widespread application of MPC/DMC over multiloop PIDs' in DWC, which is regarded as a non-linear and complex system. PID controllers are prodigiously applied in the industries [27] because of the simple structure and effectiveness to implement. In process industries more than 95 % control loops are controlled by PID controllers [28]. In view of this, present work proposes the use of fractional PID controller in DWC adapting a suitable multiloop control structure. To our knowledge, this is perhaps the very first attempt in its kind.

$PI^{\lambda}D^{\mu}$ controller is gaining popularity because of its extra flexibility in terms of its extra two degrees of freedom over the conventional PID controllers, which can meet up additional control objectives. Recently, due to the enhanced understanding of three century old fractional calculus [29, 30], the implementation of fractional order controllers has become feasible. The fractional order PID (FOPID) controller was proposed [31], design and tuning of FOPID has been receiving growing attention. (Hamamci, 2007; Hwang, Leu, & Tsay, 2002b; Leu, Tsay, & Hwang, 2002; Li, Luo, & Chen, 2010; Luo, Chao, Di, & Chen, 2011a; Luo & Chen, 2009; Luo, Li& Chen, 2011b; Luo, Wang, Chen, & Pi, 2010; Monje, Vinagre, Feliu, & Chen, 2008). Some synthesis schemes for fractional order PID controllers in feedback control systems are presented in [32-36] and those results manifested the potential of the fractional order controller to improve both the stability and robustness of the feed-back control systems. For process control applications, FO controllers have been classified in four categories among which Podlubny's $PI^{\lambda}D^{\mu}$ for FOPID [31] and Oustaloup's CRONE controller [37] and its three generations [38-40] deserve special merit. The FO phase shaper [42-43] and FO lead lag compensator are also becoming popular for the robust control. A tuning methodology for fractional order PID controllers for controlling integer order systems have been discussed in [44,45]. An optimization based frequency domain tuning method for $PI^{\lambda}D^{\mu}$ controller has been proposed by Monje et al. [46] and Dorcak et al. [47]. Dominant pole placement tuning [48,49] techniques and time domain integral techniques [50-54] are used for time domain analysis. Zamani et al. [55] proposed optimization techniques using different objective like the different characteristics of controller, Integral of absolute error (IAE), squared control signal and inverse of gain and phase margin. But there is no trade off among the objectives. Padula and Visioli [56] discussed tuning of fractional order PID using IAE minimization technique with the constraints on sensitivity. Robustness and performance can be considered as objective functions with respect to the controller parameters in optimization problem. There remains a trade-off between robustness and performance, hence, this problem can be formulated as a multiobjective optimization problem (MOP) so that the trade-off between objectives can be found consequently. Very few literature have considered the FOPID tuning with multiobjective functions. Hajiloo et al, (2012) presented multiobjective design of controllers considering

both time and frequency domain metrics as objective functions [57]. The trade-offs among design objectives were put forward using the optimal Pareto frontiers. Damarla and Kundu (2015) proposed a robust and simple technique for tuning various versions of fractional PID controllers using triangular strip operational matrix based optimal controller design [58].

Mamy methodologies have been developed for the plant wide control of chemical process. The plant wide process can be subdivided into four groups, namely process oriented (heuristics), mathematical model oriented, mixed approach, optimization approach. In heuristics approach, Govind and Power [59] proposed non-numerical and systematic procedure for simple systems to generate alternative structure. Luyben et al. [60] proposed a very effective plant wide control for entire complex plant. Knoda et al. [61] proposed an integrated framework of simulation and process oriented procedure. In optimization technique approach, Morari et al. [62] attempted the first method for self-optimizing technique. Zheng et. al [63] and Zhu et al. [64] proposed plant wide control for large scale chemical plants. In mathematical model approach, steady state and dynamic model are considered together with different tools such as relative gain array (RGA), singular value decomposition (SVD), Hankel singular value (HSV). Cao et al. [65] attempted mathematical model to calculate the best choice of manipulated variables. Groenendijk et al. [66] and Dimian et al. [67] proposed a methodology based on steady state analysis (SVD, RGA, NI) and dynamic simulation (close loop disturbance gain, performance RGA). In the mixed approach, Vasbinder and Hoo [68] presented a decision based approach, where one plant is converted in to smaller modified analytical process. Dorneanu et al. [69] proposed the model order reduction technique for decomposing the plant in to small controlled units. Panahi and Skogestad [70] proposed the plant wide control for economical efficient of CO2 capturing process plant.

Most of the process industries are multi-input-multi-output system(MIMO). MIMO systems are difficult to tune because the presence of interaction between the input and output variables. Adjusting parameters in one loop can change the performance of other loops and there might be a possibility of destabilize the system. Due to lack of proper control tuning process for MIMO system causes higher energy cost and insufficient operation. There are different methods available for the MIMO process tuning such as detuning method, sequential loop closing method, independent design method. The other approach is to design a decoupler with decentralized control system. There are different kinds of decoupler techniques are available but for higher order processes the design of decoupler is difficult. Recently researchers have been introduced the very effective equivalent transfer function (ETF) model to take into account the loop interaction in design of MIMO system. To obtain the effective transfer function model M.J.He et al. [74] derived the multiplicative model factor(MMF) for individual loop and the ETF model can be derive by the multiplication of MMF and original loop transfer function. ETF can be derived from the effective relative gain array (ERGA), relative normalized gain array (RNGA) and effective relative energy array (EREA). Xiong et al. [75] proposed ETF model by the use of ERGA. While Shen et

al. [76]derived the ETF model by using both the steady state and transient information by the RNGA matrix and then decoupler is derived. Cai et al. [77] formulated the ETF model by the use of RGA, RNGA, and relative average residence time array (RARTA). He used the ETF model instead of inverse of the process for the design of normalized decoupler technique. But this model is only applicable for first order plus delay system with two output process. Rajapandiyan et al. [78] combined the simplified decoupler approach with the ETF model approximation. The main advantage of this process is the decoupler design is not complex and model reduction steps are not required. But it is only used for the first order plus delay system. Recently Xiaoli et al. [79] proposed the more accurate ETF model by the direct analytical method. For the higher order plant system, the derivation of analytical expression is really complex and it does not guarantee the stability of the derived ETF model.

1.2 Aim and Scope

In view of this, present dissertation aims for the following objective
- Design and implementation of fractional order PID controllers in processes/plant-wide process. To ensure the aforesaid objectives following scopes are laid.

1. Design and implementation of fractional order controllers in DWC process
2. Plant-wide control in HDA process using fractional order controllers.

1.3 Organization of thesis

First chapter of the thesis provides a brief introduction on fractional controller, dividing wall column and HDA plant. The objective of thesis with chapter layout is also presented in this chapter. The second chapter involves study of different optimization techniques, equivalent transfer function model. The steady state & dynamic simulation, and result & discussion of the dividing wall column have been included in the third chapter. Fourth chapter presents the plant wide control of the HDA plant. The fifth chapter concludes the thesis describing the future scope of fractional controller design in various chemical process industries.

Chapter 2

Mathematical Postulates and Algorithms

2.1 Fractional Calculus

The derivative and integration of the non-integer systems are studied in fractional order calculus. There are different definitions of fractional order calculus. These definitions of fractional order calculus are discussed below.

2.1.1 Definition of fractional order calculus

Definition 2.1 *(Cauchy's Fractional order calculus)* [71]
This is the extension of the integer order Cauchy formula.

$$D^{\gamma} f(t) = \frac{\Gamma(\gamma+1)}{2\pi j} \int_c \frac{f(\tau)}{(\tau - t)^{\gamma+1}} \tag{2.1}$$

Where c is the smooth curve.

The generalization of fractional order differential and integral operator is denoted as ${}_aD_t^q$, which is defined as

$${}_aD_t^q = \begin{cases} \frac{d^q}{dt^q}, & R(q) > 0, \\ 1, & R(q) = 0, \\ \int_a^t (d\tau)^{-q}, & R(q) < 0, \end{cases} \tag{2.2}$$

where q is the fractional order commensurate which could be a complex number. There are two commonly used theory for fractional order differentiation and integration. Which are described below.

Definition 2.2 *(Grunwald- Letnikov definition)* [72]

$${}_aD_t^q f(t) = \lim_{x \to 0} \frac{1}{h^q} \sum_{j=0}^{[(t-q)/h]} (-1)^j \binom{q}{x} f(t - jh), \tag{2.3}$$

Definition 2.3 *(Riemann-Liouville definition)* [73]

$$ {}_aD_t^q f(t) = \frac{1}{\Gamma(n-q)} \frac{d^n}{dt^n} \int_a^t \frac{f(\tau)}{(t-\tau)^{q-n+1}} d\tau, (n-1 < q < n) \tag{2.4} $$

2.1.2 Integer order approximation of Fractional order system

The fractional order liner time invariant (LTI) system is mathematically equivalent to the interger order LTI filer. The fractional order system can be approximated as the higher integer order operator. There are two different ways to approximate the fractional order system.

1. Continuous time realization
2. Discrete time realization

Here we have used the continuous time realization approximation by using crone controller [37]. The crone approximation produces poles and zeroes. The approximated unit gain matrix of N^{th} order is given by

$$ S^{\alpha} \cong \prod_{n=1}^{N} \frac{1 + \frac{s}{\omega_{z,n}}}{1 + \frac{s}{\omega_{p,n}}} \tag{2.5} $$

The formula is valid with in a frequency range $[\ \omega_l, \omega_h]$.

2.2 Equivalent transfer function (ETF) model

For our problem we have combined the simplified decoupler approach with the ETF model derived by Xiong et al. [75]. As our HDA process is approximated as second order model, the require ETF model can be derived by only the use of dynamic relative gain.

2.2.1 Derivation of ETF model

Consider a open loop stable MIMO system with n inputs and n outputs where r_i, e_i, u_i, y_i, $i = 1, 2....., n$ are the reference inputs, errors, manipulated variables and system outputs. The process transfer function is expressed by

$$ \begin{bmatrix} \mathrm{g}_{11}(s) & \mathrm{g}_{12}(s) & \dots & \mathrm{g}_{1n}(s) \\ \mathrm{g}_{21}(s) & \mathrm{g}_{22}(s) & \dots & \mathrm{g}_{2n}(s) \\ \vdots & \vdots & \ddots & \vdots \\ \mathrm{g}_{n1}(s) & \mathrm{g}_{n2}(s) & \dots & \mathrm{g}_{nn}(s) \end{bmatrix} \tag{2.6} $$

and the decentralized controller is expressed as

$$ \begin{bmatrix} \mathrm{g}_{c1}(s) & 0 & \dots & 0 \\ 0 & \mathrm{g}_{c2}(s) & \dots & 0 \\ \vdots & \vdots & \ddots & \vdots \\ 0 & 0 & \dots & \mathrm{g}_{cn}(s) \end{bmatrix} \tag{2.7} $$

Let us consider each element of the transfer function is second order model. Most of the industrial process can be approximated as the second order process.

$$\mathrm{g}_{ij}(s) = \frac{\mathrm{g}_{ij}(0)(a_{3,ij}s+1)}{a_{2,ij}s^2 + a_{1,ij}s + 1} \tag{2.8}$$

The definition of the dynamic relative gain array (DRGA) is [80]

$$\lambda_{ij}(s) = \frac{[\int_0^{\omega_{c,ij}} (\partial y_i/\partial u_j) d\omega]_{\text{all loops open}}}{[\int_0^{\omega_{c,ij}} (\partial y_i/\partial u_j) d\omega]_{\text{all other loops closed expect for loop } y_i - u_j}} = \frac{\mathrm{g}_{ij}(s)}{\hat{\mathrm{g}}_{ij}(s)} \tag{2.9}$$

where $\hat{\mathrm{g}}_{ij}(s)$ is the ETF of $\mathrm{g}_{ij}(s)$ when all other loops are closed. The DGRA can be written in matrix form for the system,

$$\Lambda = \begin{bmatrix} \lambda_{11}(s) & \lambda_{12}(s) & \dots & \lambda_{1n}(s) \\ \lambda_{21}(s) & \lambda_{22}(s) & \dots & \lambda_{2n}(s) \\ \vdots & \vdots & \ddots & \vdots \\ \lambda_{n1}(s) & \lambda_{n2}(s) & \dots & \lambda_{nn}(s) \end{bmatrix} \tag{2.10}$$

by substituting Eq. 2.9 in 2.10 gives,

$$\Lambda = \begin{bmatrix} \mathrm{g}_{11}(s)/\hat{\mathrm{g}}_{11}(s) & \mathrm{g}_{12}(s)/\hat{\mathrm{g}}_{12}(s) & \dots & \mathrm{g}_{1n}(s)/\hat{\mathrm{g}}_{1n}(s) \\ \mathrm{g}_{21}(s)/\hat{\mathrm{g}_{11}}(s) & \mathrm{g}_{22}(s)/\hat{\mathrm{g}}_{22}(s) & \dots & \mathrm{g}_{2n}(s)/\hat{\mathrm{g}}_{2n}(s) \\ \vdots & \vdots & \ddots & \vdots \\ \mathrm{g}_{n1}(s)/\hat{\mathrm{g}}_{n1}(s) & \mathrm{g}_{n2}(s)/\hat{\mathrm{g}}_{n2}(s) & \dots & \mathrm{g}_{nn}(s)/\hat{\mathrm{g}}_{11}(s) \end{bmatrix} \tag{2.11}$$

Under the assumption of perfect control, the $\Lambda(s)$ can be obtained by [81]

$$\Lambda(s) = \begin{bmatrix} \mathrm{g}_{11}(s) & \mathrm{g}_{12}(s) & \dots & \mathrm{g}_{1n}(s) \\ \mathrm{g}_{21}(s) & \mathrm{g}_{22}(s) & \dots & \mathrm{g}_{2n}(s) \\ \vdots & \vdots & \ddots & \vdots \\ \mathrm{g}_{n1}(s) & \mathrm{g}_{n2}(s) & \dots & \mathrm{g}_{nn}(s) \end{bmatrix} \otimes \begin{bmatrix} \mathrm{g}_{11}(s) & \mathrm{g}_{12}(s) & \dots & \mathrm{g}_{1n}(s) \\ \mathrm{g}_{21}(s) & \mathrm{g}_{22}(s) & \dots & \mathrm{g}_{2n}(s) \\ \vdots & \vdots & \ddots & \vdots \\ \mathrm{g}_{n1}(s) & \mathrm{g}_{n2}(s) & \dots & \mathrm{g}_{nn}(s) \end{bmatrix}^{-T} \tag{2.12}$$

By comparing Eq 2.11 and 2.12, we obtain

$$G^{-T} = \begin{bmatrix} \mathrm{g}_{11}(s) & \mathrm{g}_{12}(s) & \dots & \mathrm{g}_{1n}(s) \\ \mathrm{g}_{21}(s) & \mathrm{g}_{22}(s) & \dots & \mathrm{g}_{2n}(s) \\ \vdots & \vdots & \ddots & \vdots \\ \mathrm{g}_{n1}(s) & \mathrm{g}_{n2}(s) & \dots & \mathrm{g}_{nn}(s) \end{bmatrix}^{-T} = \begin{bmatrix} 1/\hat{\mathrm{g}}_{11}(s) & 1/\hat{\mathrm{g}}_{12}(s) & \dots & 1/\hat{\mathrm{g}}_{1n}(s) \\ 1/\hat{\mathrm{g}}_{21}(s) & 1/\hat{\mathrm{g}}_{22}(s) & \dots & 1/\hat{\mathrm{g}}_{2n}(s) \\ \vdots & \vdots & \ddots & \vdots \\ 1/\hat{\mathrm{g}}_{n1}(s) & 1/\hat{\mathrm{g}}_{n2}(s) & \dots & 1/\hat{\mathrm{g}}_{nn}(s) \end{bmatrix} \tag{2.13}$$

It implies from Eq 2.13,

$$G^{-1}(s) = \begin{bmatrix} 1/\hat{g}_{11}(s) & 1/\hat{g}_{21}(s) & \dots & 1/\hat{g}_{n1}(s) \\ 1/\hat{g}_{12}(s) & 1/\hat{g}_{22}(s) & \dots & 1/\hat{g}_{n2}(s) \\ \vdots & \vdots & \ddots & \vdots \\ 1/\hat{g}_{1n}(s) & 1/\hat{g}_{2n}(s) & \dots & 1/\hat{g}_{nn}(s) \end{bmatrix} \tag{2.14}$$

or equivalently

$$G(s)\hat{G}^T = I \tag{2.15}$$

From Eq 2.11, we can write

$$\hat{g}_{ij}(0) = \frac{g_{ij}(0)}{\lambda_{ij}} \tag{2.16}$$

The values of λ_{ij} can be easily obtained by using Eqn 2.12 at $s = 0$. The $g_{ij}(s)$ can be written as

$$g_{ij}(s) = g_{ij}(0)g^0_{ij}(s) \tag{2.17}$$

, where $g_{ij}(0)$ is the steady state gain and $g^0_{ij}(s)$ is the normalized transfer function of $g_{ij}(s)$. ($g^0_{ij}(0) = 1$). The equivalent transfer function has same structure as the open loop transfer function. The ETF can be written as

$$\hat{g}_{ij}(s) = \hat{g}_{ij}(0)g^0_{ij}(s) \tag{2.18}$$

. The $\hat{g}_{ij}(0)$ denotes the gain change.

2.2.2 Simplified decoupler design using ETF model

There are three types of basic decoupler techniques available, which are ideal, simplified, and inverted decoupler. The decoupler($G_d(s)$) is placed between the decentralized controller ($G_C(s)$) and the process ($G(s)$). The decoupled transfer function becomes

$$G_R = G(s)G_d(s) \tag{2.19}$$

so the diagonal matrix can be written as

$$G_d(s) = G^{-1}(s)G_R(s) \tag{2.20}$$

By substituting Eq 2.14 in Eq 2.20,

$$G_d(s) = \hat{G}^T(s)G_R(s) \tag{2.21}$$

The simplified decoupler form and the decoupled transfer function can be expressed as

$$G_d(s) = \begin{bmatrix} 1 & \mathrm{g}_{d,12}(s) & \dots & \mathrm{g}_{d,1n}(s) \\ \mathrm{g}_{d,21}(s) & 1 & \dots & \mathrm{g}_{d,2n}(s) \\ \vdots & \vdots & \ddots & \vdots \\ \mathrm{g}_{d,n1}(s) & \mathrm{g}_{d,n2}(s) & \dots & 1 \end{bmatrix}, G_R(s) = \begin{bmatrix} \mathrm{g}_{R,11}(s) & 0 & \dots & 0 \\ 0 & \mathrm{g}_{R,22}(s) & \dots & 0 \\ \vdots & \vdots & \ddots & \vdots \\ 0 & 0 & \dots & \mathrm{g}_{R,nn}(s) \end{bmatrix} \tag{2.22}$$

In order to satisfy the Eq 2.21, the diagonal elements of the decoupled transfer matrix should be same as the corresponding diagonal elements of the equivalent transfer function matrix and decoupler matrix $G_d(s)$ is

$$G_d(s) = \begin{bmatrix} 1 & \mathrm{g}_{d,12}(s) & \dots & \mathrm{g}_{d,1n}(s) \\ \mathrm{g}_{d,21}(s) & 1 & \dots & \mathrm{g}_{d,2n}(s) \\ \vdots & \vdots & \ddots & \vdots \\ \mathrm{g}_{d,n1}(s) & \mathrm{g}_{d,n2}(s) & \dots & 1 \end{bmatrix} = \begin{bmatrix} 1 & \hat{\mathrm{g}}_{22}(s)/\hat{\mathrm{g}}_{12}(s) & \dots & \hat{\mathrm{g}}_{nn}(s)/\hat{\mathrm{g}}_{1n}(s) \\ \hat{\mathrm{g}}_{11}(s)/\hat{\mathrm{g}}_{21}(s) & 1 & \dots & \hat{\mathrm{g}}_{nn}(s)/\hat{\mathrm{g}}_{2n}(s) \\ \vdots & \vdots & \ddots & \vdots \\ \hat{\mathrm{g}}_{11}(s)/\hat{\mathrm{g}}_{n1}(s) & \hat{\mathrm{g}}_{22}(s)/\hat{\mathrm{g}}_{n2}(s) & \dots & 1 \end{bmatrix} \tag{2.23}$$

2.3 ev-MOGA optimization technique

The control structure for fractional order PID is

$$C(s) = K_p + \frac{K_i}{s^\lambda} + \frac{K_d}{s^\mu}$$

The control parameters to be tuned are $k = [K_p, K_i, K_d, \lambda, \mu]$ .The controller parameters can be obtained by minimizing the objective functions. In our problem the control objectives (J_1, J_2) are described in the previous section. The multi objective (MO) problem can be defined by equation 2.24.

$$\min_{k \in D \in R_5} J(k) = \min_{k \in D \in R_5} [J_1(k), J_2(k)], \tag{2.24}$$

Where $J_i \; i \in B := [1, 2]$ are the objective functions and k is the solution inside the 5-dimensional solution space D.

To solve the MO problem the Pareto Optimal set must be found. In this Pareto optimal set (K_P) one solutions does not dominate others. The Pareto optimal set (K_P) is unique and it includes infinite number of solutions. Hence a set of finite element number of solutions (K_P^*) is obtained from the(K_P). To obtain the K_P^* , we have used the ev-MOGA optimization technique [82]. This algorithm is described in the section below. From the Pareto optimal set K_P^* a unique solution k^* can be selected for the controller tuning as per the choice of the decision maker. The Pareto optimal points are non- dominated, so choosing any k^* will make the process optimal.

The ev-MOGA is an elitist multi objective evolutionary algorithm which is based on the concept of $\in$-dominance.The $\in$-Pareto set, (K_P^*), converges in a distributed manner around Pareto front $J(\theta)$ towards the Pareto optimal set (K_P). It also takes care of the solutions

which can be lost to the end of the front. The objective space is divided in to fixed number of boxes (n_box_i) for each dimension i. Each box contains only one solution. So it restricts the algorithm to converge to one point or area. There are three types of populations.

1. Main population P (t) explores the searching space (D) during the iteration. (Size-$Nind_P$)
2. Archive A (t) stores the solution (K_P^*). (Size- $Nind_A$)
3. Auxiliary population G (t). It must be an even number. (Size-$Nind_G$).

The size of A can never be higher than

$$N\_ind_max_A = \frac{\prod_{i=1}^{s}(n\_box_i + 1)}{n\_box_{max} + 1} \tag{2.25}$$

Where $n\_box_{max} = max[n\_box_1, ...n\_box_s]$. The individuals from the A (t) consists ofK_P^*. The main steps of the algorithm are described below.

1. The main population (P) is initialized at time t=0 and with the size of $Nind_P$.
2. From the search space D, the solutions are randomly selected.
3. The functional value of J(k) is computed for each individual in P(t).
4. Non dominated P(t) are detected and the maximum and minimum limits of J_i are calculated from J(k). The detected individuals are analysed and it is included in A(t) if those are not $\in$-dominated by individuals in A(t).
5. For each iteration the individuals of G(t) are created using extended linear recombination technique and random mutation with Gaussian distribution.
6. The functional value of J(k) is computed for each individuals in G(t)
7. The individuals of G(t) are included in A(t) on the basis of location in the objective space. And the Individuals from A(t) which are will be eliminated if it is $\in$- dominated by individuals of G(t)
8. P(t) is updated with individuals from G(t), if there are individuals in P(t) dominated by individuals of G(t). Finally the individuals of A(t) gives the solution K_P^*.

2.4 Cuckoo search method

The basic cuckoo search is a nature inspired metaheuristic algorithm [83] based on the natural obligate brood parasitic behavior of some cuckoo species in combination with the Lévy flight behaviour of some birds and fruit flies. Cuckoos are fascinating bird because of their beautiful sounds and aggressive reproduction strategy. Cuckoos do not lay their eggs in their own nest but in the nest of other host birds. They have the tendency to destroy the eggs of the other host bird so the possibility of the hatching of their own eggs increase. Cuckoo chicks mimics the voice of the host bird so that the chances of feeding and survival increases. If the host bird find out the truth about the cuckoo egg, they either destroy the egg or abandon the nest and build new nest somewhere. Various studies reveals that the many of animals and

insects have the characteristics of Lévy flight. Cuckoo search method follows three simple rules (1) Each cuckoo chooses a random nest and lays one egg at a time and dumps its egg (2) The eggs form the best nest will be carried out for the next generation. (3) The available nests are fixed and the probability of the host bird finds the truth is $p_a \epsilon [01]$. The pseudo code for CS algorithm [83] is:

1. Define the Objective function $f(x), x = (x_1, x_2 ... x_n)^T$
2. Generate initial population of n host nests $x_i (i = 1, 2 ... n)$
3. While (t<Max Generations) or (stop criterion)
4. Move a cuckoo randomly via Lévy flights
5. Evaluate its fitness Fi
6. Randomly choose nest among n available nests (for example j)
7. If $(Fi > Fj)$ Replace j by the new solution; Fraction Pa of worse nests is abandoned and new nests are being built;
8. Keep the best solutions or nests with quality solutions;
9. Rank the solutions and find the current best
10. Post process and visualize results

Chapter 3

Control of Dividing Wall Distillation Column

3.1 Steady state simulation

For accurate simulation of the process all the design and optimum parameters are required. The optimized value of all designed parameters must be found out such that the process and optimum cost must be low. To get the optimized value we have to take the help of steady state simulation. Steady state model performs the mass and energy balance in stationary condition. A benzene-toluene-xylene system is studied for the divided wall distillation column. The boiling point for these components are 353K, 383Kand 419K respectively. The relative volatility of these components are 7.1, 2.2 and 1 respectively. Using DWC the feed stream is separated in to three product streams. In which benzene is the top product, xylene in the bottom product and toluene in the side product. For simulating the divided wall column we have used Aspen plus software. We have used four column divided wall column model. In DWC, a single column is separated into 4 columns by inserting a wall in it. The left section is known as Prefractionator column, the top section as rectifying column, the bottom section as stripping column and the right section as side column. Feed composition is 30 mol % benzene, 30 mol% toluene and 40 mol% xylene. The feed is introduced in to 12th stage of the prefractionator. In our simulation we have used 24 trays for the prefractionator (without reboiler and condenser), 9 trays for the rectifying column (with condenser and no reboiler), 13 trays for the stripping column (with a rebolier and no condenser) and 24 trays for the side column (without reboiler and condenser). In the rectifying column the condenser is at 1 atm and the condenser pressure drop is 0.068 atm. In all other columns the stage 1 is at 1 atm and the stage pressure drop is 0.05 bar. The split fraction for liquid and vapor are 0.55 and 0.43 respectively. The values of all feed composition, feed flow rate, number of stages etc. are referred from Ling and Luyben [22].

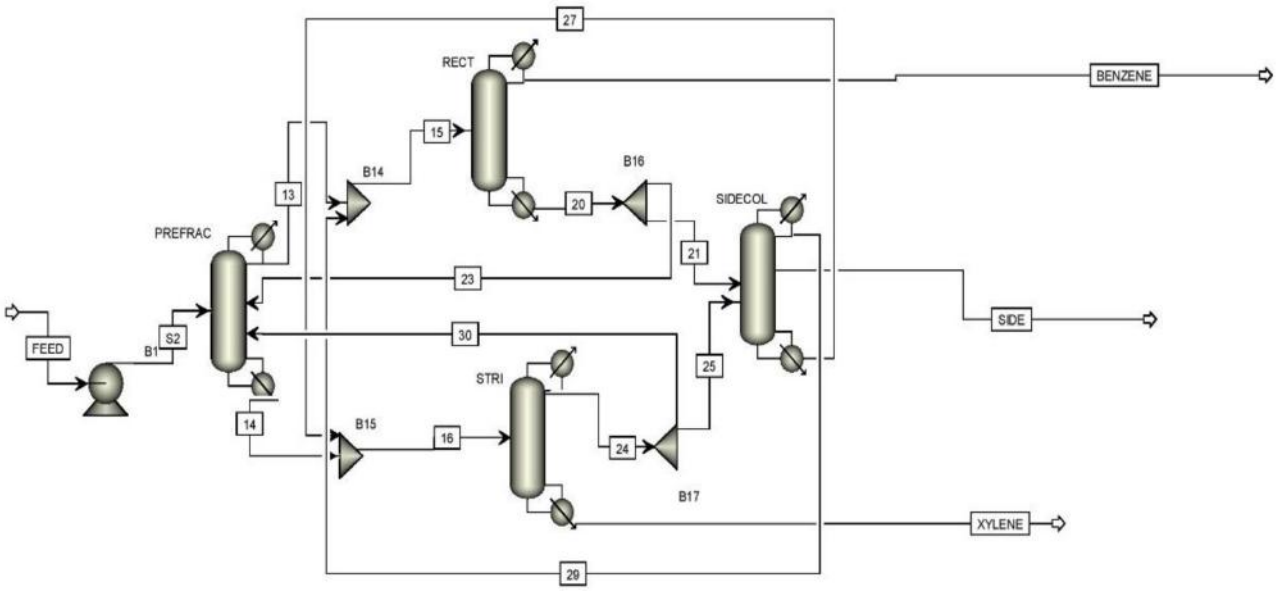

Figure 3.1: Flow Sheet

The temperature profile is shown in figure 2. As from the figure we can conclude that the bottom trays are at high temperature because the heavy components are accumulating in the bottom trays. The tray temperature varies from 80 to 116 for the rectification column, 115 to 163 for stripping column, 105 to 145 for prefractionator and 104 to 143 for side column. The composition profile is shown in figure 3. In the rectifying column the benzene is the top product with 99% purity. In the side column the toluene purity is 99.9912% and in the bottom column the o-xylene purity is 99.29%.

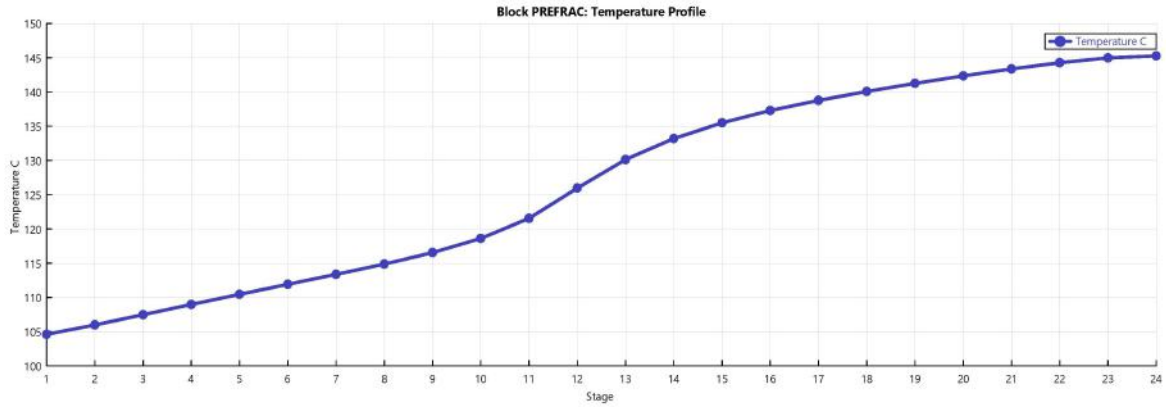

(a)

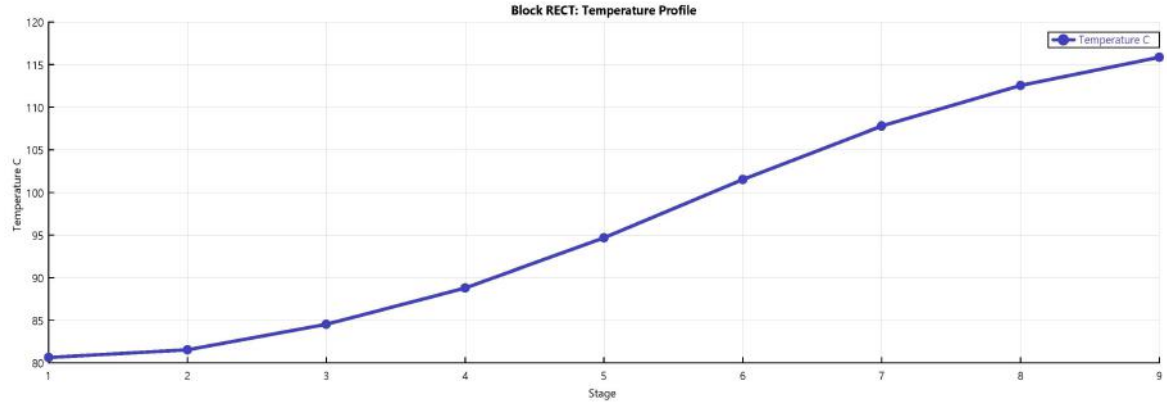

(b)

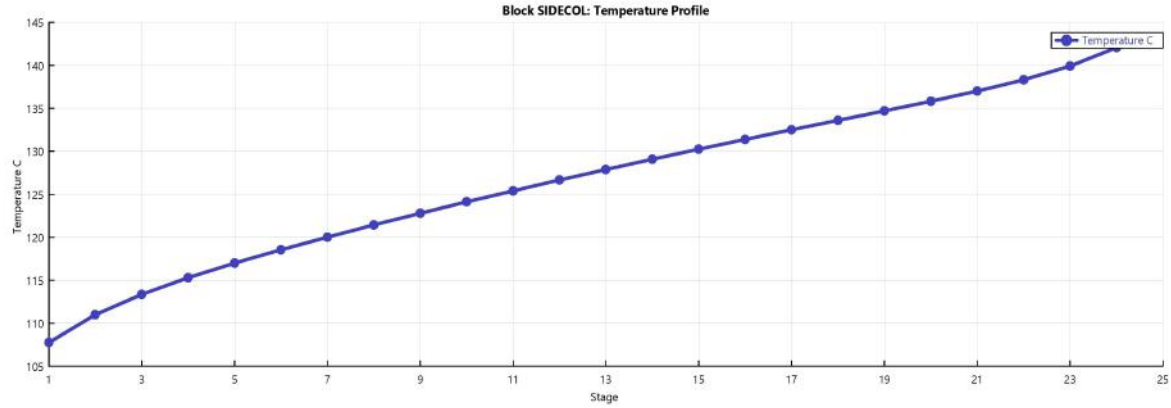

(c)

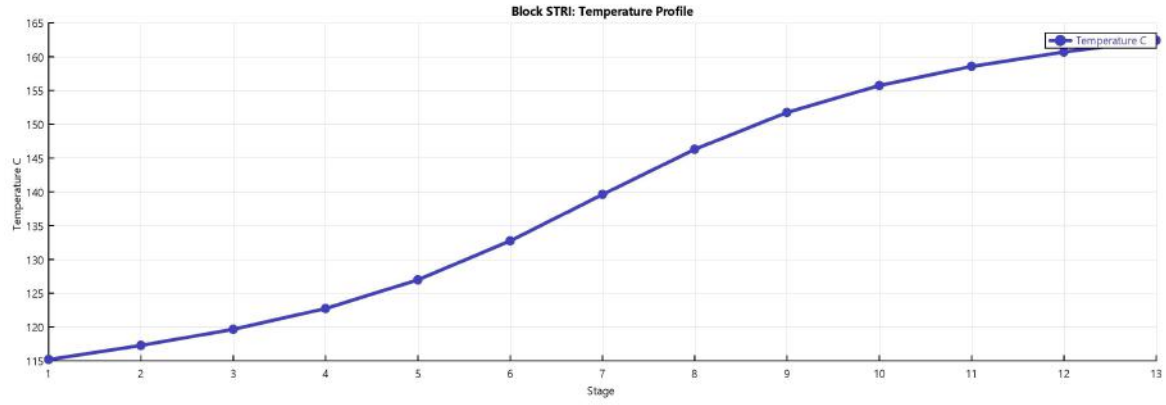

(d)

Figure 3.2: Temperature profile in divided wall column

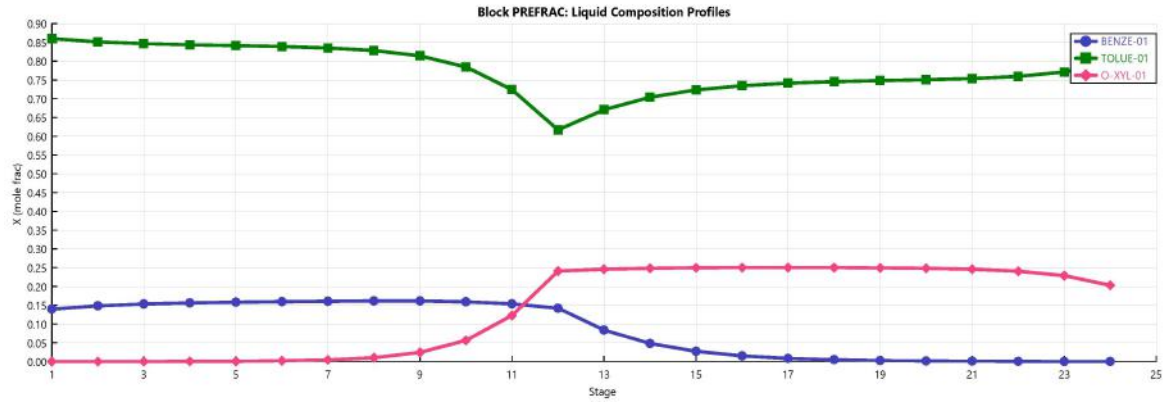

(a)

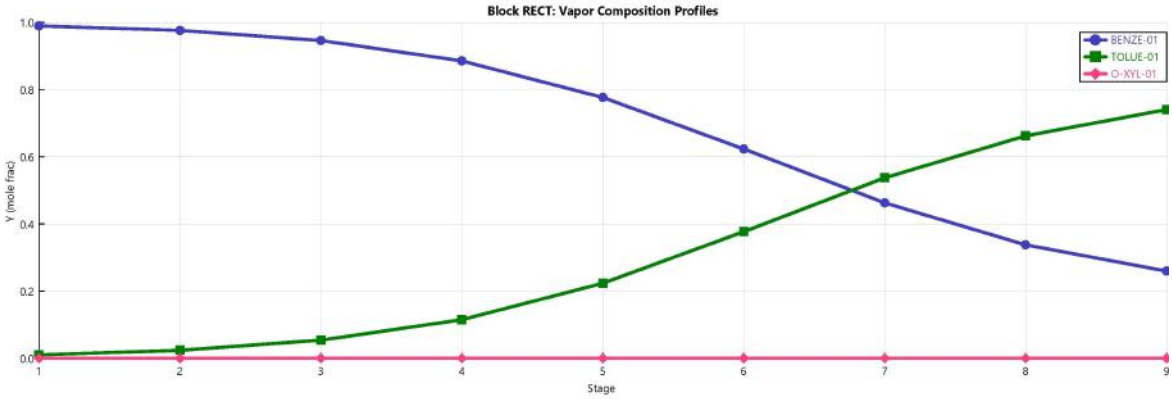

(b)

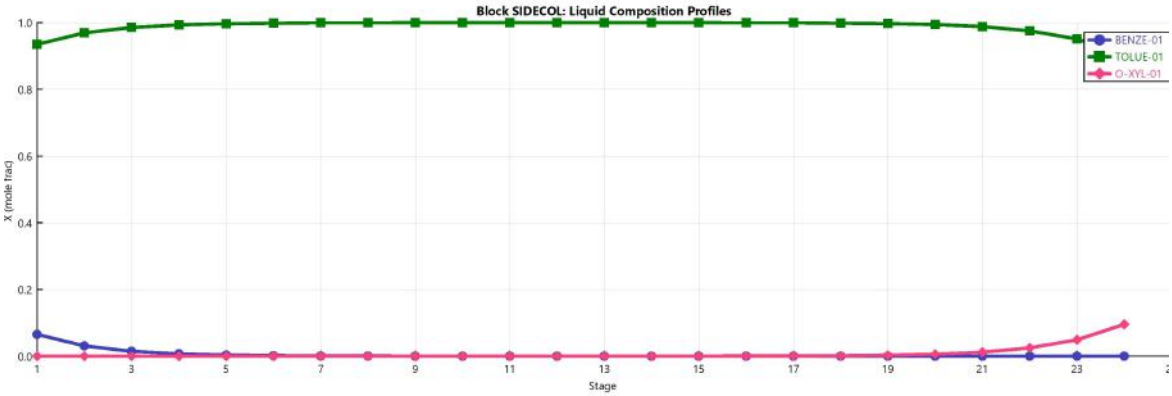

(c)

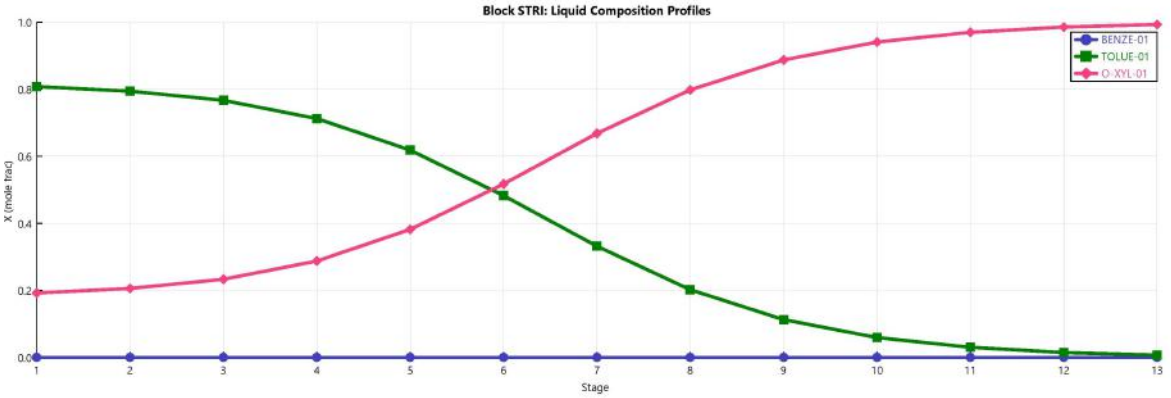

(d)

Figure 3.3: Composition profile in divided wall column

3.2 Dynamic Simulation

The dynamic simulation is performed in Aspen plus dynamics. The steady-state model is imported to Aspen Plus Dynamics (APD) for a flow-driven simulation. This neglects actuator dynamics and assumes accurate regulation of manipulated flow rates. By default the aspen plus dynamics add PI controller for pressure, liquid level controls and temperature. But for our case it was intentionally removed. For dynamic simulation the tray hydraulics, tower sump geometry, and the reflux drum size is specified. For all the columns the tray spacing is used as 0.6096 meter and weir height as 0.05 meter. Aspen Plus Dynamics provides a features to linearizes a dynamic model at a specified condition. This linearization is done by the control design interface tool (CDI). For the dynamic system input variables have been considered as:

1. Rebolier duty(QRebR)
2. Condenser duty(Qr)
3. Side draw flow(FR)
4. Feed flow rate

Three product specification should be used as control variables. Since online analyser is very difficult to implement for the analysis of product composition. So it is desirable to use tray temperature instead of composition. The output variables are:

1. Last tray temperature in the rectifying column.
2. 11^{th} tray temperature in the main column.
3. Bottom tray temperature of the stripping column

First the script file is created in the Aspen plus dynamics and this file contains all the information of input and output variable. The model is initialized in the steady state nominal steady state condition. After invoking the script file we have generated the A, B, and C matrices of the standard continuous-time LTI state-space model along with the list of model variables, nominal values and the gain matrices. All these generated matrices are sparse matrices. By using MATLAB the state space matrices are converted into state space model. The original model has 282 number of states. In this process we have scaled our plant model. The scaled plant model is used for both model reduction and controller design. For the scaling we have defined a span for each output and input. The span is the expected difference between the maximum and minimum value. The nominal conditions from engineering units have been converted in to the percentage.

3.2.1 Model order reduction

The number of states for the process is very high. So the model order reduction technique is used to reduce the complexity of the large scale complex problems. In this technique the input-output relation can be reproduced with negligible error and acceptable time. The goals of the model order reduction is the output of lagre order system can be approximated by the

reduced order, so that it can be evaluated significantly as well as the physical property of the reduced order should be preserved. The Hankel singular value plot 4.2 suggests that there are four dominant states in this system. However, the contribution of the remaining states are still significant. So we have discarded the remaining states to find a 4^{th} oder reduced model. The approximate error can be visualized by two different ways.

1. Step response
2. Singular value plot

Figure 3.5 shows the step responses of the input variables of the original order model is compared with the reduced order model. It can be seen that the step change in rebolier heat duty and condenser heat duty are nearly same for the original and the reduced model. But for the step change in the side stream flow rate and the feed flow rate the reduced model is slightly different than the original one. But the error is very less. The figure 3.6 shows the singular value (SV) plot of the frequency response of both the reduced and the original system. The singular values of the frequency response extend the Bode magnitude response for MIMO systems.The singular value response of a SISO system is identical to its Bode magnitude response. It can be observed that the reduction error is less compared to the original system. So the reduced model provides the better approximation to the original model.

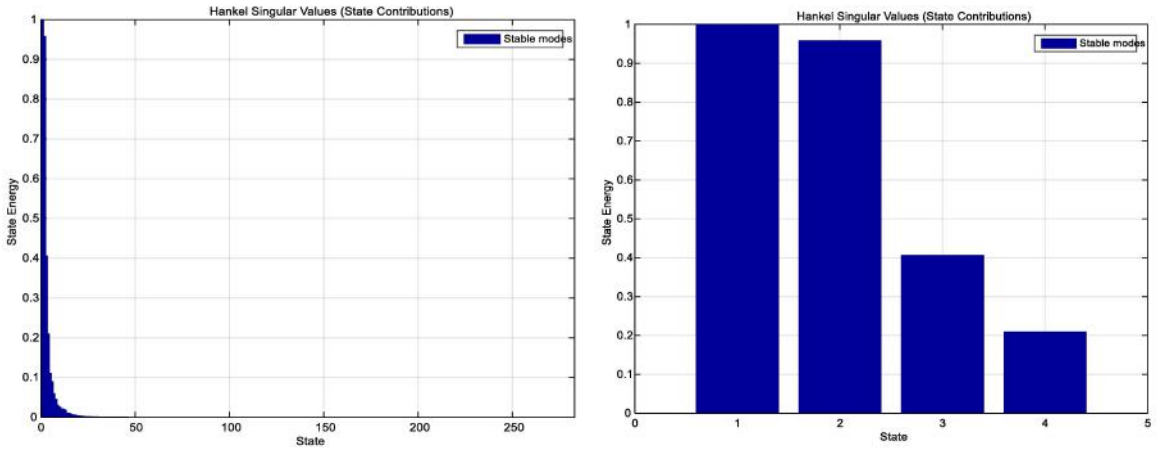

(a) (b)

Figure 3.4: (a)Hankel Singukar Value, (b)Reduced Hankel singular value

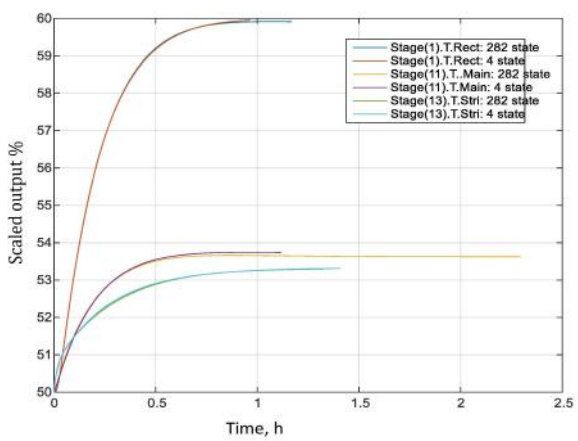

(a) Step change on rebolier duty

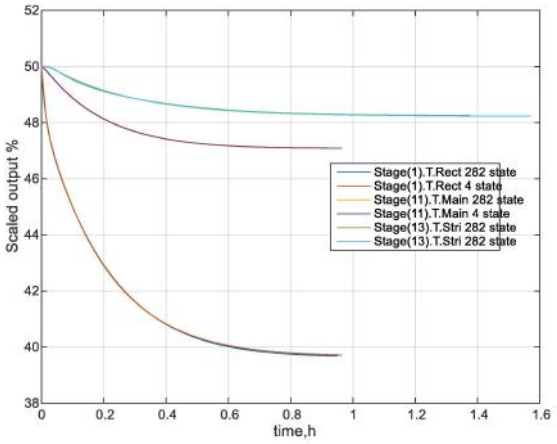

(b) Step change on condenser duty

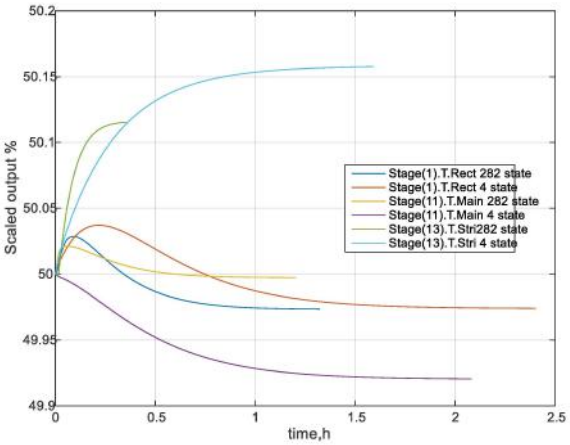

(c) Step change on side stream flow rate

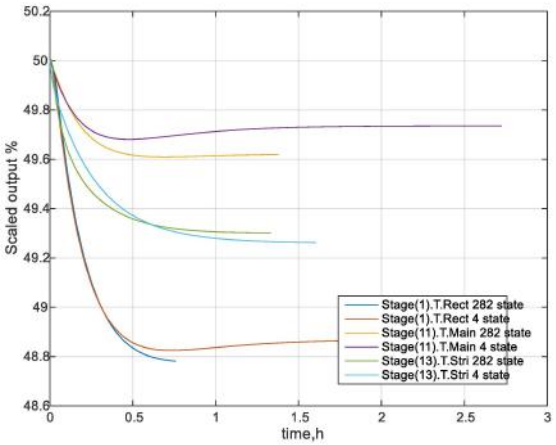

(d) Step change on feed flow rate

Figure 3.5: Step Response of inputs

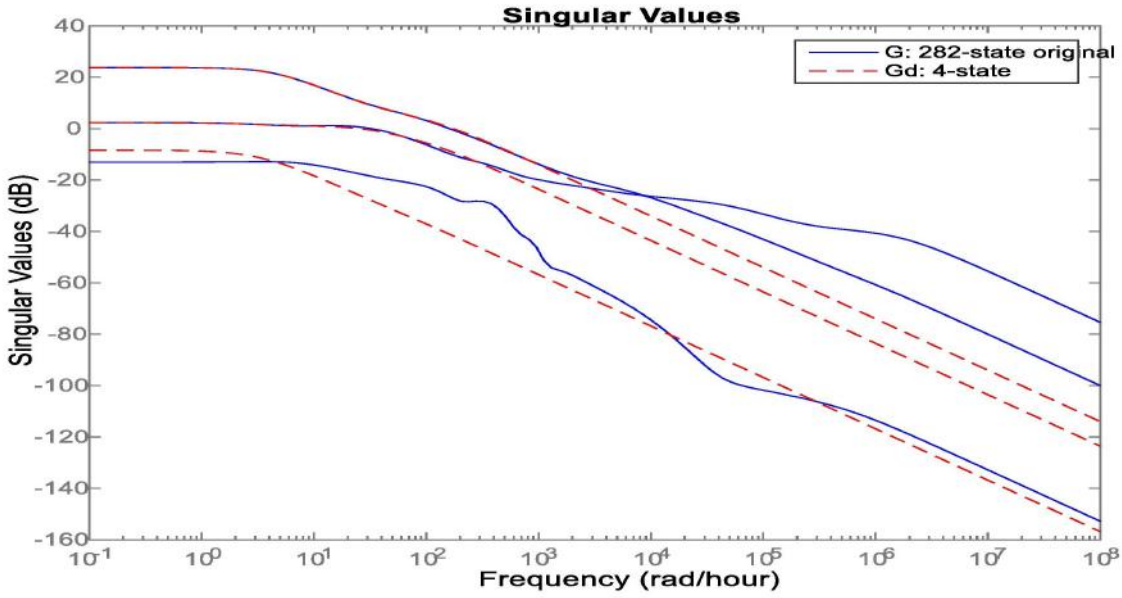

Figure 3.6: Singular value

Table 3.1: Transfer Function Matrix

	Condenser heat duty	Rebolier heat duty	Side draw flow	Feed flow rate
Stage(1).T.Rect	$\frac{-199.2s^3-2.5e04s^2-5.9e05-1.3e06}{s^4+209.6s^3+1.1e04s^2+7.5e04s+1.3e05}$	$\frac{-2.731s^3-258s^2+4.695e05s+1.35e06}{s^4+209.6s^3+1.1e04s^2+7.5e04s+1.3e05}$	$\frac{0.8937s^3+89.56s^2+4190s-3534}{s^4+209.6s^3+1.1e04s^2+7.5e04s+1.3e05}$	$\frac{0.7152s^3-180.3s^2-6.602e04s-1.534e05}{s^4+209.6s^3+1.1e04s^2+7.5e04s+1.3e05}$
Stage(11).T.Main	$\frac{-2.63s^3-2058s^2-1.489e05s-3.914e05}{s^4+209.6s^3+1.1e04s^2+7.5e04s+1.3e05}$	$\frac{10.37s^3+3351s^2+1.961e05s+5.029e05}{s^4+209.6s^3+1.1e04s^2+7.5e04s+1.3e05}$	$\frac{-0.2044s^3-22.22s^2-680s-1.081e04}{s^4+209.6s^3+1.1e04s^2+7.5e04s+1.3e05}$	$\frac{-1.686s^3-423.5s^2-2.238e04s-3.587e04}{s^4+209.6s^3+1.1e04s^2+7.5e04s+1.3e05}$
Stage(13).T.Stri	$\frac{0.9939s^3+347.7s^2-6.292e04s-2.413e05}{s^4+209.6s^3+1.1e04s^2+7.5e04s+1.3e05}$	$\frac{65.07s^3+8743s^2+1.523e05s+4.512e05}{s^4+209.6s^3+1.1e04s^2+7.5e04s+1.3e05}$	$\frac{0.9945s^3+161.3s^2+5990s+2.146e04}{s^4+209.6s^3+1.1e04s^2+7.5e04s+1.3e05}$	$\frac{-7.6s^3-1148s^2-3.02e04s-1.004e05}{s^4+209.6s^3+1.1e04s^2+7.5e04s+1.3e05}$

3.2.2 Transfer Function Matrix

The state space model is transferred into the transfer function model. The model is given below in table 3.1. In this model we have considered 3 manipulated variable and 1 measured disturbance. The outputs are all measurable. The 3 manipulated variables are Rebolier duty(QRebR), Condenser duty(Qr) and Side draw flow(FR). Feed flow rate is considered as the process disturbance.

3.2.3 Decoupler design

As we have the MIMO (Multi-input and Multi-output) system, so there is a control loop interaction. The manipulated variable affects more than one controlled output. One of the very effective way to handle this problem is to introduce a decoupler in the control system. The purpose of this decoupler is to cancel the interaction between the loops and produce non-interacting loops. The main advantage of this process is it allows independent tuning of each controllers with out affecting the stability of the process. In this problem the simplified decoupling technique has been used. In the decoupler technique we have decoupled the manipulated variables. The disturbance variable is not taken in to consideration for the decoupling. For the third order simplified decoupler matrix is:

$$D = \begin{bmatrix} 1 & D_{12} & D_{13} \\ D_{21} & 1 & D_{23} \\ D_{31} & D_{32} & 1 \end{bmatrix}$$

The transfer function of decoupled matrix is:

$$G*D= \begin{bmatrix} GD_{11} & 0 & 0 \\ 0 & GD_{22} & 0 \\ 0 & 0 & GD_{33} \end{bmatrix}$$

$$\begin{bmatrix} GD_{11} & 0 & 0 \\ 0 & GD_{22} & 0 \\ 0 & 0 & GD_{33} \end{bmatrix} = \begin{bmatrix} G_{11} & G_{12} & G_{13} \\ G_{21} & G_{22} & G_{23} \\ G_{31} & G_{32} & G_{33} \end{bmatrix} \begin{bmatrix} 1 & D_{12} & D_{13} \\ D_{21} & 1 & D_{23} \\ D_{31} & D_{32} & 1 \end{bmatrix}$$

For the simplified decoupling the off diagonal elements of G*D matrix are zero. So by equating the above equation the expressions for the decoupling matrix can be obtained as:

$$D_{12} = \frac{G_{13}G_{32} - G_{12}G_{33}}{G_{11}G_{33} - G_{31}G_{13}}$$

$$D_{13} = \frac{G_{23}G_{12} - G_{22}G_{13}}{G_{22}G_{11} - G_{21}G_{12}}$$

$$D_{21} = \frac{G_{31}G_{23} - G_{21}G_{33}}{G_{33}G_{22} - G_{23}G_{32}}$$

$$D_{32} = \frac{G_{31}G_{12} - G_{32}G_{11}}{G_{11}G_{33} - G_{31}G_{13}}$$

$$D_{23} = \frac{G_{21}G_{13} - G_{23}G_{11}}{G_{22}G_{11} - G_{21}G_{12}}$$

$$D_{31} = \frac{G_{32}G_{21} - G_{31}G_{22}}{G_{33}G_{22} - G_{23}G_{32}}$$

Apply the D matrix equation in GD matrix to get the diagonal value of GD matrix. After this GD matrix is converted in to 3 SISO systems to control 3 output variables.
The Diagonal elements of the GD matrix is given by:

$$\begin{aligned} GD_{11} &= \frac{-0.914s - 4.482}{0.0047s^2 + 0.2644s + 1} \\ GD_{22} &= \frac{0.3631s + 1.712}{0.002s^2 + 0.3097s + 1} \\ GD_{33} &= \frac{0.075s + 0.291}{0.117s^2 + 0.6882s + 1} \end{aligned}$$

3.2.4 Fractional Controller

Fractional calculus is a 300 years old topic. Fractional order calculus has the advantage to describe and design a model more accurately than integer order calculus. Especially, the controllers which are designed by use of fractional order of derivatives and integrals shows more superior performance than the other integer order controller. Fractional order $PI^{\lambda}D^{\mu}$ are described by fractional order control. The fractional order controller is the expansion of integer order control. In PID controller there are 3 design parameters but in the fractional order PID controller there are 5 design parameters. The extra 2 degrees of freedom gives more flexibility to improve the performance of the controller. The transfer function representation of a FOPID controller is given by :

$$C(s) = K_p + \frac{K_i}{s^{\lambda}} + K_d s^{\mu}$$

The FOPID controller generalizes the conventional integer order PID controller and In other words it can be said that it is the expansion of point to plane. For $\lambda = 1$ and $\mu = 1$ the controller becomes a classical PID controller.
On the other hand the fractional order differentiator and integrator has the infinite dimensional nature which creates hardware issue in the industrial application of FOPID controller. A fractional order linear time invariant system is mathematically equivalent to the infinite dimensional LTI filter. The fractional order system can be approximated as the higher order polynomial which consists of integer order operators. There are two different ways for the approximation.

1. Continuous time realization
2. Discrete time realization

Here we have used crone controller which is the crone continuous time approximation. This formula is valid with in a frequency range $[w_l, w_h]$. In the present study the 5^{th} order approximation is done with in a limit of $w \in [0.001, 1000]$ rad/sec.

For the fractional order controller design we have used multi objective optimisation technique. The main question arises why we need multi-objective optimisation technique. There are different design control objective like H_2, H_∞ or L_1, which can be satisfied by minimizing the closed loop weighted function norm. Minimization of each norm has its own advantage and it satisfy the required criteria, but it does not say anything about the other design specification. For example by minimising the H_∞ imply a good closed loop robust stability but may not give guarantee about the system stability in presence of the disturbances. On the other hand the H_2 norm give close loop stabilization in presence of disturbance. It is difficult to satisfy different specifications like disturbance rejection, set point tracking and robust stability with the help of single norm. Thus multi-objective algorithm is very effective to trade-off among different design objective.
In our problem we have used two objective functions which are the ITAE criteria for the set point tracking (J_1) and the ITAE for the load disturbance(J_2). J_1 tries to minimise the set point tracking error while the J_2 tries to minimize the deviation from the set-point from the process disturbance.

$$\begin{aligned} J_1 &= ITAE_{setpoint} = \int_0^\infty t|e(t)|_{sp}dt \\ J_2 &= ITAE_{loaddisturbance} = \int_0^\infty t|e(t)|_{ld}dt \end{aligned}$$

For the multiobjective optimization we have used the *ev*-MOGA optimization technique.

3.3 Results and Discussion

In this section we have discussed the step point tracking and the disturbance rejection for each of the outputs.Three different SISO loops have been obtained from the decoupler design for tuning. The nominal set point of the all the variables are set at 50% because we have already scaled our system.

3.3.1 The last tray temperature in the rectifying column

The Pareto frontiers for the two contradictory objective function J_1 and J_2 are shown in Figure 3.7 while the representative solutions on the Pareto front are reported in Table 3.2. Figure 3.8 and Table 3.3 presents the set point tracking performance of the controllers in nominal cases $A1, B1, C1$. While the Figure 4.3 and Table 3.4 reveals the disturbance rejection of the three controllers. The open loop bode plots are shown in Figure 3.10 and it can be observed that the system is stable when the loop is closed.

Table 3.2: Representation solutions on the Pareto front for 1^{st} output

Solution	J_1	J_2	K_p	K_i	K_d	λ	μ
A1	7.67e-17	0.0124	-42.2717	-990.7795	-969.5525	0.9275	0.9274
B1	6.286e-12	5.178e-04	-1000	-1000	-1000	1	0.01
C1	1.313e-08	6.241e-05	1000	-1000	-1000	1	0.01

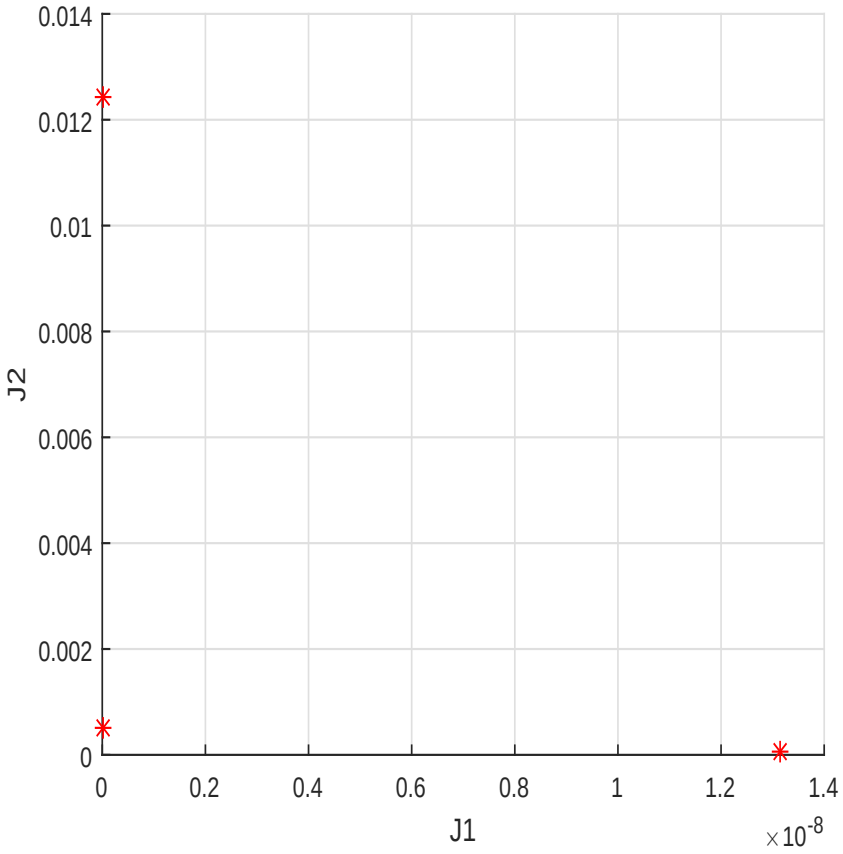

Figure 3.7: Pareto front of the objective J_1 and J_2

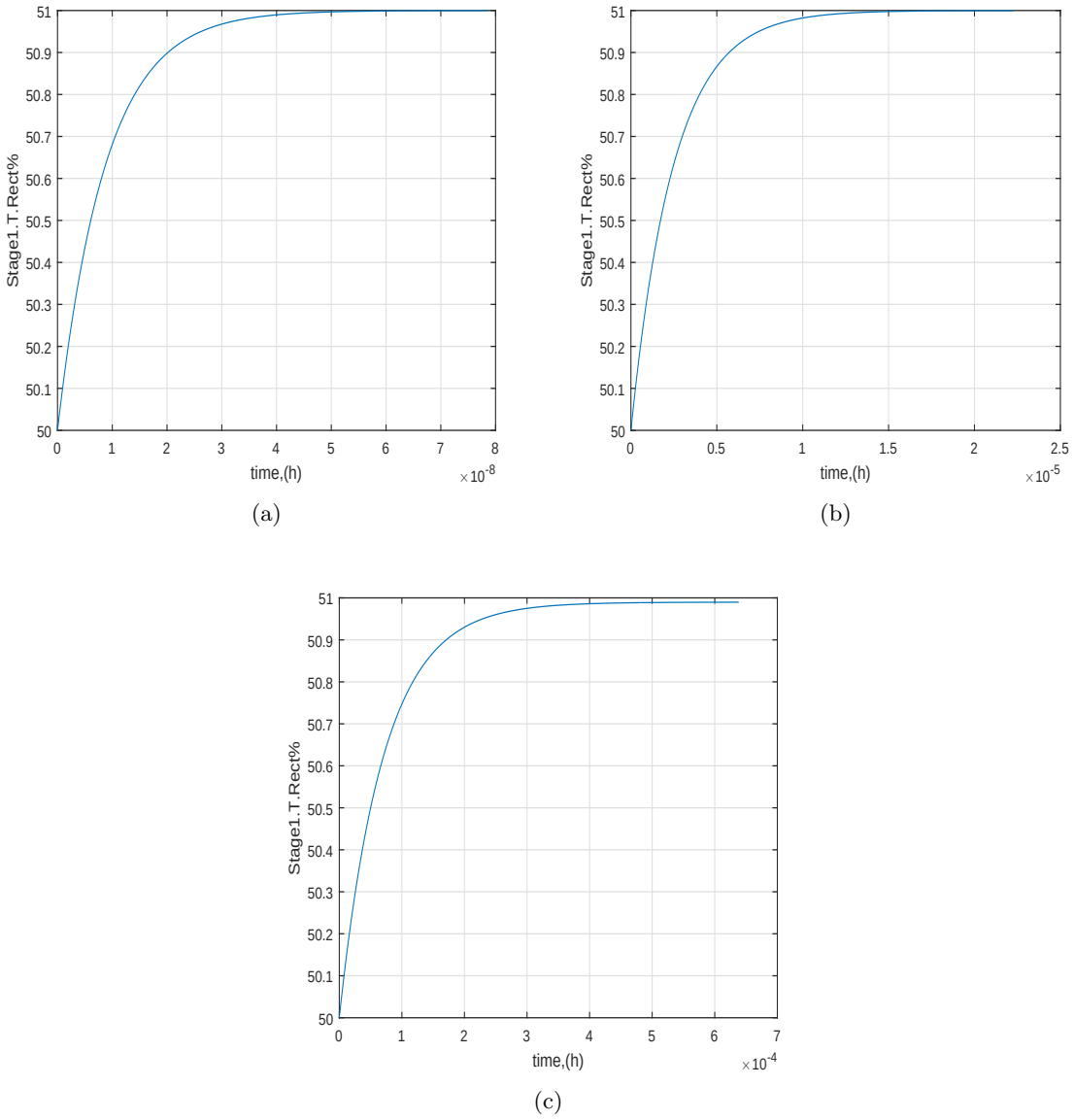

Figure 3.8: Step response characteristic performance of controllers corresponding to three Pareto solutions as presented in Table 3.2

Table 3.3: Step Response characteristics of various controllers corresponding to the Pareto solutions as presented in Table 3.2

Solution	Rise time (t_r)	Overshoot(OS)	Settling Time(t_s)	Peak Time(t_p)
A1	1.923e-08	0	3.4245e-08	9.2305e-08
B1	5.4525e-06	0	9.7201e-06	2.6158e-05
C1	1.6325e-04	0	3.2946-04	0.0022

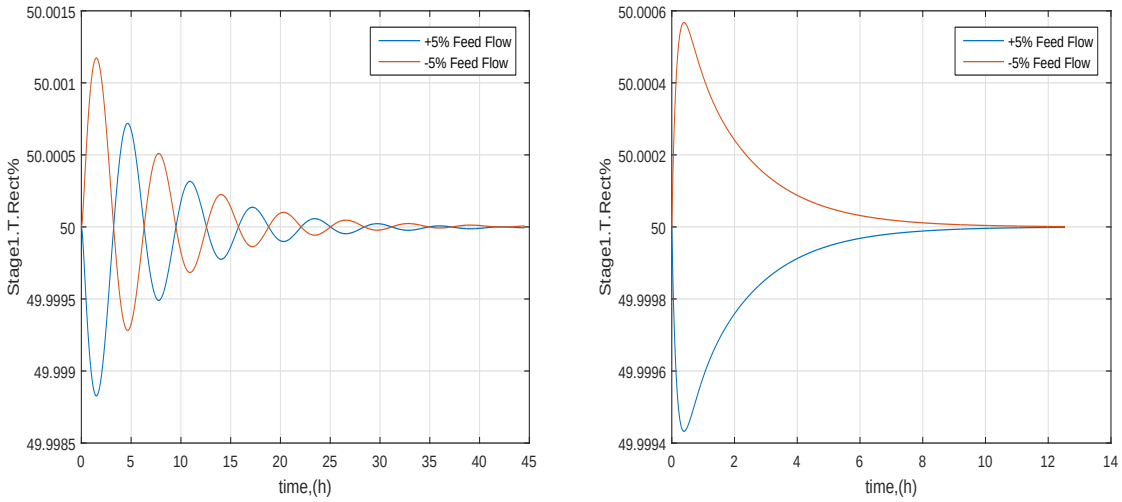

(a) (b)

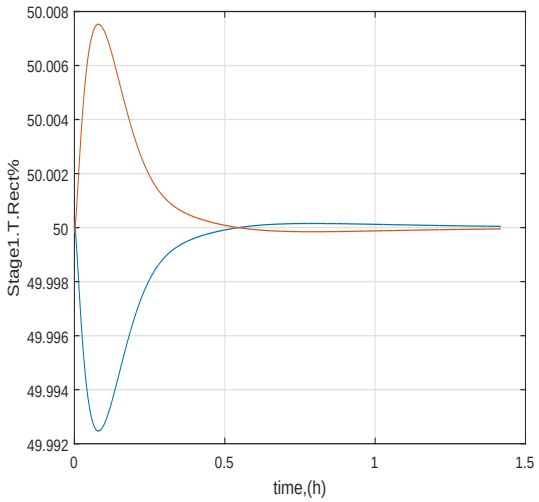

(c)

Figure 3.9: Disturbance rejection performance of controllers corresponding to three Pareto solutions as presented in Table 3.2 due to ±5% change in feed flow

Table 3.4: Disturbance rejection characteristics of various controllers corresponding to the Pareto solutions as presented in Table 3.2 due to ±5% change in feed flow

Solution	Rise time (t_r)	Peak	Settling Time(t_s)	Peak Time(t_p)
A1	0.0153	50.012	29.9916	1.5035
B1	0	50.00056	8.0089	0.3947
C1	0	50.0075	0.8334	0.0794

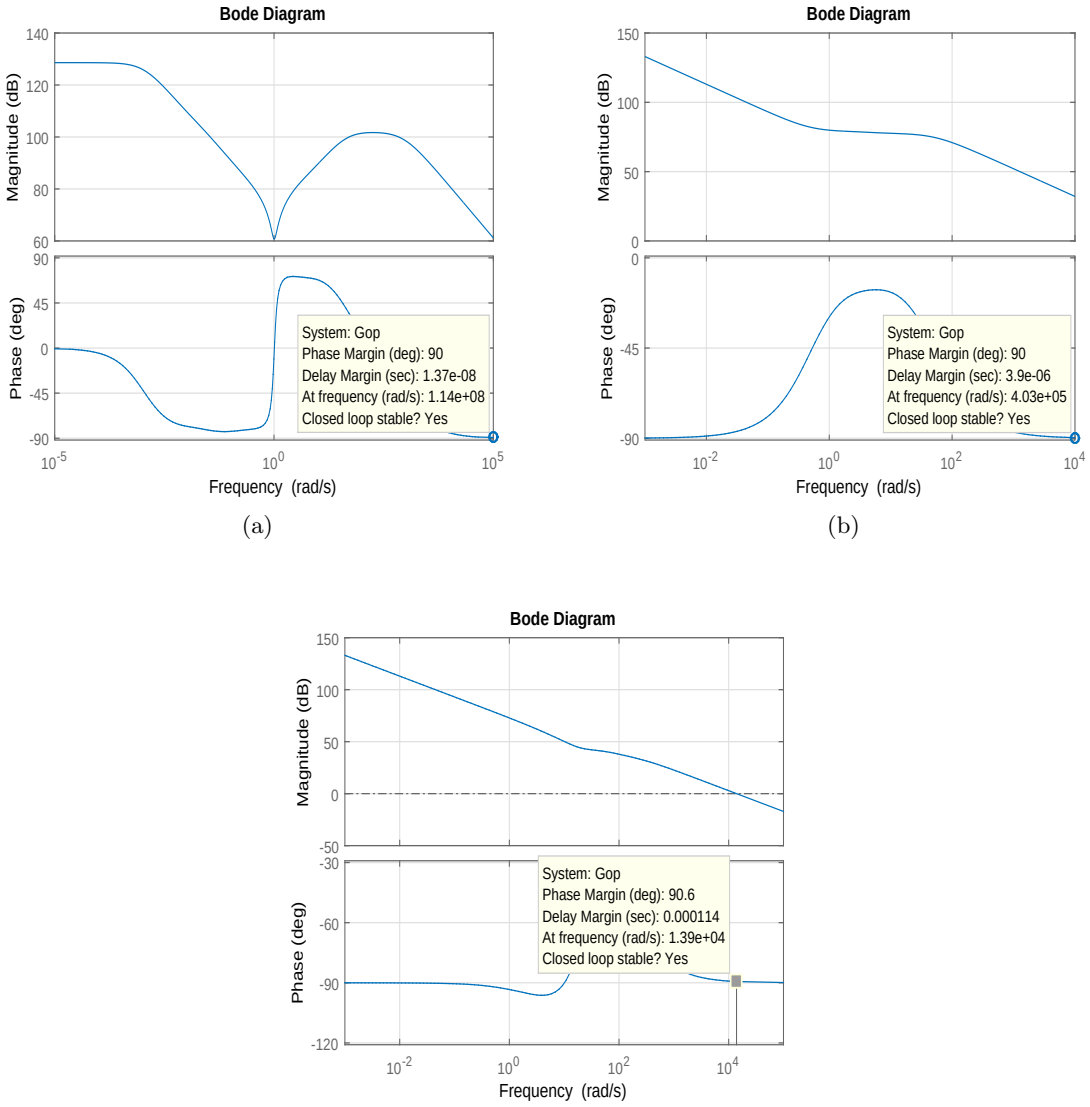

Figure 3.10: Open loop bode plot for (a) Solution A1 (b) Solution B1 (c) Solution C1 in loop 1

3.3.1.1 Robustness analysis of the obtained solutions

The controllers have been designed for the nominal condition. The controller need to be tuned in such a way to work under different operating conditions. The main of the robust controller is to achieve robustness and stability in presence of modelling errors which are bounded. The robustness of a controller can be checked by varying the process gain and time parameter. In our problem we have varied our gain and time constant values with in a certain range of -30% to $+30\%$ to that of nominal value. Figure 3.11 shows the robustness analysis of the solution A1 for gain parameter change and time constant change for both the step and load change. Figure 3.11 and Figure 3.12 show the robustness analysis for the solution B1 and solution C1 respectively as done for solution A1. Form Figure 3.11, 3.11, 3.12 are representing performances indicates sufficient robustness of the designed controllers

at the face of variation of process gain and time constant.

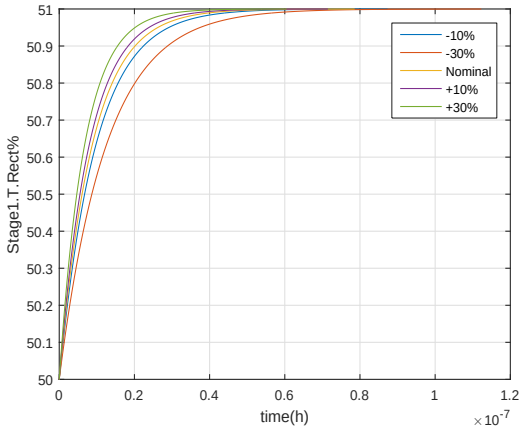

(a) Set point tracking performance under gain variation

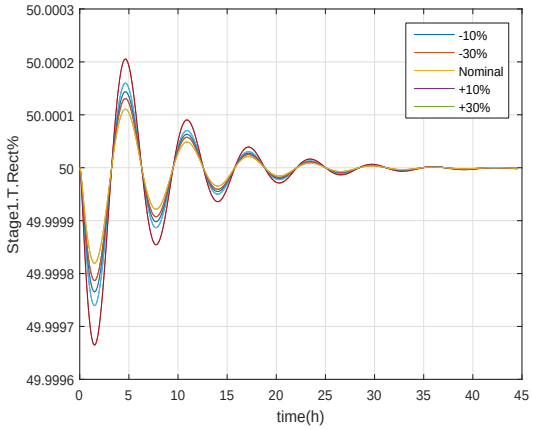

(b) Disturbance rejection performance under gain variation

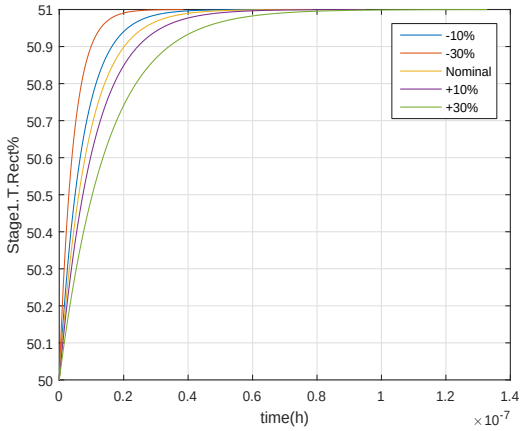

(c) Set point tracking performance under time constant variation

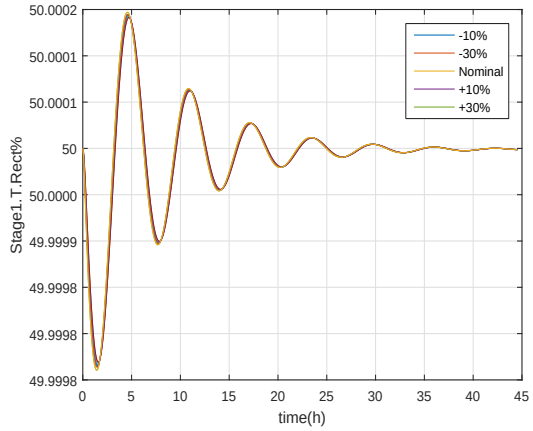

(d) Disturbance rejectio performance under time constant variation

Figure 3.11: Robustness analysis for solution A1

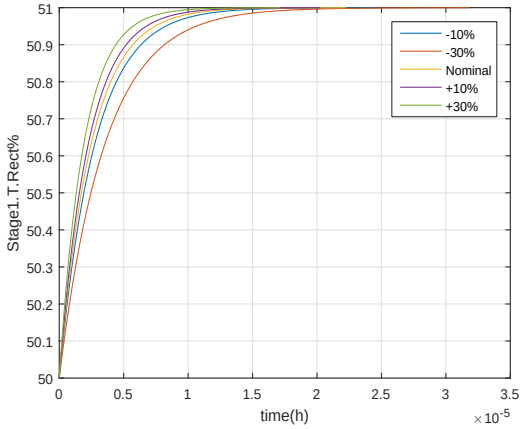

(a) Set point tracking performance under gain variation

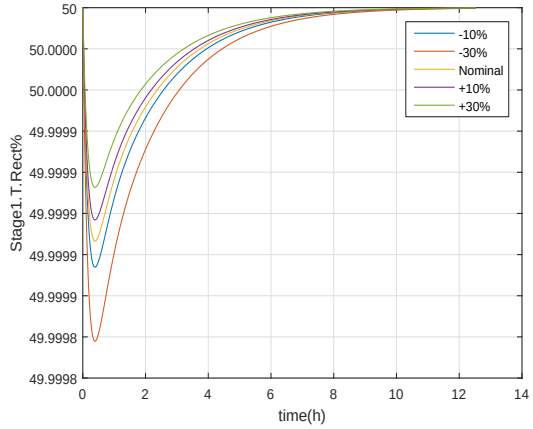

(b) Disturbance rejection performance under gain variation

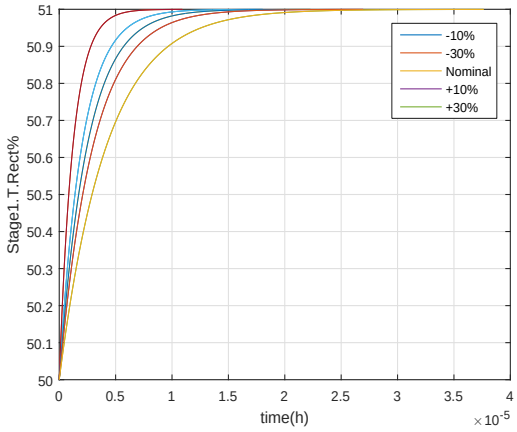

(c) Set point tracking performance under time constant variation

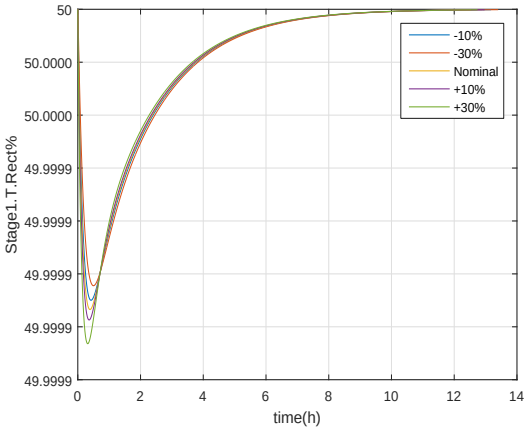

(d) Disturbance rejection performance under time constant variation

Figure 3.11: Robustness analysis for solution B1

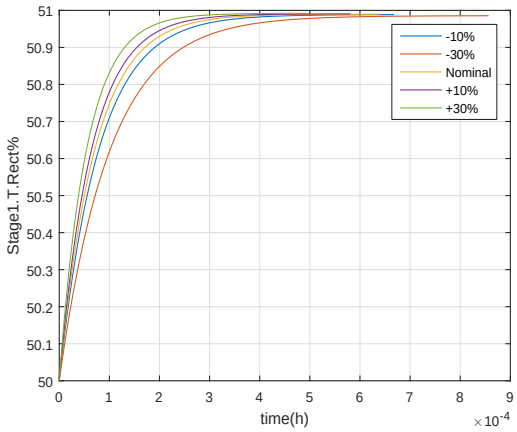

(a) Set point tracking performance under gain variation

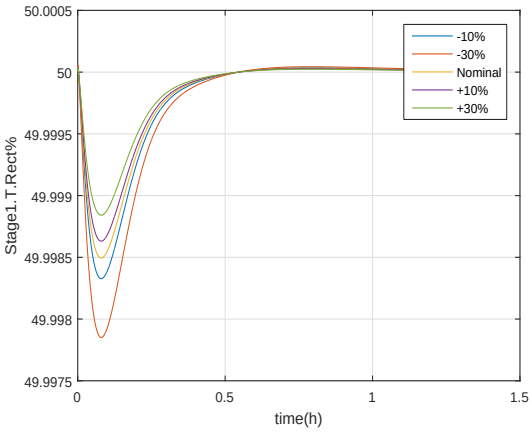

(b) Disturbance rejection performance under gain variation

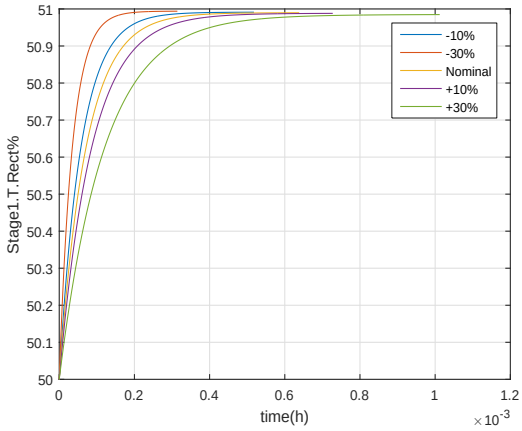

(c) Set point tracking performance under time constant variation

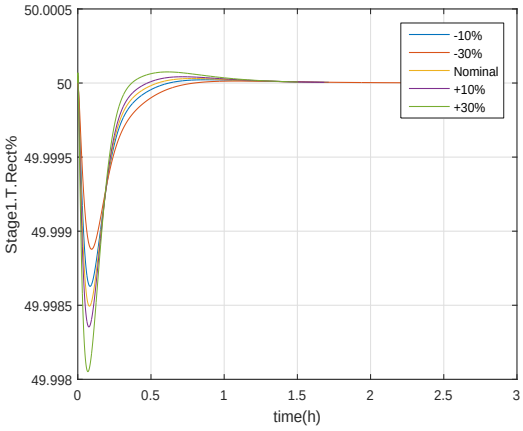

(d) Disturbance rejectio performance under time constant variation

Figure 3.12: Robustness analysis for solution C1

3.3.2 The 11^{th} tray temperature in the main column

The Pareto frontiers for the two contradictory objective function J_1 and J_2 are shown in Figure 3.13 while the representative solutions on the Pareto front are reported in Table 3.5. Figure 3.14 and Table 3.6 presents the set point tracking performance of the controllers in nominal cases $A2, B2, C2$. While the Figure 4.3 and Table 3.7 presents the disturbance rejection of the three controllers. The open loop bode plots are shown in Figure 3.16 and it can be observed that the system is stable when the loop is closed.

Table 3.5: Representation solutions on the Pareto front for 2^{nd} output

Solution	J_1	J_2	K_p	K_i	K_d	λ	μ
A2	1.32e -09	1.2969e-04	-634.6040	833.0344	613.5093	0.9429	0.0476
B2	9.9624e-15	4.4208e-04	787.5673	525.2540	219.947	0.9986	0.7987
C2	4.4255e-17	0.5818	687.1901	749.3356	831.5049	0.6109	0.993

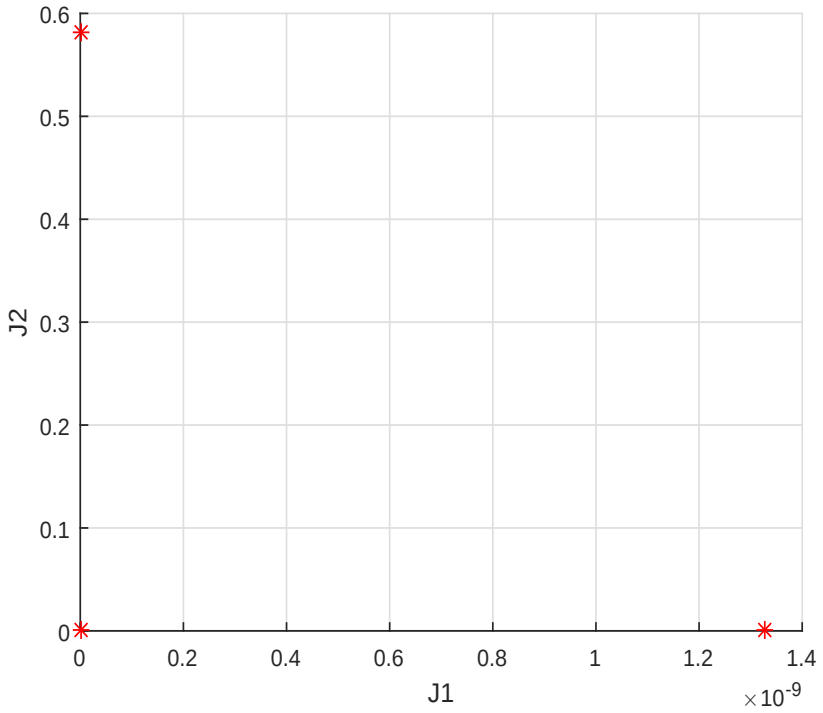

Figure 3.13: Pareto front of the objective J_1 and J_2

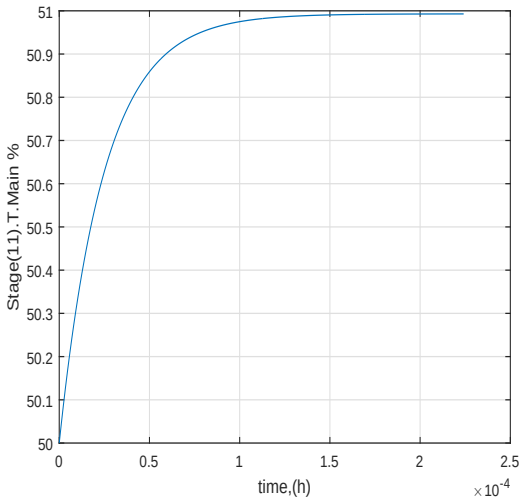

(a)

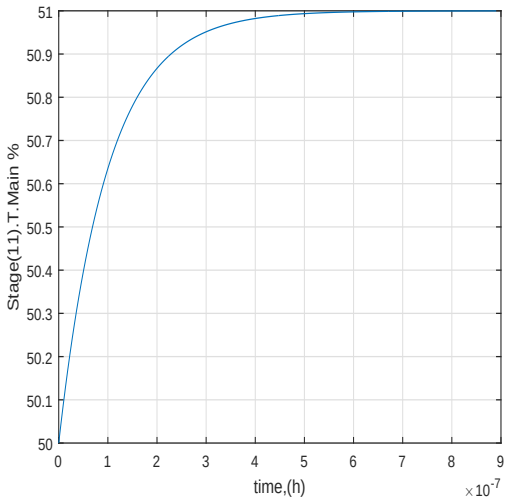

(b)

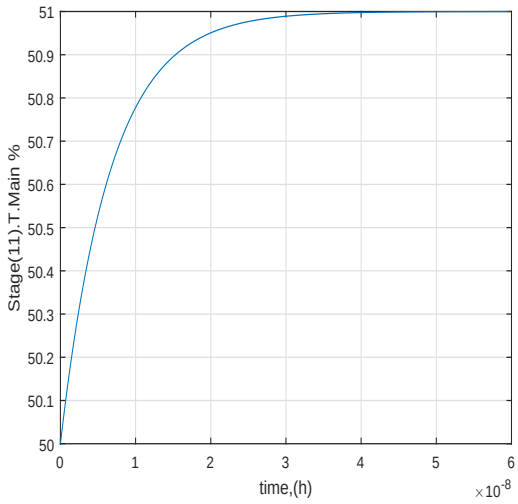

(c)

Figure 3.14: Step response characteristic performance of controllers corresponding to three Pareto solutions as presented in Table 3.5

Table 3.6: Step Response characteristics of various controllers corresponding to the Pareto solutions as presented in Table 3.5

Solution	Rise time (t_r)	Overshoot(OS)	Settling Time(t_s)	Peak Time(t_p)
A2	5.4667e-05	0	1.0831e-04	2.6320e-04
B2	2.1788e-07	0	3.8825e-07	1.0455e-06
C2	1.4607e-08	0	2.6008e-08	7.0114e-08

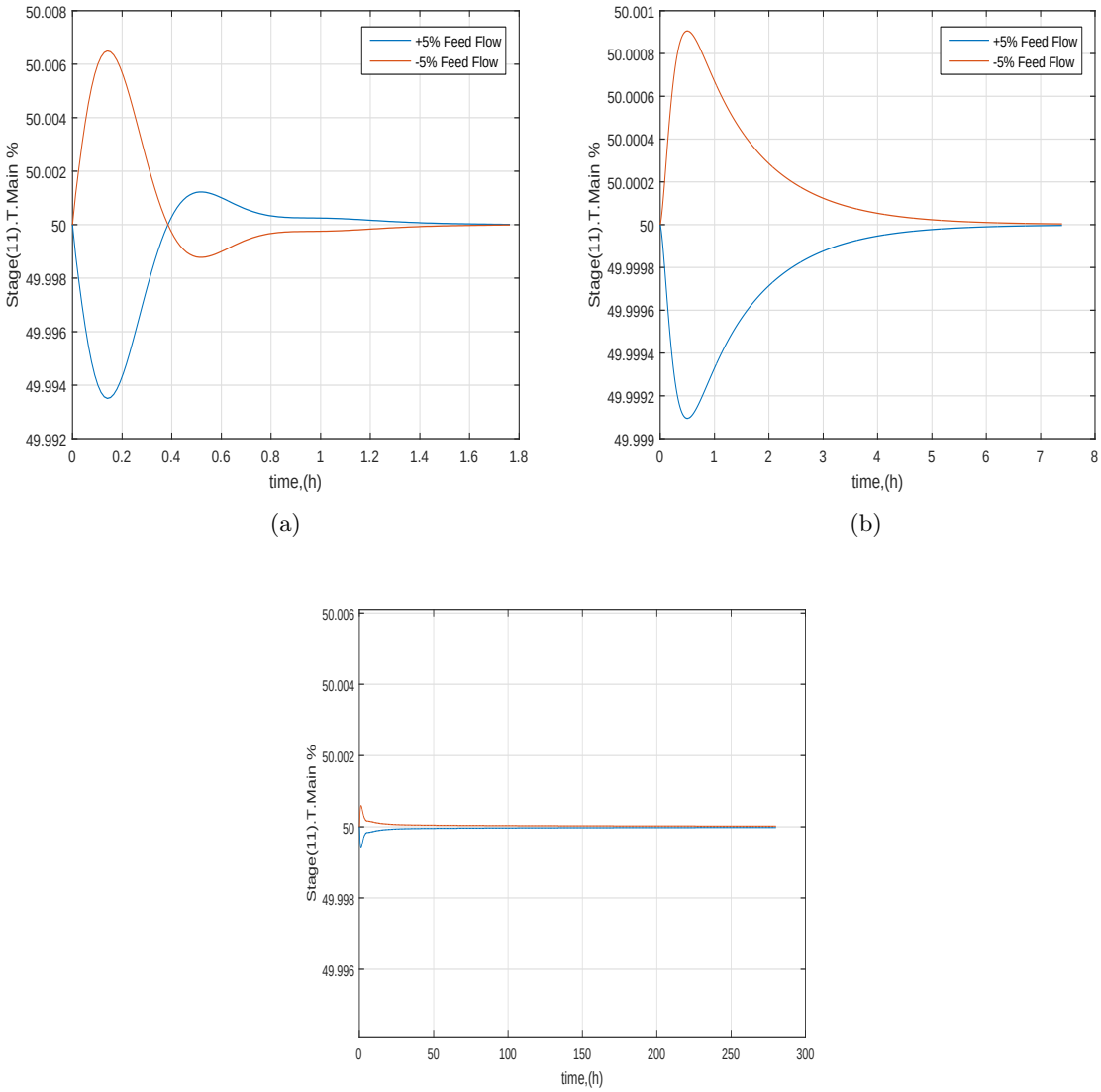

Figure 3.15: Disturbance rejection performance of controllers corresponding to three Pareto solutions as presented in Table 3.5 due to ±5% change in feed flow

Table 3.7: Disturbance rejection characteristics of controllers corresponding to three Pareto solutions as presented in Table 3.5 due to ±5% change in feed flow

Solution	Rise time (t_r)	Peak	Settling Time(t_s)	Peak Time(t_p)
A2	1.2249-05	50.0065	1.2678	0.1405
B2	9.6461e-04	50.0009	5.1953	0.4957
C2	0.0370	50.0006	152.7841	1.1331

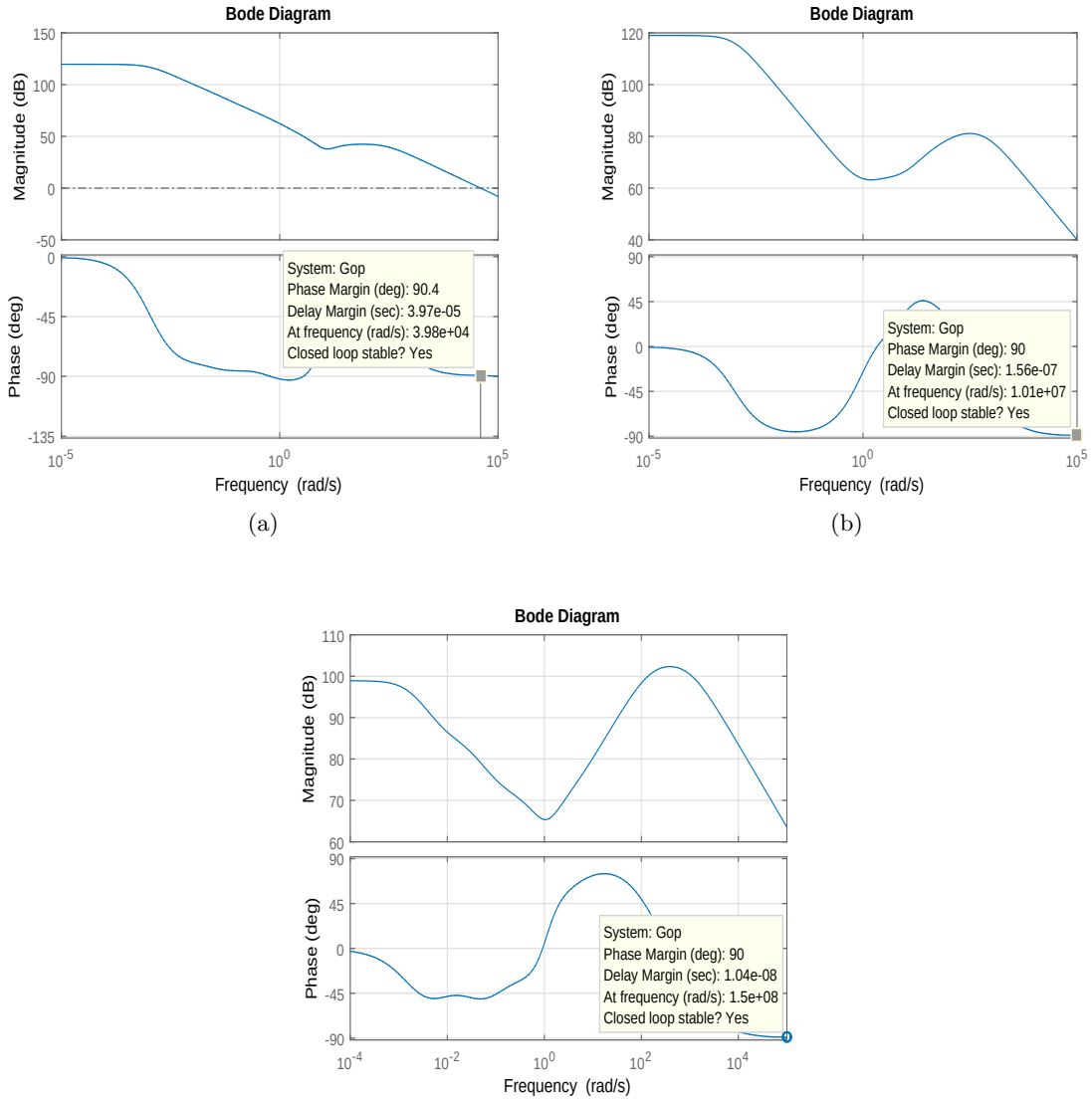

Figure 3.16: Open loop bode plot for (a) Solution A2 (b) Solution B2 (c) Solution C2 in loop 2

3.3.2.1 Robustness analysis of the obtained solutions

The controllers have been designed for the nominal condition. we have varied our gain and time constant values with in a certain range of -30% to $+30\%$ to that of nominal value. Figure 3.17 shows the robustness analysis of the solution A2 for gain parameter change and time constant change for both the step and load change. Figure 3.17 and Figure 3.18 show the robustness analysis for the solution B2 and solution C2 respectively as done for solution A2.

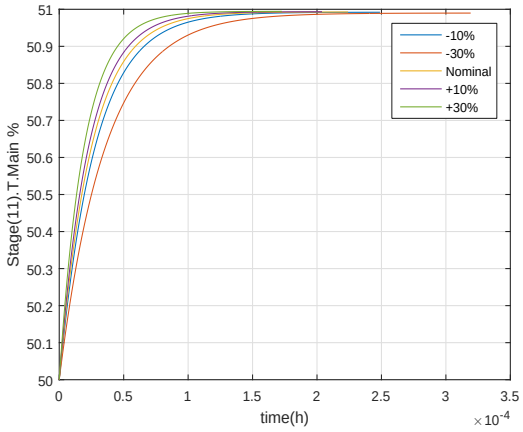

(a) Set point tracking performance under gain variation

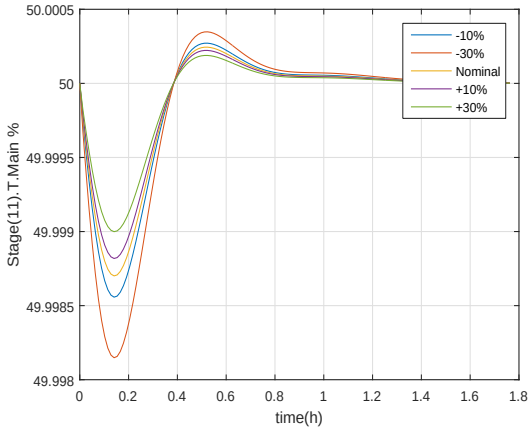

(b) Disturbance rejection performance under gain variation

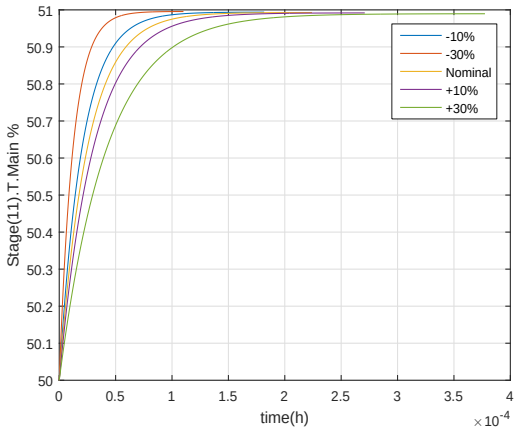

(c) Set point tracking performance under time constant variation

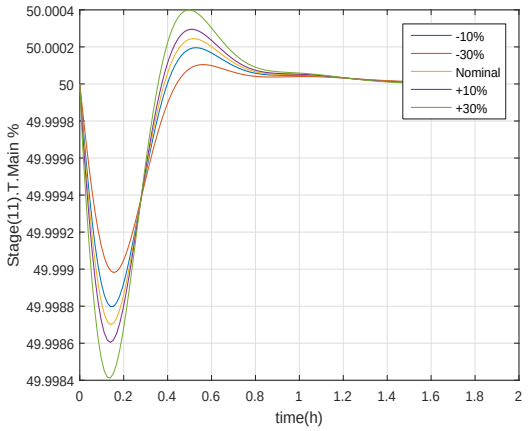

(d) Disturbance rejection performance under time constant variation

Figure 3.17: Robustness analysis for solution A2

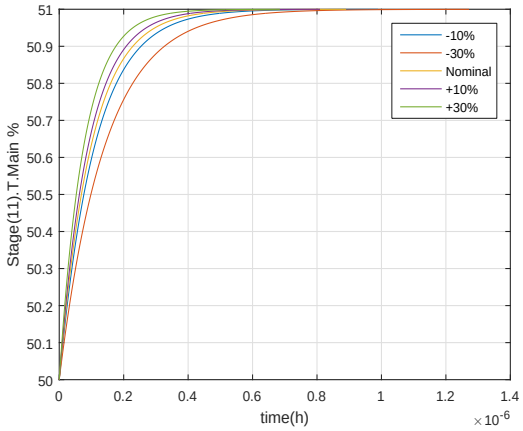

(a) Set point tracking performance under gain variation

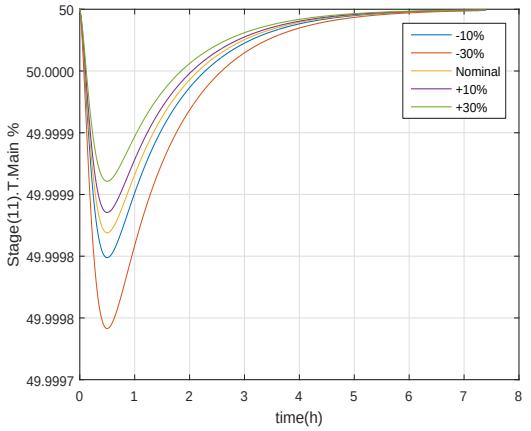

(b) Disturbance rejection performance under gain variation

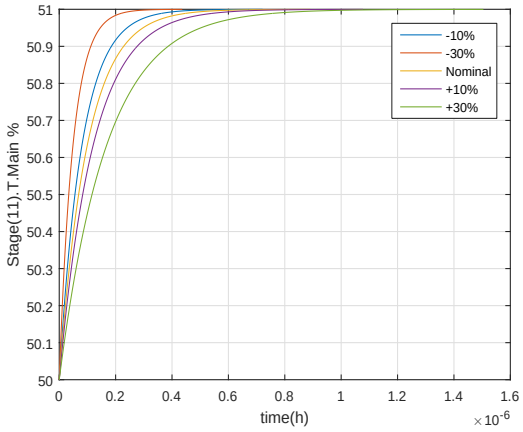

(c) Set point tracking performance under time constant variation

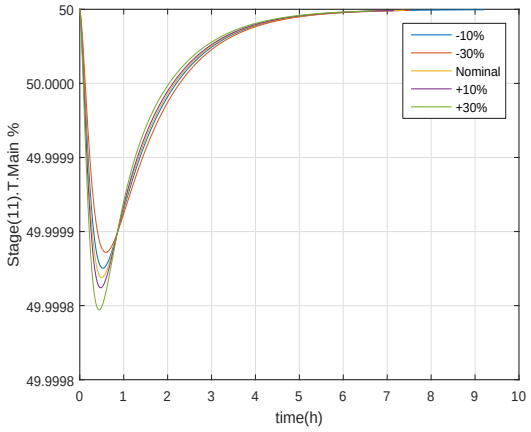

(d) Disturbance rejection performance under time constant variatio

Figure 3.17: Robustness analysis for solution B2

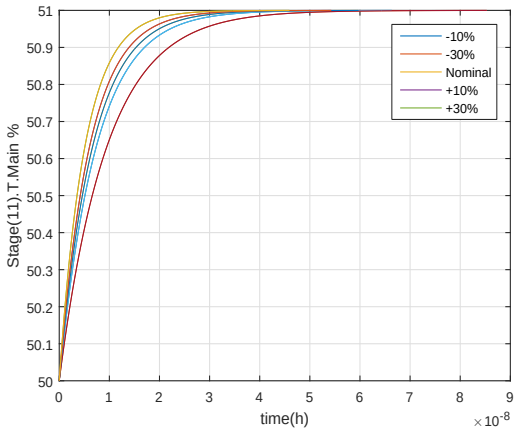

(a) Set point tracking performance under gain variation

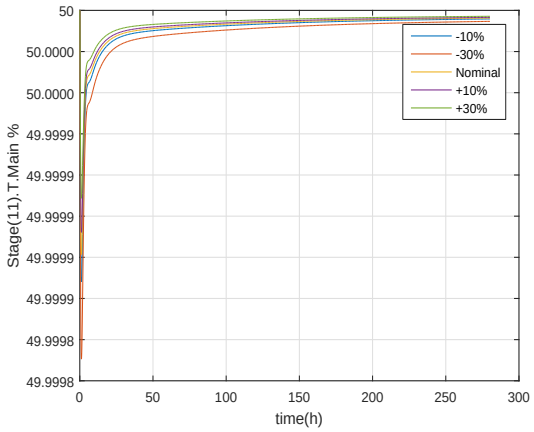

(b) Disturbance rejection performance under gain variation

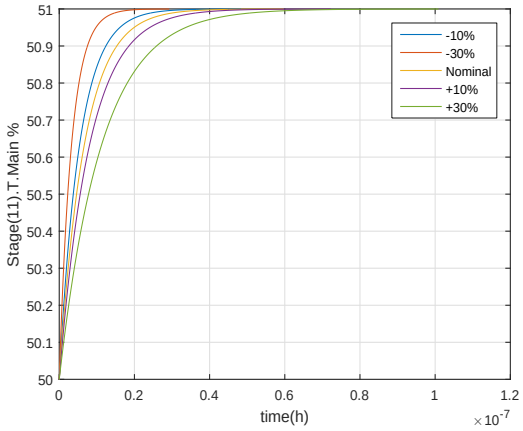

(c) Set point tracking performance under time constant variation

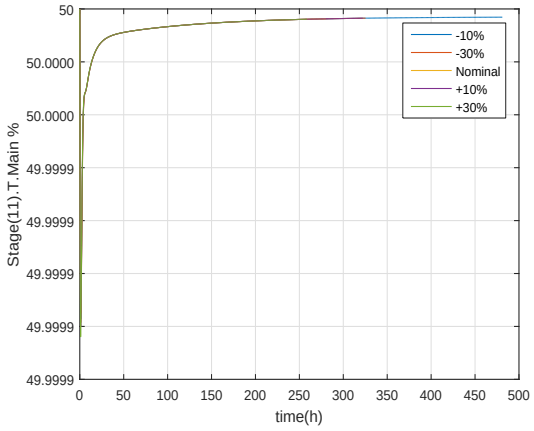

(d) Disturbance rejection performance under time constant variation

Figure 3.18: Robustness analysis for solution C2

3.3.3 The 13^{th} tray temperature in the stripping column

The Pareto frontiers for the two contradictory objective function J_1 and J_2 are shown in Figure 3.19 while the representative solutions on the Pareto front are reported in Table 3.8. Figure 3.20 and Table 3.9 presents the set point tracking performance of the controllers in nominal cases $A3, B3, C3$. While the Figure 3.21 and Table 3.10 reveals the disturbance rejection of the three controllers. The open loop bode plots are shown in Figure 3.22 and it can be observed that the system is stable when the loop is closed.

Table 3.8: Representation solutions on the Pareto front for 3^{rd} output

Solution	J_1	J_2	K_p	K_i	K_d	λ	μ
A3	9.6297e-14	0.009	5.1284e+03	2.9600e+03	5.5755e+03	0.9042	0.9814
B3	2.9583e-13	0.001	5.0017e+03	7.458e+03	2.921e+03	0.9389	0.9961
C3	2.789e-04	5.5056e-05	-10000	10000	10000	1	0.01

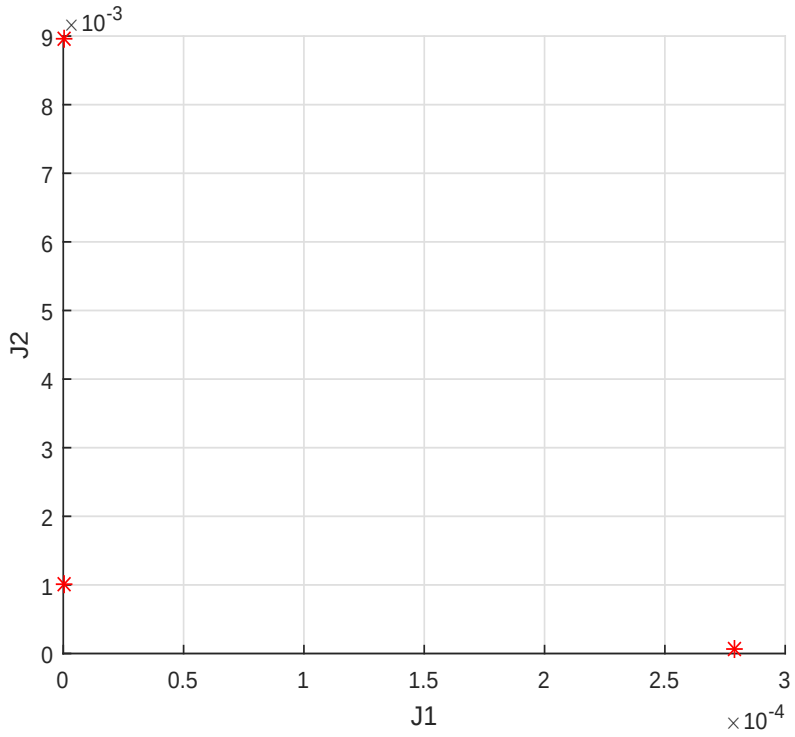

Figure 3.19: Pareto front of the objective J_1 and J_2

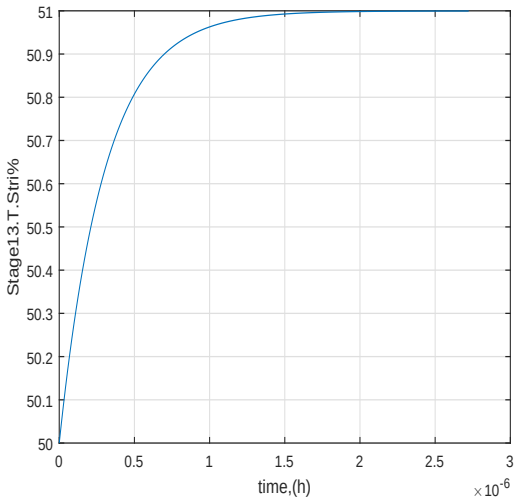

(a)

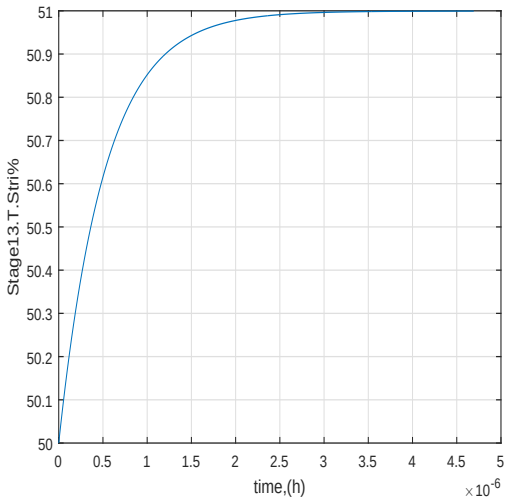

(b)

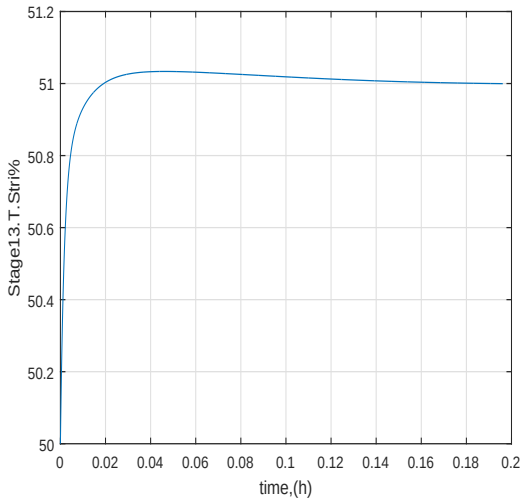

(c)

Figure 3.20: Step response characteristic performance of controllers corresponding to three Pareto solutions as presented in Table 3.8

Table 3.9: Step Response characteristics of various controllers corresponding to the Pareto solutions as presented in Table 3.8

Solution	Rise time (t_r)	Overshoot(OS)	Settling Time(t_s)	Peak Time(t_p)
A3	6.6701e-07	0	1.1907e-06	3.1978e-06
B3	1.1505e-06	0	2.0578e-06	5.5108e-06
C3	0.0077	0	0.0958	0.0462

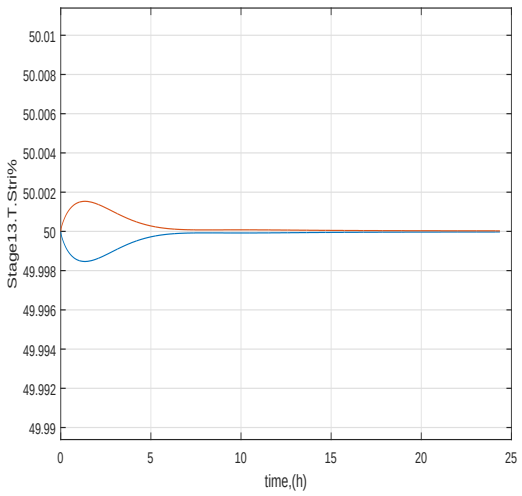

(a)

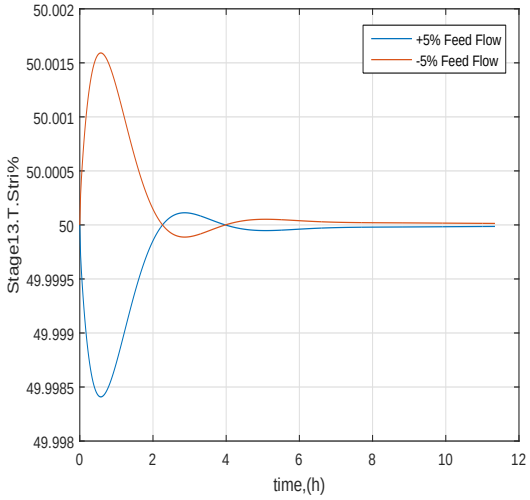

(b)

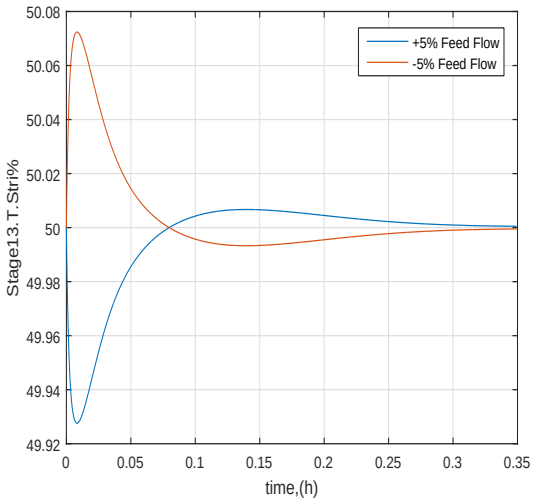

(c)

Figure 3.21: Disturbance rejection performance of controllers corresponding to three Pareto solutions as presented in Table 3.8 due to ±5% change in feed flow

Table 3.10: Disturbance rejection characteristics of various controllers corresponding to the Pareto solutions as presented in Table 3.8

Solution	Rise time (t_r)	Peak	Settling Time(t_s)	Peak Time(t_p)
A3	9.2448e-04	50.0015	18.0490	1.3489
B3	1.6535e-04	50.0016	6.2597	0.5840
C3	0	0.0724	50.2755	0.0082

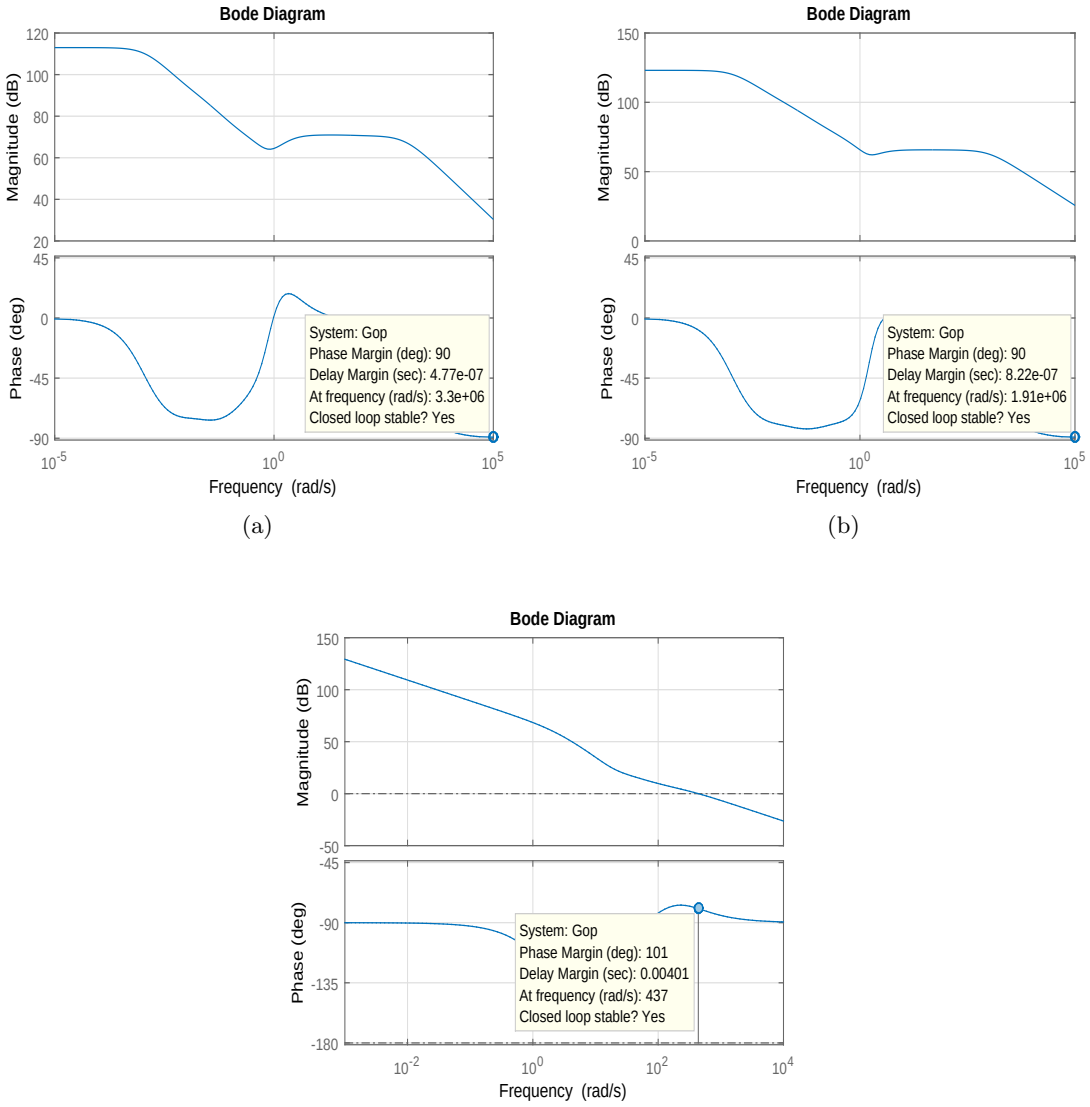

Figure 3.22: Open loop bode plot for (a) Solution A3 (b) Solution B3 (c) Solution C3 in loop 3

3.3.3.1 Robustness analysis of the obtained solutions

The controllers have been designed for the nominal condition. The controller need to be tuned in such a way to work under different operating conditions. The main of the robust controller is to achieve robustness and stability in presence of modelling errors which are bounded. The robustness of a controller can be checked by varying the process gain and time parameter. In our problem we have varied our gain and time constant values with in a certain range of -30% to $+30\%$ to that of nominal value. Figure 3.23 shows the robustness analysis of the solution A3 for gain parameter change and time constant change for both the step and load change. Figure 3.23 and Figure 3.24 show the robustness analysis for the solution B3 and solution C3 respectively as done for solution A3.

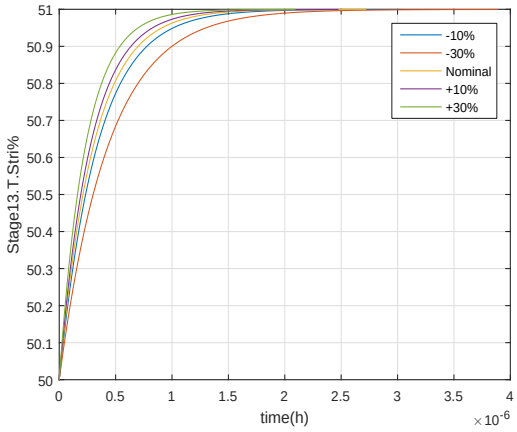

(a) Set point tracking performance under gain variation

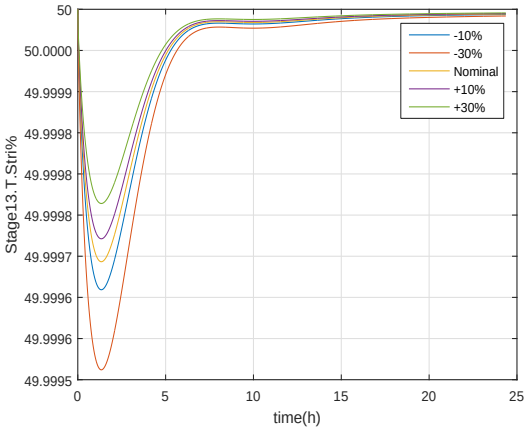

(b) Disturbance rejection performance under gain variation

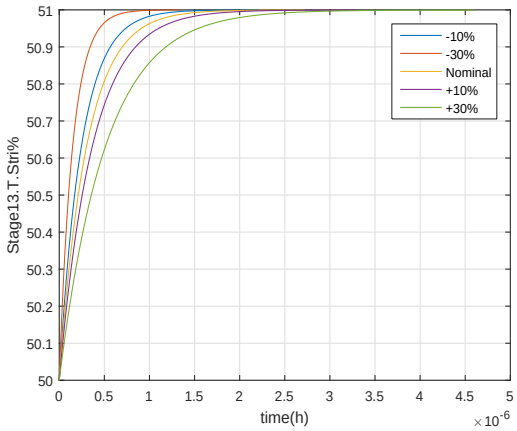

(c) Set point tracking performance under time constant variation

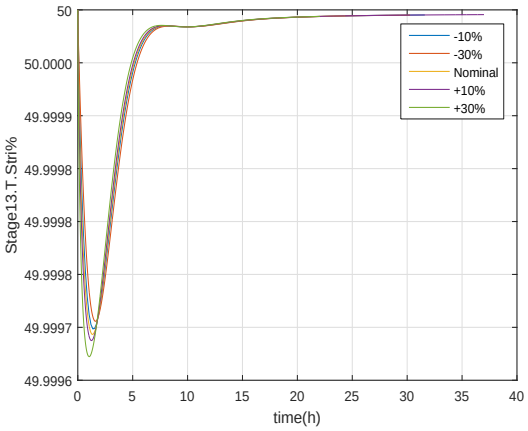

(d) Disturbance rejection performance under time constant variation

Figure 3.23: Robustness analysis of solution of solution A3

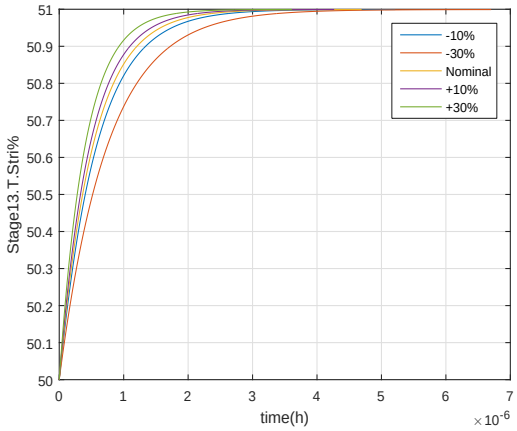

(a) Set point tracking performance under gain variation

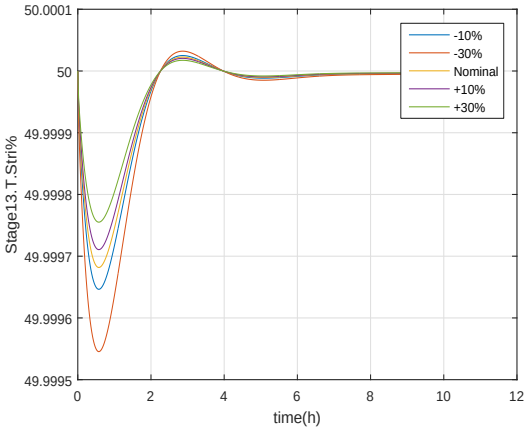

(b) Disturbance rejection performance under gain variation

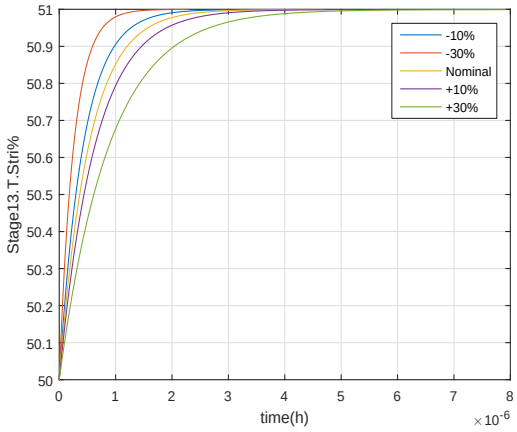

(c) Set point tracking performance under time constant variation

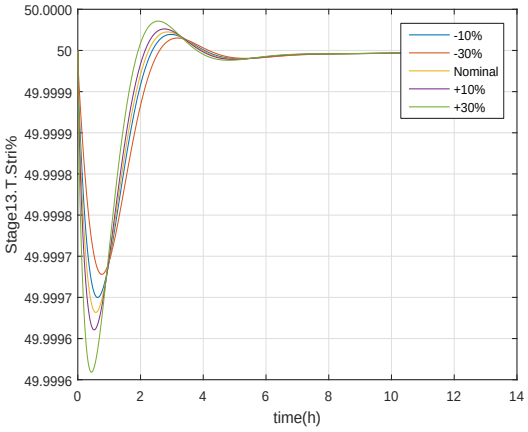

(d) Disturbance rejection performance under time constant variation

Figure 3.23: Robustness analysis of solution B3

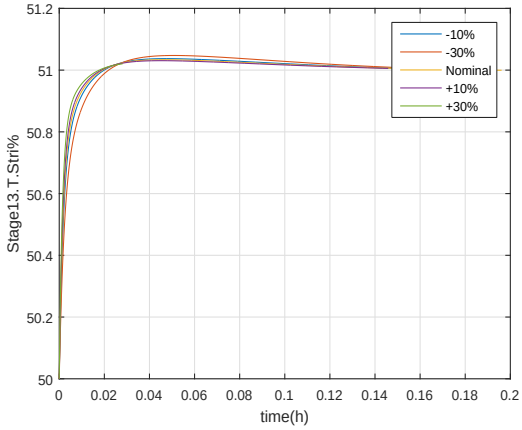

(a) Set point tracking performance under gain variation

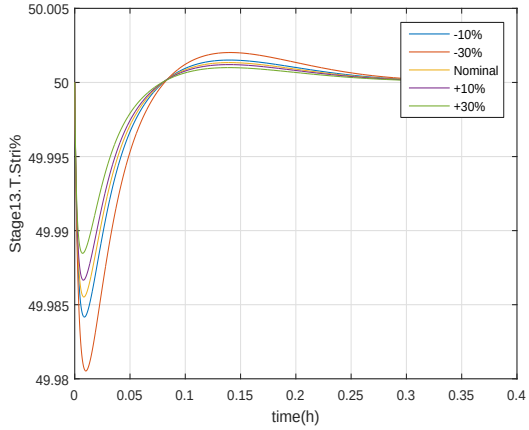

(b) Disturbance rejection performance under gain variation

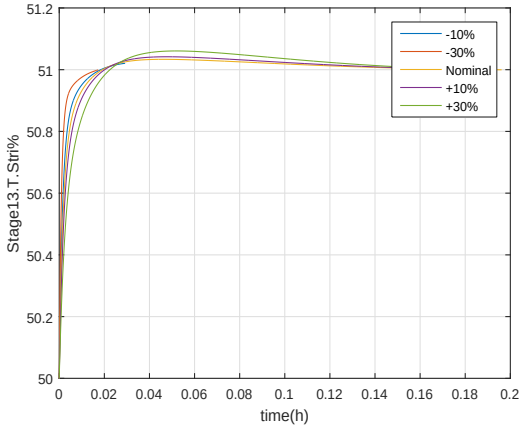

(c) Set point tracking performance under time constant variation

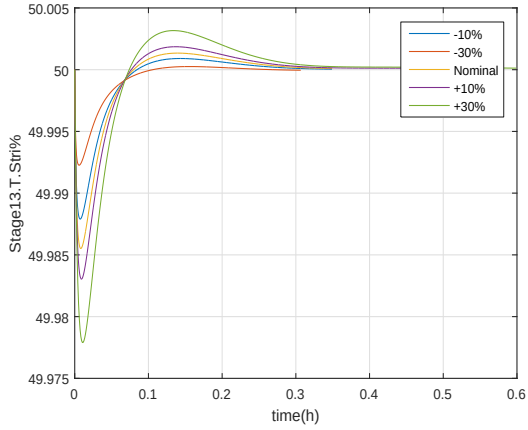

(d) Disturbance rejection performance under time constant variation

Figure 3.24: Robustness analysis of solution C3

The multiobjective optimisation algorithm produces set of solution on the pareto front, which is useful for the trade offs for the different objective functions. When making the final choice of the controller, one has to choose the controller from the set depending on which objective is more important.If one requires the controller which can tolerate the load disturbance and the set point tracking is not very essential. Then the designer can choose a solution form the Pareto front which gives better disturbance rejection than set point tracking.

Chapter 4

Plant wide Control : HDA Process

In HDA process the feed is fresh toluene and hydrogen (95% H_2 and 5% CH_4) which are mixed with recycled toluene and hydrogen. This mixed feed stream is preheated in heat exchanger with the help of rector effluent stream. Then it is heated to the reactor temperature in the furnace and fed in to the adiabatic reactor. Two main reactions in the reactor are

$$Toluene + H_2 \rightarrow Benzene + CH_4$$

$$2Benzene \leftrightarrow Diphenyl + H_2$$

The reactor effluent is quenched with the recycle liquid , which is useful for the prevention of coking. Before sending to the flash separator, it is cooled in the heat exchanger and cooler. The over head product of the separator is sent to the separating membrane permeator unit. In this unit the methane is separated from the hydrogen, which is useful to avoid accumulation of hydrogen. The hydrogen stream is compressed and recycled back to the fresh hydrogen stream. The bottom product of the separator is sent to the separation section. The separation section is consists of three distillation units. The first distillation column (stabilizer) removes H_2 and CH_4 as the top product. Benzene is the required product from the second distillation unit (product). In the third distillation column (Recycle) toluene is separated from the diphenyl and recycled back to the toluene fresh stream.

4.1 Steady state simulation

For a simulation of real process two important parameters are required that is design and optimum parameter. For a low cost in process and optimum cost, the optimized value of optimized parameter must be found out. One of the best way to find the optimized value of the process is steady state simulation. The steady state simulation model is developed in the Aspen plus. The fresh hydrogen stream feed flow rate is 393.9 lbmol/hr while the fresh toluene feed flow rate is 274.2 lbmol/hr. The shell and tube heat exchanger is used to preheat the mixed feed stream. The temperature in the furnace is specified as 1200F at 500 psia. The required reaction is specified in the plug flow reactor. Temperature of the separator is specified as 90F. As discussed in above the separating unit consists of three different distillation units. In the stabilizer column the number of trays are specified as 10 and the condenser pressure is 109.12 psia with 0.1 psia pressure drop in each tray. The

Product column is designed with 25 number of stages and 20 psia of condenser pressure with 0.1 psia pressure drop. The specifications of the final distillation column are 7 number of trays and 20 psia condenser pressure.

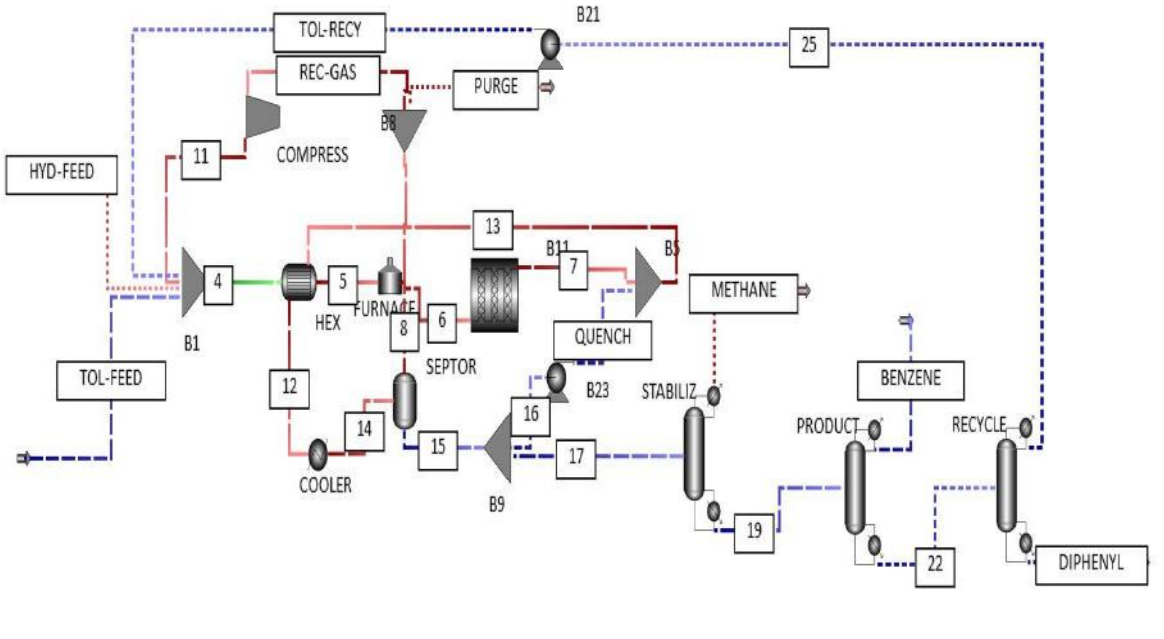

Figure 4.1: HDA process flowsheet

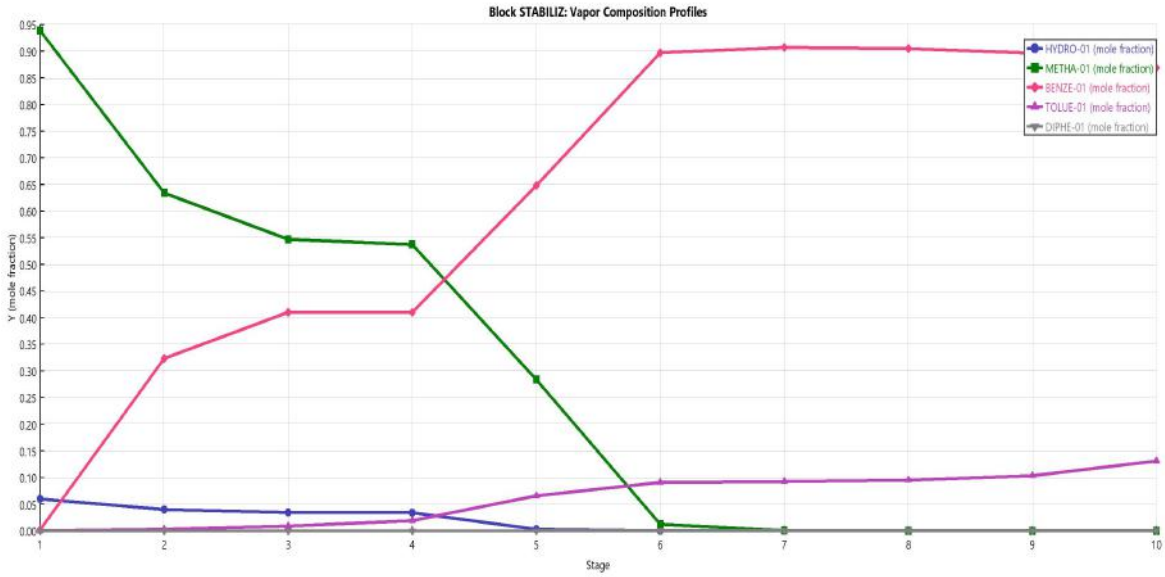

(a)

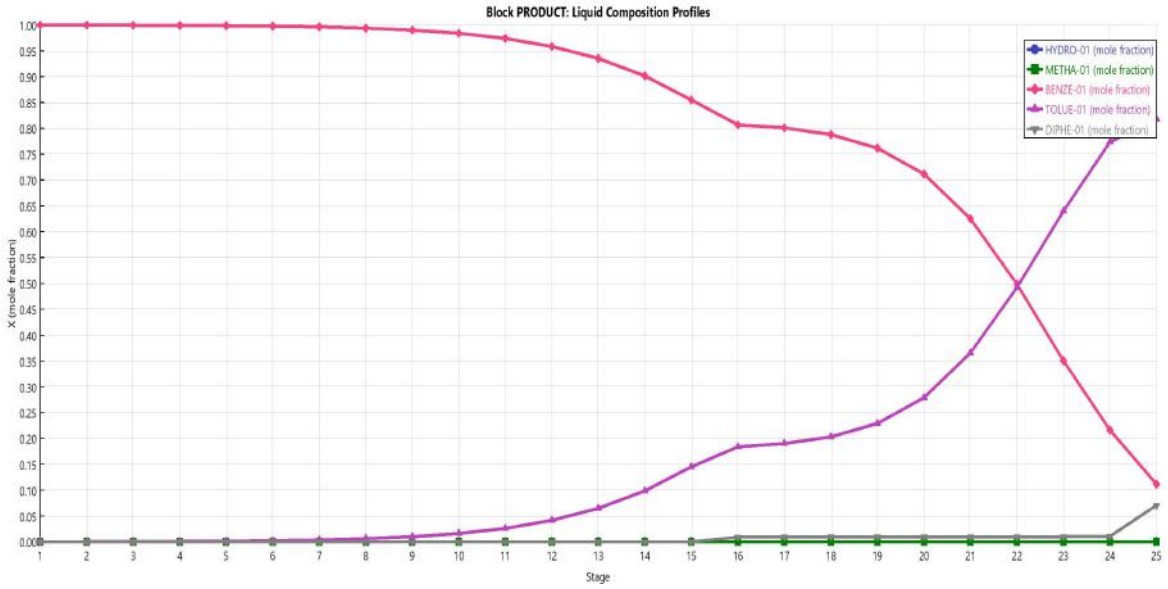

(b)

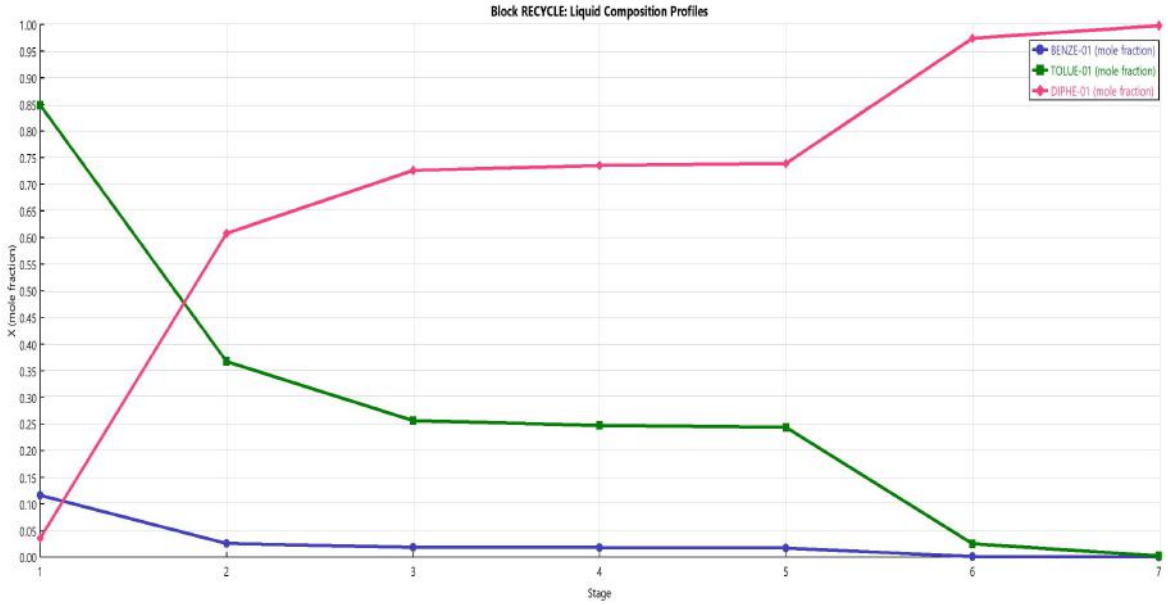

(c)

Figure 4.1: Composition profile in HDA process

All the values of the parameters for the steady state are same as the value in [84]. The composition profile is presented in figure 4.1. In the stabilizer column the methane is the top product with 93.81% purity. While in the product column the benzene composition in the distillate is 99.99%. In the recycle column the bottom product is Diphenyl with 99.77% purity.

4.2 Dynamic simulation

For the dynamic simulation we have used aspen dynamics. The dynamic model has the same physical property and flow-sheet of the steady state model. So it is easy in aspen dynamics to

import the steady state model. The steady state model can be imported into aspen dynamics by two different ways such as flow driven and pressure driven. For our problem we have used the flow driven simulation. For the dynamic simulation some extra parameters have to be specified such as plumbing, pressure-flow specification and equipment sizing. In dynamic mode the extra pressure-flow specification is required because the resulting equation is solved by the implicit Euler numerical integration technique with the fixed step size. The equipment sizing is necessary for the dynamic simulation because for a real plant the dynamics of a system is depended upon the size of the equipment. A systematic procedure is required to be followed for the plumbing and equipment sizing, which are explained in Luyben(2002) .The aspen plus dynamics by default adds PI controller for the temperature, pressure and level. We have intentionally removed the controller. Aspen plus has the feature to linearise the dynamic model at a specified condition.
The script file is created in the Aspen control design interface tool (CDI) which contains the information about the input and output variables. The input variables are considered as

1. Furnace heat duty
2. Cooler inlet temperature
3. Condenser heat duty of stabilizer
4. Rebolier duty of stabilizer
5. Condenser heat duty of product column
6. Rebolier duty of product column
7. Condenser heat duty of recycle
8. Toluene feed flow rate
9. Hydrogen feed flow rate

Product specification should be used as control variables. Since online analyser is very difficult to implement for the analysis of product composition. So it is desirable to use tray temperature instead of composition. The output variables are:

1. Furnace outlet temperature
2. Cooler outlet temperature
3. 1^{st} stage temperature of the stabilizer
4. 8^{th} stage temperature of the stabilizer
5. 1^{st} stage temperature of the product column
6. 22^{nd} stage temperature of the product column
7. 1^{st} stage temperature of the recycle

The dynamic model is initialized in the nominal steady state condition. The standard A, B, C matrices of the continuous LTI state space model is generated along with the model variables. nominal value, gain matrices after invoking the script file. By using MATLAB(2015) the generated sparse matrices is converted into state space model. The original model has

370 state variables which is reduced by the model order reduction technique. One of the important criteria for the model order reduction is the scaling of the plant. We have scaled our plant for model order reduction as well as for controller design. A span matrix is defined for the input and output variables. Span matrix can be defined as the expected difference between the maximum and minimum value. The nominal conditions has been converted it to the percentage.

4.2.1 Model order reduction

One of the effective way to reduce the complexity of a large scale plant is model order reduction. The input and output relation can be reproduced by the reduced order with a negligible error. From the Hankel value plot (4.2), we can observe that there are 7 dominant states. Hence the other states are discarded to find a 7^{th} order model. The approximated error can be visualized by singular value plot of both the reduced and original order system. The singular value plot represents the extended Bode magnitude of MIMO system. The singular value of the SISO system is identical to the Bode magnitude response. Figure 4.3 indicates that the approximated error is less compared to the original system.

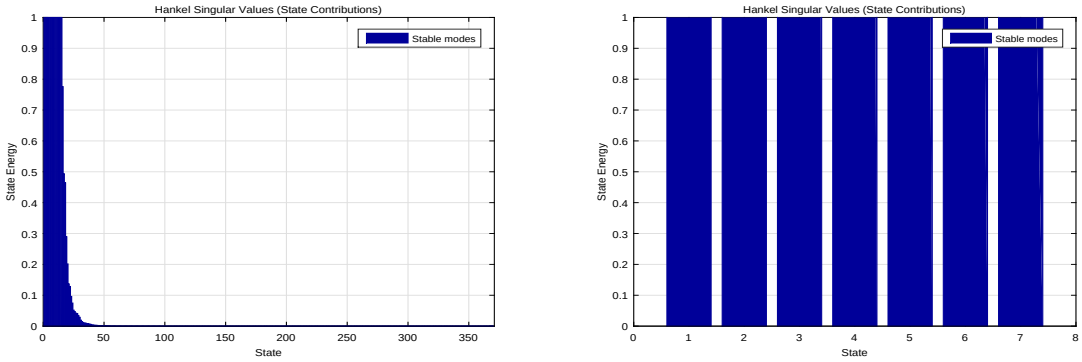

(d) (e)

Figure 4.2: (a) Hankel singular value (b) reduced hankel singular value

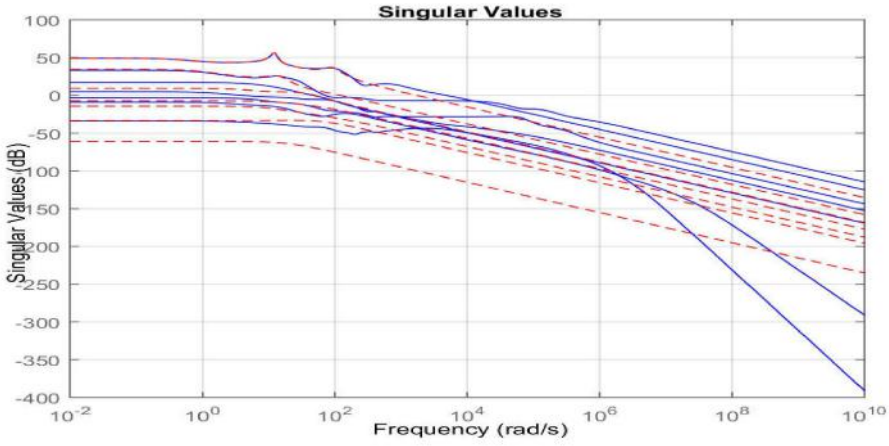

Figure 4.3: Singular value

4.3 Controller design

The state space model is transferred into transfer function model. In this model there are 7 manipulated variable, 7 measured outputs and 2 measured disturbances. Feed flow rate of hydrogen and Toluene are considered as disturbances. There are controller structure interaction between the loops . As discussed in chapter 2, the problem can be handled by using the equivalent transfer function model. The seventh order systems are approximated as the second order transfer functions. The simplified decoupler is designed by using the equivalent transfer function model. The decoupler converts the MIMO system into 7 SISO loops and that can be tuned independently. For the control of the process we have used the fractional order PID. The tuning of the controller is performed by minimizing the objective function. There are many types of objective functions are available. In this process we have considered the time domain ITAE criteria for the load disturbance rejection.

$$J_1 = ITAE_{loaddisturbance} = \int_0^\infty t|e(t)|_{ld}dt \tag{4.1}$$

In a plant wide process there are different design specifications and the objective function can be formed according to the users necessity. Here we have design controllers with disturbance rejection as the single objective functions but the results, which discussed in the next section indicates the designed controllers have the capability to handle disturbance rejection, set point tracking and robustness. For the optimization we used the very new cuckoo search optimization technique. Detailed of the algorithm is described in chapter 2.

4.4 Results and Discussion

In this section we have discussed the set point tracking and the disturbance rejection for each of the outputs. In figure 4.3 we have shown the disturbance rejection of $\pm 5\%$ change in toluene feed flow for all outputs. Figure 4.3 shows the disturbance rejection performance of $\pm 5\%$ change in the Hydrogen feed flow rate for all the seven outputs and Figure 4.3 presents the set point tracking of controllers for all the outputs. The set point tracking and disturbance rejection performance seems satisfactory for all the outputs. Figure 4.3 shows the open loop bode plots and which are stable for all the outputs indicating the stability of the close loop system. The time unit for HDA process is in hours.

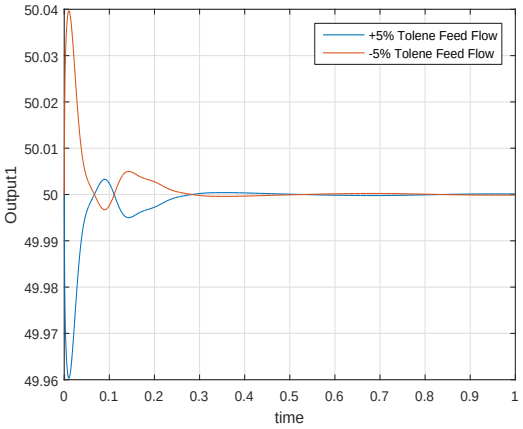
+5% Tolene Feed Flow
-5% Tolene Feed Flow
Output1
time

(a)

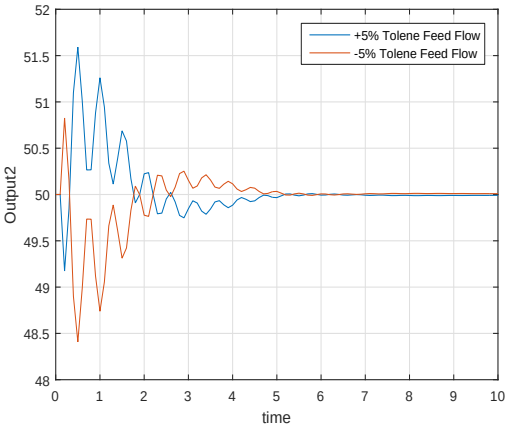
+5% Tolene Feed Flow
-5% Tolene Feed Flow
Output2
time

(b)

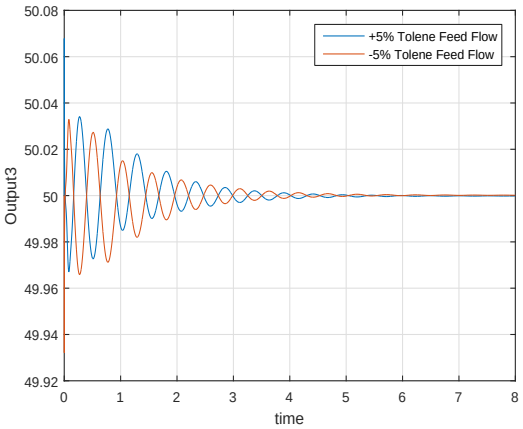
+5% Tolene Feed Flow
-5% Tolene Feed Flow
Output3
time

(c)

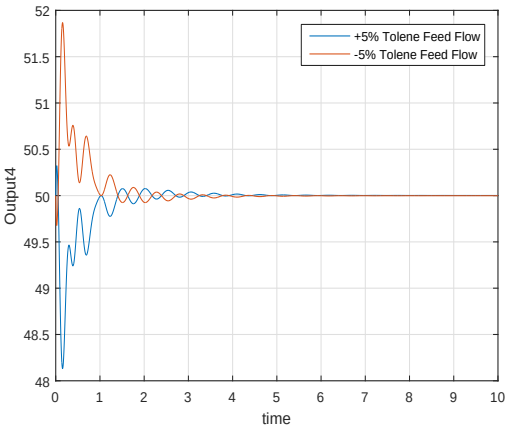
+5% Tolene Feed Flow
-5% Tolene Feed Flow
Output4
time

(d)

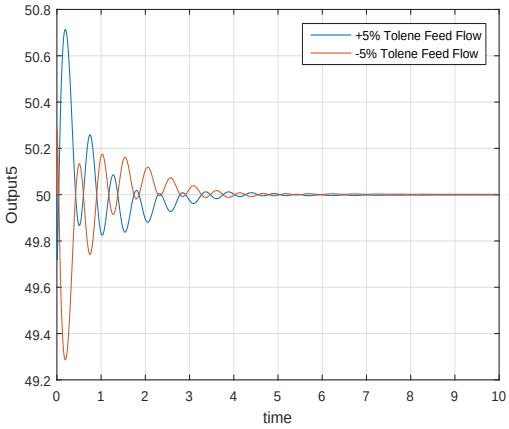
+5% Tolene Feed Flow
-5% Tolene Feed Flow
Output5
time

(e)

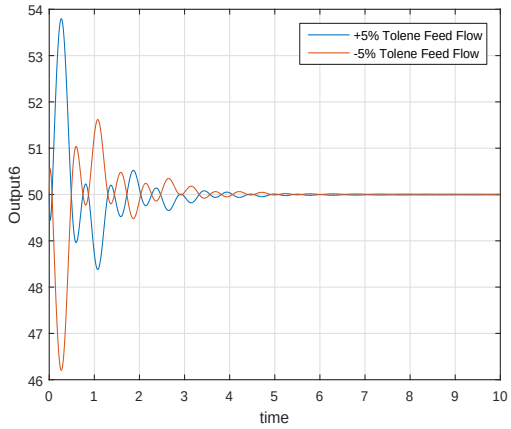

(f)

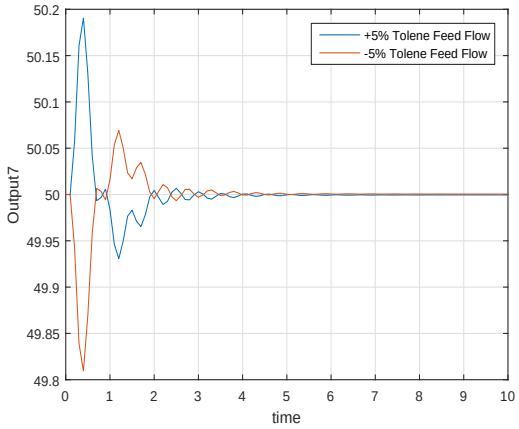

(g)

Figure 4.3: Disturbance rejection of ±5% change in Toluene feed flow

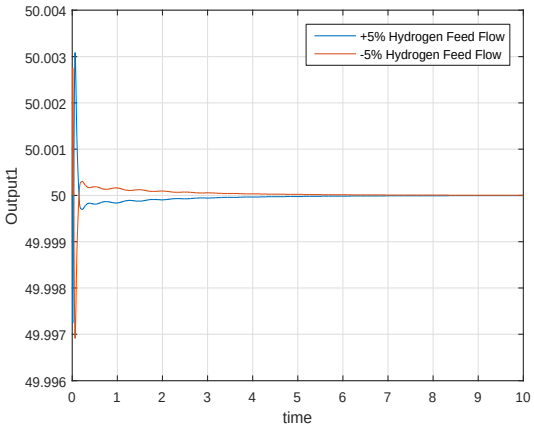

(a)

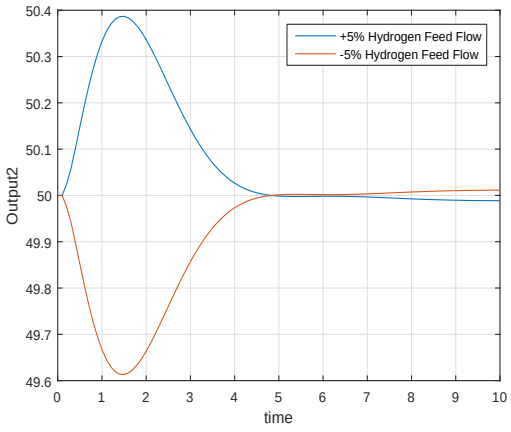

(b)

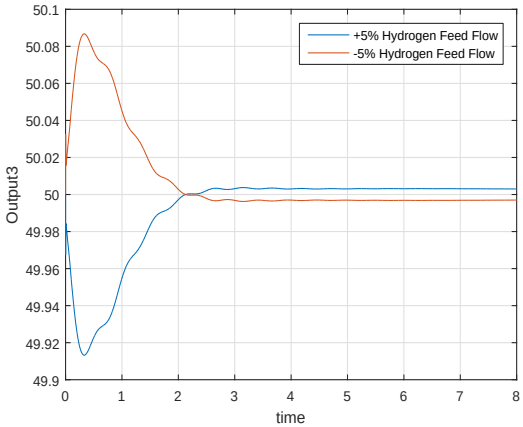

(c)

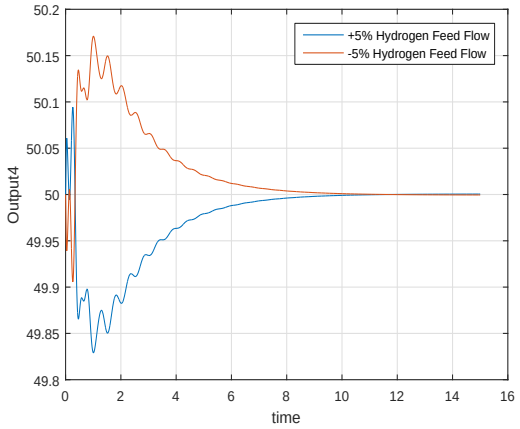

(d)

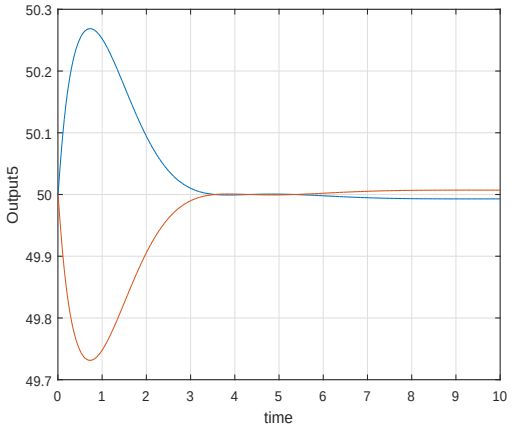

(e)

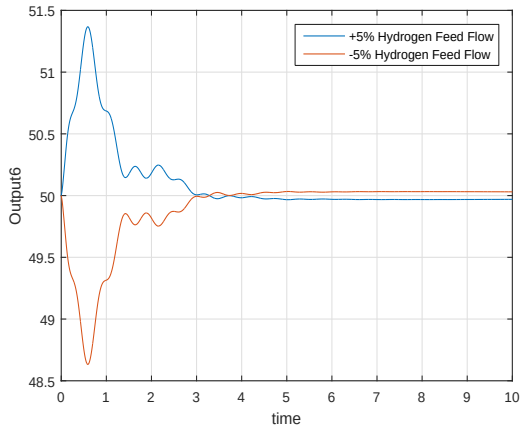

(f)

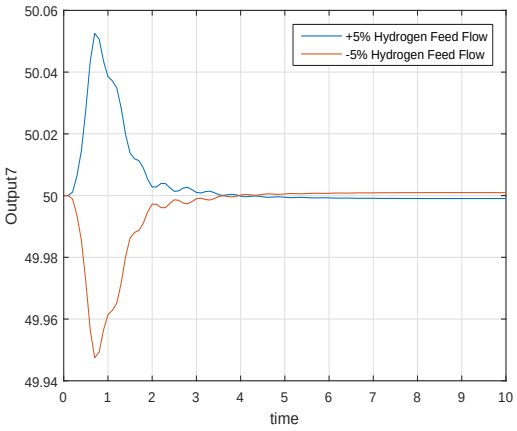

(g)

Figure 4.3: Disturbance rejection of ±5% change in Hydrogen feed flow

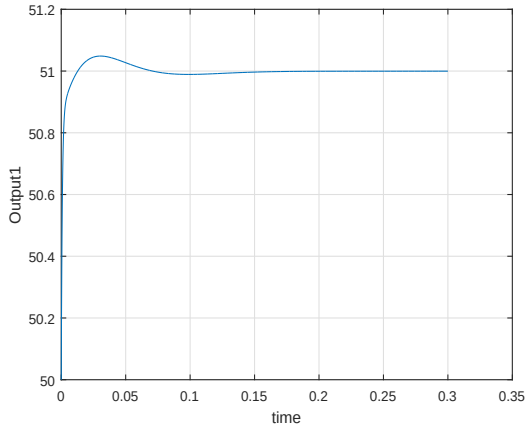

(a)

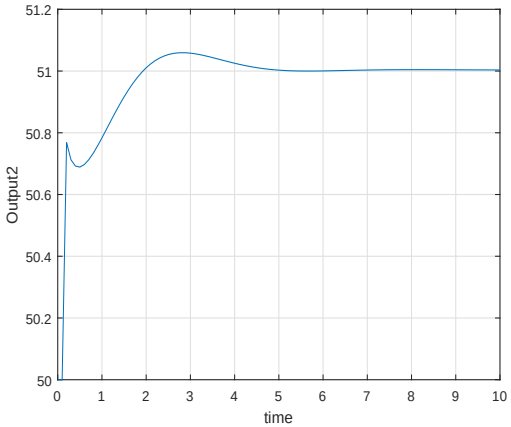

(b)

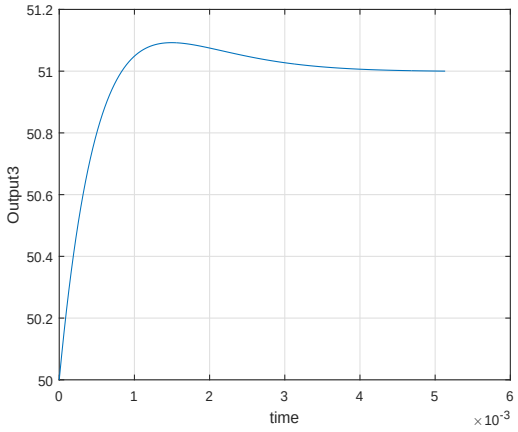

(c)

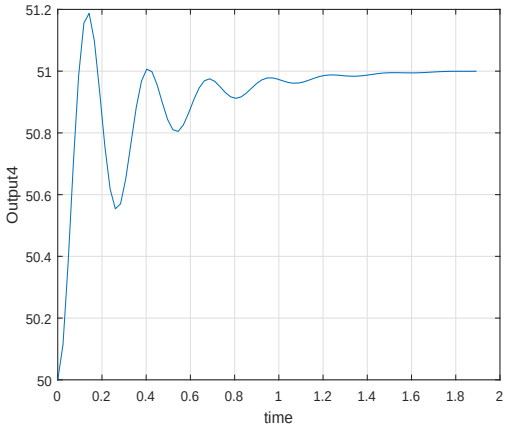

(d)

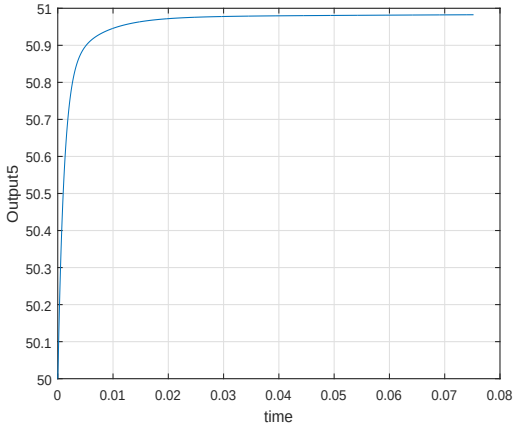

(e)

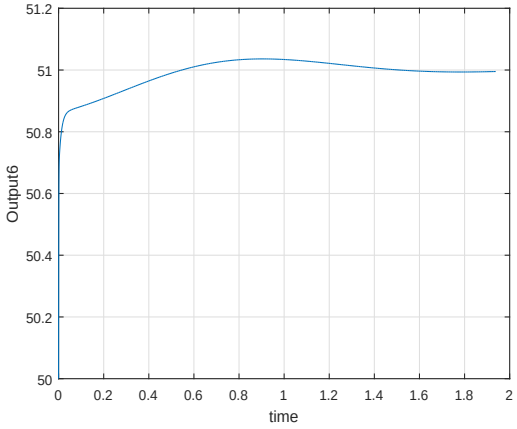

(f)

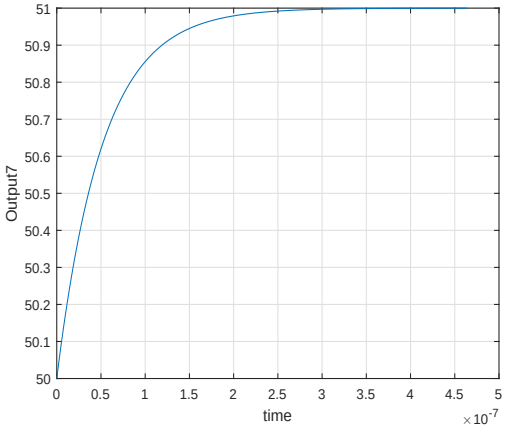

(g)

Figure 4.3: Step point tracking

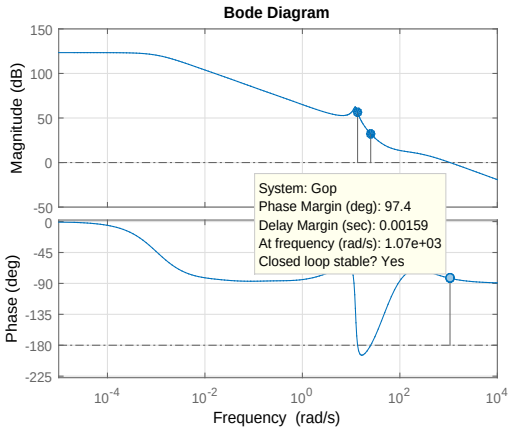
Bode Diagram
Magnitude (dB)
Phase (deg)
Frequency (rad/s)
System: Gop
Phase Margin (deg): 97.4
Delay Margin (sec): 0.00159
At frequency (rad/s): 1.07e+03
Closed loop stable? Yes

(a)

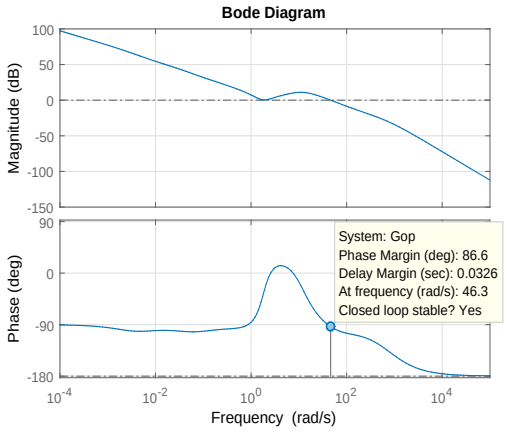
Bode Diagram
Magnitude (dB)
Phase (deg)
Frequency (rad/s)
System: Gop
Phase Margin (deg): 86.6
Delay Margin (sec): 0.0326
At frequency (rad/s): 46.3
Closed loop stable? Yes

(b)

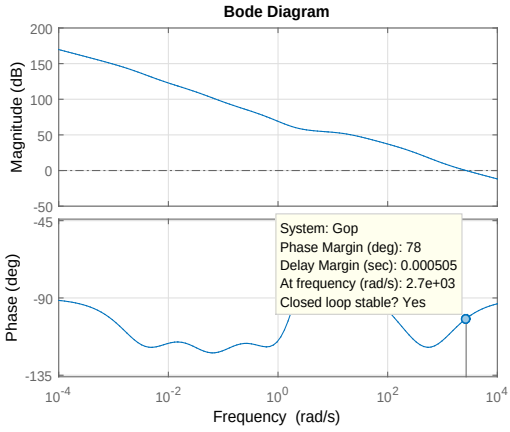
Bode Diagram
Magnitude (dB)
Phase (deg)
Frequency (rad/s)
System: Gop
Phase Margin (deg): 78
Delay Margin (sec): 0.000505
At frequency (rad/s): 2.7e+03
Closed loop stable? Yes

(c)

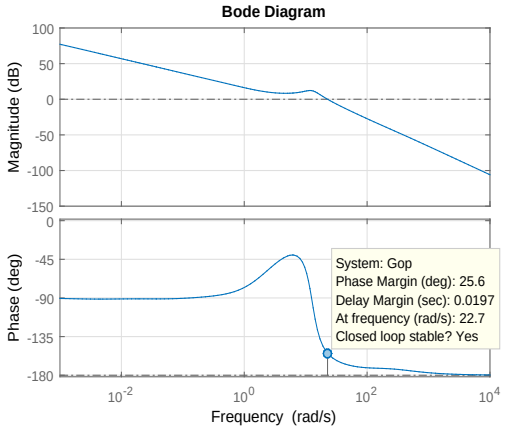
Bode Diagram
Magnitude (dB)
Phase (deg)
Frequency (rad/s)
System: Gop
Phase Margin (deg): 25.6
Delay Margin (sec): 0.0197
At frequency (rad/s): 22.7
Closed loop stable? Yes

(d)

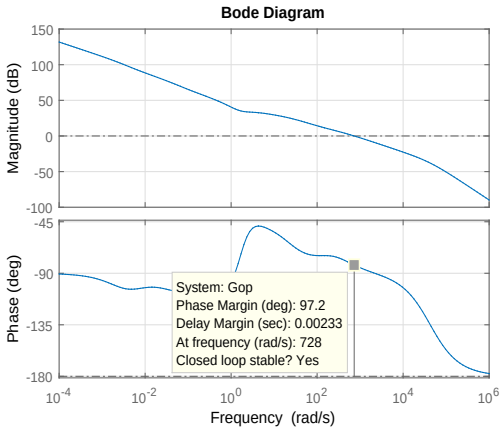
Bode Diagram
Magnitude (dB)
Phase (deg)
Frequency (rad/s)
System: Gop
Phase Margin (deg): 97.2
Delay Margin (sec): 0.00233
At frequency (rad/s): 728
Closed loop stable? Yes

(e)

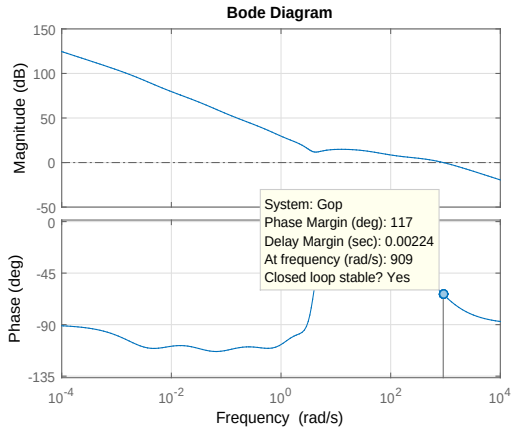

(f)

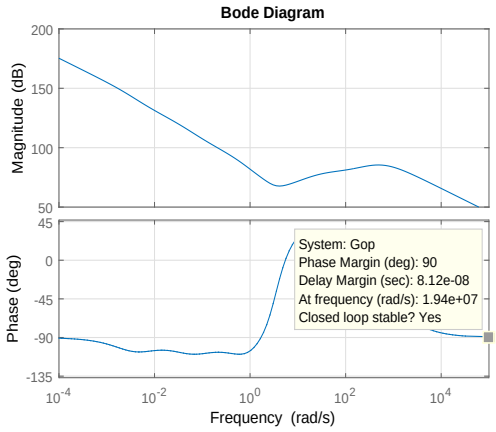

(g)

Figure 4.3: Open loop Bode plot

4.4.1 Robustness of the obtained solutions

The controllers have been designed in the nominal conditions. The system should show satisfactory results for all other operating conditions. The system should be robust to change the parameters. In this section we have shown the robustness of the controllers due to change in the process gain parameter. There is variation with in a range of $-30\%$to$+30\%$. Figure 4.3 shows the disturbance rejection performance under the process gain variation of $\pm 5\%$ change in Toluene feed flow rate, while Figure 4.3 shows the load rejection under the gain variation of $\pm 5\%$ change in Hydrogen feed flow rate. Figure 4.3 4.3 indicates the sufficient robustness for variation of process gain.

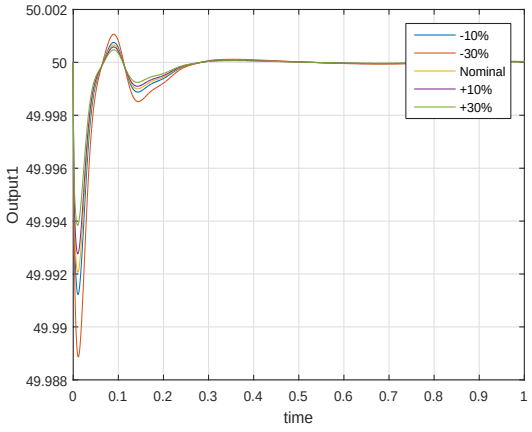

(a)

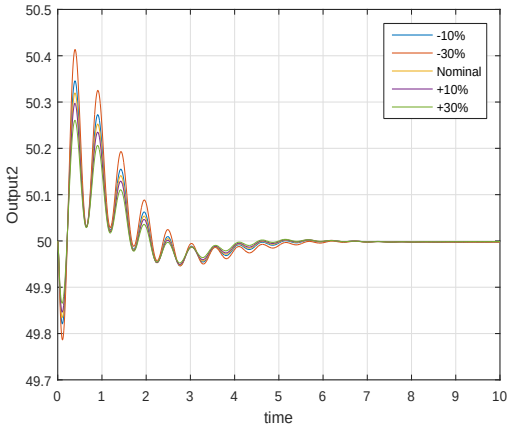

(b)

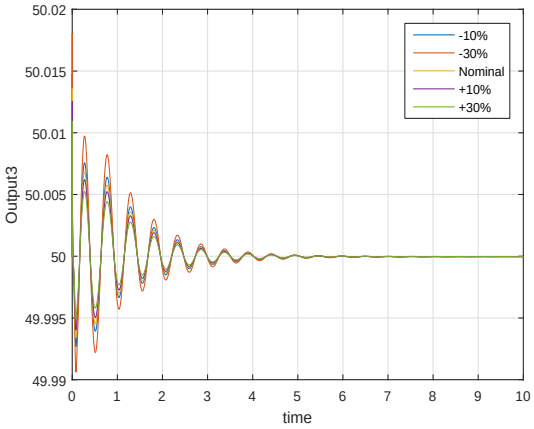

(c)

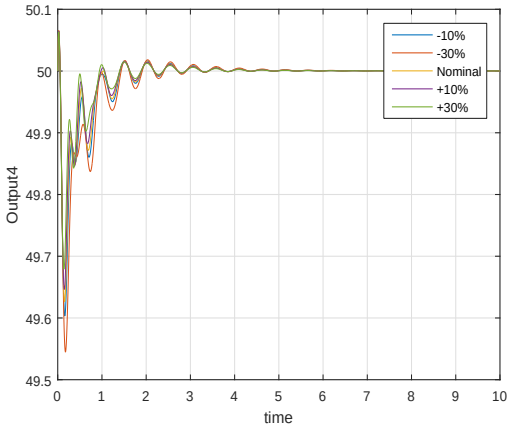

(d)

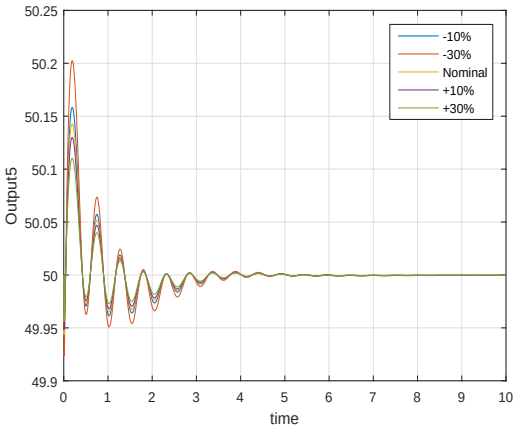

(e)

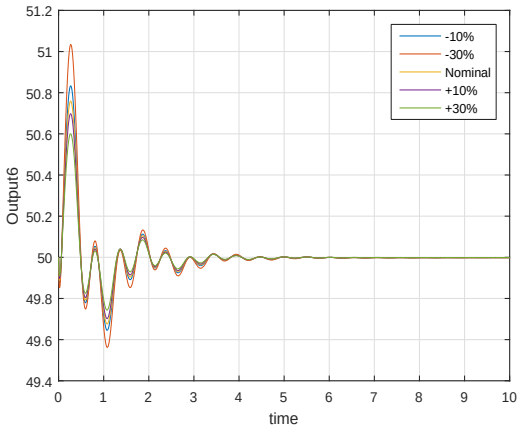

(f)

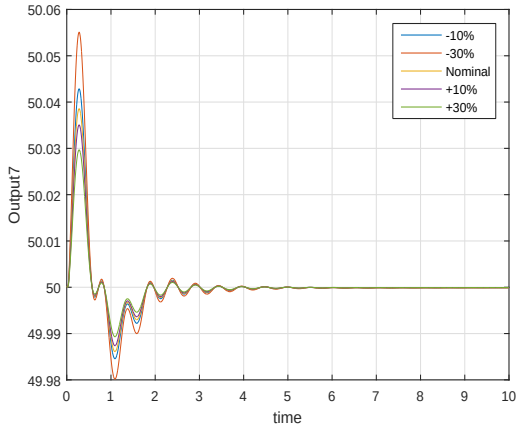

(g)

Figure 4.3: Disturbance rejection performance of controllers for ±5% change in Toluene feed flow rate under gain variation

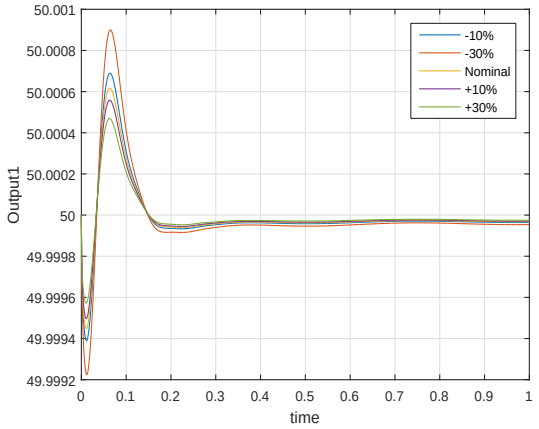
Output1
time
-10%
-30%
Nominal
+10%
+30%

(a)

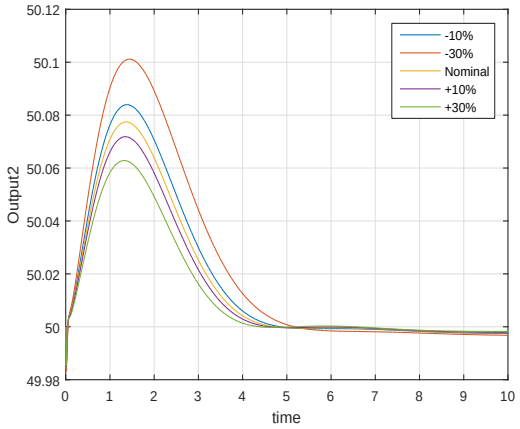
Output2
time
-10%
-30%
Nominal
+10%
+30%

(b)

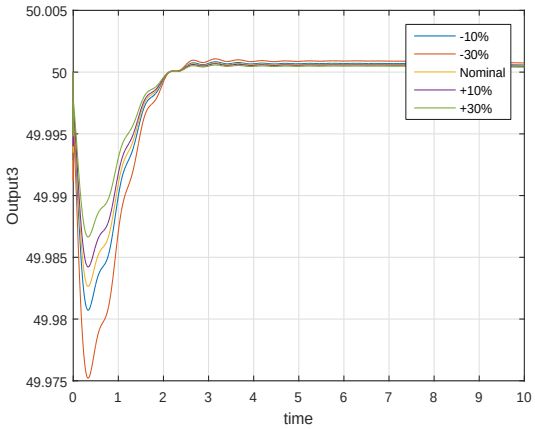
Output3
time
-10%
-30%
Nominal
+10%
+30%

(c)

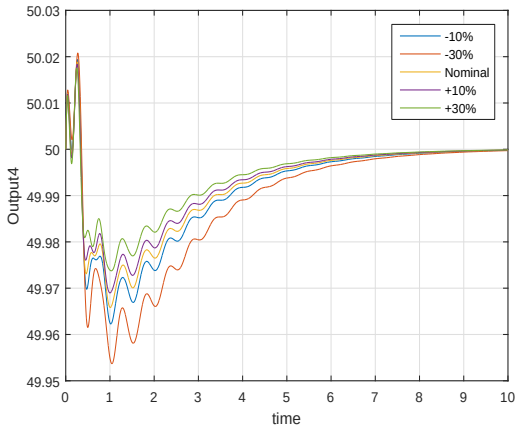
Output4
time
-10%
-30%
Nominal
+10%
+30%

(d)

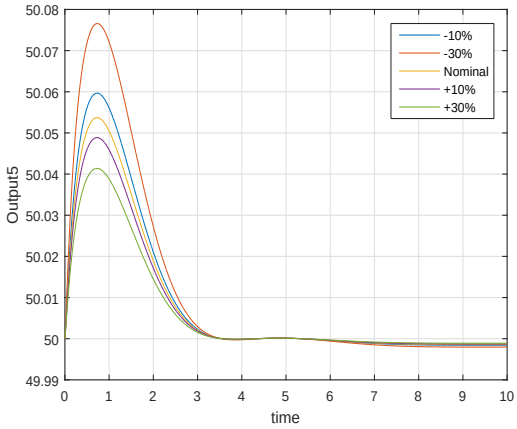
Output5
time
-10%
-30%
Nominal
+10%
+30%

(e)

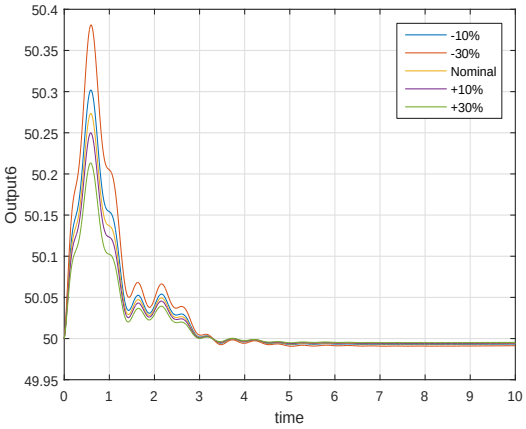

(f)

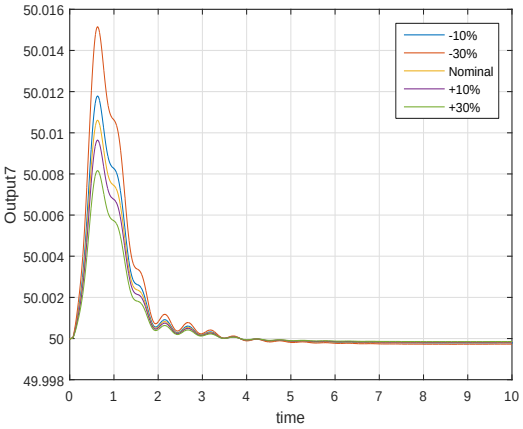

(g)

Figure 4.3: Disturbance rejection performance of controllers for ±5% change in Hydrogen feed flow rate under gain variation

Chapter 5

Conclusions and Future Recommendations

We have designed the fractional order controller for the both the DWC and the HDA process. In the DWC process we have optimized the multiobjective objective function to get the values of the controller parameter while in the HDA process we have used the single objective function. For both the process the designed controllers have the ability to satisfy different specifications like set point tracking, disturbance rejection and robust stability. The advantages of our control methodology are the use of fractional order controller which has the extra flexibility than the conventional PID control and for the HDA process the designed controllers have capability to reduce the interaction in the process. In view of this, present work proposes the use of fractional PID controller in plant wide control and a complex nonlinear system adapting a suitable multiloop control structure. To our knowledge, this is perhaps the very first attempt in its kind.

5.0.1 Future recommendations

Multicomponent system consisting more than 3 components in the DWC can be attempted. The centralized control by the fractional order controller can be designed for MIMO system.

References

[1] R. Agrawal, "Synthesis of distillation column configurations for a multicomponent separation", Ind. Eng. Chem. Res. 35 (1996) 1059–1071.

[2] J.A. Caballero, I.E. Grossmann, Design of distillation sequences: from conventional to fully thermally coupled distillation systems, Comp. Chem. Eng. 28(2004) 2307–2329.

[3] I.E. Grossmann, P.A. Aguirre, M. Barttfeld, Optimal synthesis of complex distillation columns using rigorous models, Comp. Chem. Eng. 29 (2005) 1203.

[4] Z.T. Fidkowski, Distillation configurations and their energy requirements, AIChE J. 52 (2006) 2098–2106.

[5] F. Henrich, C. Bouvy, C. Kausch, K. Lucas, M. Preu, G. Rudolf, P. Roosen,Economic optimization of non-sharp separation sequences by means of evolutionary algorithms, Comp. Chem. Eng. 32 (2008) 1411–1432.

[6] Petlyuk, F.B., Platonov, V.M., Slavinskii, D.M., 1965. Thermodynamically optimal method for separating multicomponent mixtures. Int. Chem. Eng. 5, 555–561.

[7] Draghiciu, L., Isopescu, R., Woinaroschy, A., 2009. Capital cost reduction by the use of divided wall distillation column. Rev. Chim. 60, 1056–1060.

[8] Errico, M., Tola, G., Rong, B.G., Demurtas, D., Turunen, I., 2009. Energy saving and capital cost evaluation in distillation column sequences with a divided wall column. Chem. Eng. Res. Des. 87, 1649–1657.

[9] Dejanovic, I., Matijasevic, Lj., Olujic, Z., 2010. Dividing wall column—a breakthrough towards sustainable distilling. Chem. Eng. Process.: Process Intensification 49, 559–580.

[10] Asprion, N., Kaibel, G., 2010. Dividing wall columns: Fundamentals and recent advances. Chem. Eng. Process. 49, 139–146.

[11] Midori, S., Zheng, S.N., Yamada, I., 2001. Azeotropic distillation process with vertical divided-wall column. Kagaku Kogaku Ronbunshu 27, 756–760.

[12] Bravo-Bravo, C., Segovia-Hernandez, J.G., Gutierrez-Antonio, C., Duran, A.L., Bonilla-Petriciolet, A., Briones-Ramırez, A., 2010. Extractive dividing wall column: Design and optimization. Ind. Eng. Chem. Res. 49, 3672–3688.

[13] Kiss, A.A., Pragt, H., van Strien, C., 2009. Reactive dividing-wall columns—how to get more with less resources? Chem. Eng. Commun. 196, 1366–1374.

[14] Ling, H., Luyben, W.L., 2009. New control structure for divided-wall columns. Ind. Eng. Chem. Res. 48, 6034–6049.

[15] Kiss, A.A., Bildea, C.S., 2011. A control perspective on process intensification in dividing-wall columns. Chem. Eng. Process.: Process Intensification 50, 281–292.

[16] Kiss, A.A., Rewagad, R.R., 2012. Dynamic optimization of a dividing-wall column using model predictive control, Chemical Engineering Science 68 (2012) 132–142.

[17] Wolff, E. A.; Skogestad, S. Operation of integrated three-product (Petlyuk) distillation columns. Ind. Eng. Chem. Res. 1995, 34, 2094–2103.

[18] Abdul Mutalib, M. I.; Smith, R. Operation and control of dividing wall columns Part 1: Degree of freedom and dynamic simulation. Trans.Inst. Chem. Eng., Part A 1998, 76, 308–318.

[19] Abdul Mutalib, M. I.; Zeglam, A. O.; Smith, R. Operation and controlof dividing wall columns Part 2: Simulation and pilot plant studies using temperature control. Trans. Inst. Chem. Eng., Part A 1998, 76, 319–334.

[20] Adrian, R., Schoenmakers, H., Boll, M., 2004. MPC of integrated unit operations:control of a DWC. Chem. Eng. Process. 43, 347–355.

[21] Wang, S.; Lee, C.; Jang, S. Plant-wide design and control of acetic acid dehydration system via heterogeneous azeotropic distillation and divided wall distillation. J. Process Control 2008, 18, 45–60.

[22] Ling, H., Luyben, W.L., 2010. Temperature control of the BTX divided-wall column. Ind. Eng. Chem. Res. 49, 189–203.

[23] Wang, S.; Wong, D. Controllability and energy efficiency of high- purity divided wall column. Chem. Eng. Sci. 2007, 62, 1010–1025.

[24] Serra, M.; Perrier, Esuna, A.; Puigjaner, L. Analysis of different control possibilities for the divided wall column: feedback diagonal and dynamic matrix control. Comput. Chem. Eng. 2001, 25, 859–866.

[25] Woinaroschy, A., Isopescu, R., 2010. Time-optimal control of dividing-wall distillation columns. Ind. Eng. Chem. Res. 49, 9195–9208.

[26] Kvernland, M., Halvorsen, I., Skogestad, S., 2010. Model predictive control of a Kaibel distillation column. In: Proceedings of the 9th International Symposium on Dynamics and Control of Process Systems (DYCOPS), July 2010, pp. 539–544.

[27] Astrom, K., Hagglund, T. (1995). PID controllers: theory, design and tuning. Research Triangle Park: Instrument Society of America.

[28] Astrom, K., Hagglund, T. (2006). Advanced PID control. ISA–The Instrumentation, Systems, and Automation Society.

[29] Podlubny, I. (1999a). Fractional differential equations. Academic Press.

[30] Kenneth S. Miller , Bertram Ros (1993). An Introduction to the Fractional Calculus and Fractional Differential Equations, Wiley-Blackwell (6 July 1993)

[31] Podlubny, I. (1999b). Fractional-order systems and $PI^{\lambda}D^{\mu}$ controller. IEEE Transactions on Automatic Control, 44(1), 208–214.

[32] Hamamci, S. (2007). An algorithm for stabilization of fractional-order time delay systems using fractional-order PID controllers. IEEE Transactions on Automatic Control, 52(10), 1964–1969.

[33] Leu, J. F., Tsay, S. Y., & Hwang, C. (2002). Design of optimal fractional-order PID controllers. Journal of the Chinese Institute of Chemical Engineers, 33(2), 193–202.

[34] Luo, Y.,& Chen, Y. Q. (2009). Fractional-order [proportional derivative] controller for a class of fractional order systems. Automatica, 45(10), 2446–2450.

[35] Luo, Y., Li, H., & Chen, Y. (2011b). Experimental study of fractional order proportional derivative controller synthesis for fractional order systems. Mechatronics, 21, 204–214.

[36] Monje, C. A., Vinagre, B. M., Feliu, V.,& Chen, Y. Q. (2008). Tuning and auto-tuning of fractional order controllers for industry applications. Control Engineering Practice, 16, 798–812.

[37] Alain Oustaloup and Pierre Melchior, "The great principles of the CRONE control", in International Conference on Systems, Man and Cybernetics, 1993, 'Systems Engineering in the Service of Humans', Volume 2, pp. 118-129, 17-20 October 1993, Le Touquet.

[38] A. Oustaloup and M. Bansard, "First generation CRONE control", in International Conference on Systems, Man and Cybernetics, 1993, 'Systems Engineering in the Service of Humans', Volume 2, pp. 130-135, 17-20 October 1993, Le Touquet.

[39] Alain Oustaloup, Benoit Mathieu and Patrick Lanusse, "Second generation CRONE control", in International Conference on Systems, Man and Cybernetics, 1993, 'Systems Engineering in the Service of Humans', Volume 2, pp. 136-142, 17-20 October 1993, Le Touquet.

[40] Patrick Lanusse, Alain Oustaloup and Benoit Mathieu, "Third generation CRONE control", in International Conference on Systems, Man and Cybernetics, 1993, 'Systems Engineering in the Service of Humans', Volume 2, pp. 149-155, 17-20 October 1993, Le Touquet.

[41] Concepcion A. Monje, Antonio J. Caderon, Blas M. Vinagre and Vicente Feliu, "The fractional order lead compensator", in Second IEEE International Conference on Computational Cybernetics, ICCC 2004, pp. 347-352, Vienna

[42] YangQuan Chen, Kevin L. Moore, Blas M. Vinagre and Igor Podlubny, "Robust PID controller autotuning with a phase shaper", in Proceedings of the first IFAC Symposium on Fractional Differentiation and its Application (FDA04), Bordeaux, France, 2004.

[43] Suman Saha, Saptarshi Das, Ratna Ghosh, Bhaswati Goswami, R. Balasubramanian, A.K. Chandra, Shantanu Das and Amitava Gupta, "Fractional order phase shaper design with Bode's integral for iso-damped control system", ISA Transactions, Volume 49, Issue 2, pp. 196-206, April 2010.

[44] Concepcion A. Monje, Antonio J. Calderon, Blas M. Vingre, YangQuan Chen and Vicente Feliu, "On fractional PI^{λ} controllers: some tuning rules for robustness to plant uncertainties", Nonlinear Dynamics, Volume 38, Numbers 1-2, pp. 369-381, December 2004.

[45] HongSheng Li, Ying Luo and YangQuan Chen, "A fractional order proportional and derivative (FOPD) motion controller: tuning rule and experiments", IEEE Transactions on Control System Technology, Volume 18, Issue 2, pp. 516-520, March 2010.

[46] Concepcion A. Monje, Blas M. Vinagre, Vicente Feliu and YangQuan Chen, "Tuning and auto-tuning of fractional order controllers for industry applications", Control Engineering Practice, Volume 16, Issue 7, pp. 798-812, July 2008.

[47] Lubomir Dorcak, Jan Terpak, Marcela Papajova, Frantiska Dorcakova and Ladislav Pivka, "Design of the fractional-order $PI^{\lambda}D^{\mu}$ controller based on the optimization with self-organizing migrating algorithm", Acta Montanistica Slovaca, Volume 12, Number 4, pp. 285-293, 2007.

[48] Arijit Biswas, Swagatam Das, Ajith Abraham and Sambarta Dasgupta, "Design of fractional-order $PI^{\lambda}D^{\mu}$ controllers with an improved differential evolution", Engineering Applications of Artificial Intelligence, Volume 22, Issue 2, pp. 343-350, March 2009.

[49] Deepyaman Maiti, Mithun Chakraborty, Ayan Acharya and Amit Konar, "Design of a fractional-order self-tuning regulator using optimization algorithms", in Proceedings of 11 th International Conference on Computer and Information Technology, ICCIT 2008, pp. 470-475, 24-27 December 2008, Khulna, Bangladesh.

[50] Jun-Yi Cao and Bing-Gang Cao, "Design of fractional order controllers based on particle swarm optimization", International Journal of Control, Automation and Systems, Volume 4, Issue 6, pp. 775-781, December 2006.

[51] Jun-Yi Cao and Bing-Gang Cao, "Optimization of fractional order PID controllers based on genetic algorithm", in Proceedings of the International Conference on Machine Learning and Cybernetics, ICMLC 2005, pp. 5686-5689, Guangzhou, 18-21 August 2005.

[52] Deepyaman Maiti, Ayan Acharya, Amit Konar and Ramadoss Janarthanan, "Tuning PID and $PI^{\lambda}D^{\mu}$ controllers using the integral time absolute error criterion", in 4 th International Conference on Information and Automation for sustainability, ICIAFS 2008, pp. 457-462, 12-14 December 2008, Colombo.

[53] Muwaffaq Irsheid Alomoush, "Load frequency control and automatic generation control using fractional-order controllers", Electrical Engineering, Volume 91, Number 7, pp. 357-368, March 2010.

[54] Mohammad Saleh Tavazoei, "Notes on integral performance indices in fractional order control systems", Journal of Process Control, Volume 20, Issue 3, pp. 285-291, March 2010.

[55] Majid Zamani, Masoud Karimi-Ghartemani, Nasser Sadati and Mostafa Parniani, "Design of a fractional order PID controller for an AVR using particle swarm optimization", Control Engineering Practice, Volume 17, Issue 12, pp. 1380-1387, December 2009.

[56] Fabrizio Padula and Antonio Visioli, "Tuning rules for optimal PID and fractional-order PID controllers", Journal of Process Control, 21 (2011) 69–81

[57] A. Hajiloo, , N. Nariman-zadeh, , Ali Moein, Pareto optimal robust design of fractional-order PID controllers for systems with probabilistic uncertainties, Mechatronics, 22 (2012) 788–801.

[58] Damarla, Seshu, K. and Kundu, M., (2015). Design of robust fractional PID controller using triangular strip operational matrices, Fractional Calculus and Applied Analysis, Vol. 18(5), 1291-1326

[59] Govind, R. and Powers, G.J. Control System Synthesis Strategies. AIChE J., 28, pp.60-73. 1982.

[60] Luyben, M.L.; Tyreus, B.D.; Luyben, W.L. Plant-Wide Control Design Procedure. AIChE J., 43, pp.3161-3174. 1997.

[61] Konda, N.V.S.N.M.; Rangaiah, G.P.; Krishnaswamy, P.R. Plant-Wide Control of Industrial Processes: An Integrated Framework of Simulation and Heuristics. Ind. Eng. Chem. Res., 44, pp.8300-8313. 2005.

[62] Morari, M.; Arkun, Y.; Stephanopoulos, G. Studies in the Synthesis of Control Structures for Chemical Processes. Part 1: Formulation of the Problem - Process Decomposition and the Classification of the Control Tasks. Analysis of the Optimizing Control Structures. AIChE J., 26, pp.220-232. 1980.

[63] Zheng, A.; Mahajanam, R.V.; Douglas, J.M. Hierarchical Procedure for Plant-Wide Control System Synthesis. AIChE J., 45, pp.1255-1265. 1999.

[64] Zhu, G.Y.; Henson, M.A.; Ogunnaike, B.A. A Hybrid Model Predictive Control Strategy for Non-Linear Plant-Wide Control. J. Proc. Cont., 10, pp.449-458. 2000.

[65] Cao, Y.; Rossiter, D.; Owens, D. Input Selection for Disturbance Rejection under Manipulated Variable Constraints. Comput. Chem. Eng., 21, pp.S403-S408. 1997.

[66] Groenendijk, A.J.; Dimian, A.C.; Iedema, P.D. Systems Approach for Evaluating Dynamics and Plant-Wide Control of Complex Plants. AIChE J., 46, pp.133-145. 2000.

[67] Dimian, A.C.; Groenendijk, A.J.; Iedema, P.D. Recycle Interaction Effects on the Control of Impurities in a Complex Plant. Ind. Eng. Chem. Res., 40, pp.5784-5794. 2001.

[68] Vasbinder, E.M. and Hoo, K.A. Decision-Based Approach to Plant-Wide Control Structure Synthesis. Ind. Eng. Chem. Res., 42, pp.4586-4598. 2003.

[69] Dorneanu, B.; Bildea, C.S.; Grievink, J. On the Application of Model Reduction to Plant-Wide Control. Comput. Chem. Eng., 33, pp.699-711. 2009

[70] Panahi, M. and Skogestad, S. (2011) Economically efficient operation of CO2 capturing process partI: self-optimizing procedure for selecting the best controlled variables. Industrial & Engineering Chemistry Research, 50, 247–253.

[71] K.S. Miller, B. Ross "An Introduction to the Fractional Calculus and Fractional Differential Equations", NewYork: Wiley, 1993.

[72] D. Xue, Y.Q. Chen MATLAB Solutions to Advanced Applied Mathematical Problems. Beijing: Tsinghua University Press, 2004.

[73] R. Hilfer "Applications of Fractional Calculus in Physics", Singapore: World Scientific, 2000.

[74] M.J.He, W.J. Cai, " Simple decentralized PID controller design method based on denamis analysis," Ind. Eng. Chem., 8334-8344, 2005

[75] Q. Xiong, " Equvalent transfer function method for PID controller design", journal of process control, 665-673, 2007.

[76] Shen, Y.; Cai, W. J.; Li, S.Multivariable Process Control: Decentralized, Decoupling, or Sparse? Ind. Eng. Chem. Res. 2010, 49 (2) 761– 771.

[77] Cai. w.J, He Mj, " Normalized decoupling - a new approach for MIMO process", Ind. Eng. Chem, 7347-56, 2008.

[78] C. Rajapandiyan and M. Chidambaram, "Controller design for MIMO processes based on simple decoupled equivalent transfer functions and simplified decoupler," Ind. Eng. Chem. Res., vol. 51, no. 38, pp. 12398-12410, 2012.

[79] Xiaoli and W. J. Cai, "Effective transfer function method for decentralized control system design of multi-input multi-output processes," Journal of Process Control, vol. 16, no. 8, pp. 773-784, 2015

[80] Bristol E.H, " On a new measure of interaction of multi variable system,", IEEE Trans, 133-134, 1966

[81] P. Grosdidier, M. Morari, Interaction measures under decentralized control, Automatica 22 (1986) 309–319.

[82] M. Herrero, S. García-Nieto, X. Blasco, V. Romero-García, J. V. Sánchez-Pérez and L. M. Garcia- Raffi. "Optimization of sonic crystal attenuation properties by ev-MOGA multiobjective evolutionary algorithm. Structural and Multidisciplinary Optimization". Vol. 39, num. 2, pp. 203 - 215, 2009 (ISSN:1615-1488)

[83] X.-S. Yang; S. Deb (December 2009). "Cuckoo search via Lévy flights". World Congress on Nature and Biologically Inspired Computing (NaBIC 2009). IEEE Publications. pp. 210–214.

[84] Truls larsson* and Sigurd skogestad "Plantwide control—A review and a new design procedure", Modeling , identification and control, 2000.